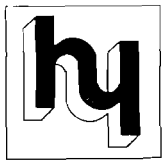

HR Wallingford

Hydro-geotechnical performance of rubble mound breakwaters

NWH Allsop & AF Williams

Report SR 183
February 1991

Address: **Hydraulics Research Ltd,** Wallingford, Oxfordshire OX10 8BA, United Kingdom.
Telephone: 0491 35381 International + 44 491 35381 Telex: 848552 HRSWAL G.
Facsimile: 0491 32233 International + 44 491 32233 Registered in England No. 1622174

FUNDING SUPPORT

This report describes work funded in part by the Department of the Environment under Research Contract PECD 7/6/108 for which the nominated officer was Dr R P Thorogood. It is published on behalf of the Department of the Environment, but any opinions expressed in this report are not necessarily those of the Department. The work was carried out in the Maritime Engineering Department of Hydraulics Research, Wallingford, under the management of Dr S W Huntington.

Mr Lee, Mr Fung, Mr A Thompson, Dr I C Pyrah, and Dr W Anderson were supported by the Science and Engineering Research Council and the University of Sheffield. Dr T J T Whittaker was supported by The Queen's University of Belfast. Mr R Tong was supported by the Science and Engineering Research Council, Hydraulics Research and the University of Bristol. Dr Z C Sun and Mr H Y Pan were supported by the British Council, Hydraulics Research and Dalian University of Technology, China.

The support of Ove Arup Partnership and OASYS Ltd in the supply of computer software for slope stability calculation is gratefully acknowledged.

Further assistance was afforded to this project by contributors to a workshop at HR in November 1989 on "Wave impacts on coastal structures"; see Appendix A to this report.

HYDRO-GEOTECHNICAL PERFORMANCE OF RUBBLE MOUND BREAKWATERS

Report SR 183 February 1991

ABSTRACT

Rubble mound breakwaters, and related structures, are used worldwide to protect harbours, shorelines, and other sensitive areas against wave action. Such structures may face large wave forces and cost of the order £10 to £50 million per kilometre. The porosity and permeability of such structures allows wave pressures and flows to pass into, and sometimes through, the mound. High pressure gradients within the structure may initiate geotechnical instability.

A research project has been conducted to examine and quantify the behaviour of rubble mounds subjected to wave action, with particular emphasis on the fluid/structure interactions. This report describes studies to extend design and analysis methods. The responses addressed in this study are those that relate to the overall stability of the mound, rather than the performance of the armour layer. The general objectives were to:

- Improve the description of material properties and develop techniques to define the flow within properties of granular material;
- Develop numerical models to calculate flows and pressures at and within rubble mounds;
- Develop methods to estimate the geotechnical stability of rubble mounds;
- Instrument prototype structures to give validation data for the numerical models and other design procedures.

This report describes work conducted primarily at Hydraulics Research, and includes some details of complimentary work conducted elsewhere. A brief resume of the overall approach is given. The main results of the study may be summarised:

- Permeability data, and simple empirical methods, describing the flow properties of a wide range of single-sized or wide-graded rubble materials, giving input data for numerical models;
- Numerical models of overall hydraulic performance, and of wave flows/pressures over and within the mound;
- Calculation methods for the stability of slopes and internal stability of mounds;
- Development of field measurement equipment for flows/pressures, intended to derive calibration data for numerical models.

NOTATION

a,b	Forchhiemer coefficients
C_o, C_7	den Adel's coefficients
C_1, C_2	coefficients used in Shih's equation
c	Cohesion
dh	pressure head drop
g	gravitational acceleration
h	water depth
h_o	mean water level
h_1 h_2	water depths used in Madsen & White model
i	hydraulic gradient
i_{cr}	critical hydraulic gradient for suffusion
k	permeability
k_L	air content for a breaking wave
k_w	wave number
n	porosity
t	time
u	discharge
A	cross-sectional area
D	representative particle diameter
D_n	particle diameter
D_*	modified representative particle diameter
F	measure of particle grading
F_R	non-linear friction term
H	measure of particle grading
H_b	maximum breaking wave height
H_c	height of wave crest
L	wave length
L_t	distance between tappings
P_{total}	total pressure
P_{stat}	hydrostatic pressure
P_{dyn}	hydrodynamic pressure
P_A	percentage air content of a breaking wave
U_c	Hazen's uniformity coefficient
U_n	depth averaged horizontal velocity
U_1, U_2	discharge velocities used in Madsen & White model
Q	flow rate
S	wave maker stroke length
α_o	Engehund coefficients
$\alpha_1\alpha_2$	modified Engelund coefficients
β_1 β_2	modified Engelund coefficients
γ	fluid weight density (ρg)
η	free surface elevation
η_m	perturbation of the free surface
ν	kinematic viscosity
ρ	water density
τ_b	bottom shear stress
$\emptyset$	velocity potential
$\emptyset'$	slip angle
ψ	stream function

HYDRO-GEOTECHNICAL PERFORMANCE OF RUBBLE MOUND BREAKWATERS

Report SR 183 February 1991

CONTENTS

CONTENTS (CONT'D)

1. INTRODUCTION

1.1 Project objectives

Rubble mound breakwaters are widely used to protect harbour and coastal areas from wave action. Rubble mounds dissipate much of the incident wave action in the voids within the armour, underlayers and core. The porosity and permeability of such structures allows the transmission of pressures and flows within, and sometimes through, the mound. Pore pressures vary markedly within the structure, and high pressure gradients may initiate geotechnical instability.

During a previous research study for Department of Environment (DOE) PECD 7/6/52, a review was conducted of methods available to quantify flows and pressures within rubble mound breakwaters, and to predict their geotechnical responses (Ref 1). This review concluded that the design methods available at the time, 1986/7, were not well supported, and required advances in four areas. These may be summmarised:

(a) improve the description of material properties;
(b) develop new techniques to define the hydraulic flow properties of granular material;
(c) develop numerical models to calculate flows and pressures at and within rubble mounds;
(d) instrument prototype structures and/or large scale models to give validation data for the numerical models and other design procedures.

In 1987 a new research project funded under DOE contract PECD 7/6/108 was started to address some of these points. The objectives for the new project were "to examine and quantify fundamental aspects of the behaviour of porous mounds subjected to wave action, with particular emphasis on the fluid/structure interactions".

1.2 Project organisation

The review work conducted under the previous project (Ref 1) had been performed jointly by Hydraulics Research, Wallingford (HR) and Dr LA Wood of South Bank Polytechnic, London (SBP). The plan for the new project envisaged that work at HR would address the main hydraulic aspects, whilst studies at SBP would concentrate on the main geotechnical aspects. The project was expected to run for three years only. During the first year of the contract, it became clear that funding would not be available for SBP to complete the work required within the time remaining. The contract was extended to four years, and some aspects of the emphases in the initial programme were

revised, without changing the objectives. The work at HR was addressed under five main headings:

Wave flume experiments
Permeameter tests
Field measurements of flows/pressures
Stability calculations for rubble slopes

During the course of the project a number of other researchers, designers, and owners contributed to the project by conducting, or by funding, additional work. Particular assistance was given by:

Ove Arup & Partners, OASYS
Kirk McClure & Morton
States of Guernsey, Technical Services Dept
University of Bristol, School of Mathematics
The Queen's University of Belfast, Department of Civil Engineering
University of Sheffield, Department of Civil and Structural Engineering
Dalian University of Technology, China.

1.3 Outline of report

This report describes the work conducted primarily by Hydraulics Research and, where possible, summarises those aspects of the work conducted elsewhere. A description of the general approach to the research project is given in Chapter 2. The main aspects of the study are covered in Chapters 3 to 6.

A considerable proportion of the study effort has been devoted to quantifying the flow properties of rubble. This has been addressed principally by measuring the permeability of a wide range of granular materials. The design of initial wave flume tests to identify the range of hydraulic gradients needed, the design of the permeameter and ancilliary equipment, the tests themselves, and the analysis of the results, are all described in Chapter 3.

During this study a programme of field data collection was initiated. The design of the instrumentation and its deployment are covered in Chapter 4.

The previous review had identified the considerable importance of numerical models in the description of flows and pressures within rubble structures. Numerical models of wave action on the outer surface of a structure, and other models of conditions within the mound, are described in Chapter 5. Examples of the use of the models are also discussed.

The final chapter in this main section of the report, Chapter 6, describes work on the stability analysis of rubble structures. This includes examples of slope stability calculations, and tests for internal stability.

The main conclusions of the project, and recommendations for further work, are summarised in Chapter 7.

2. OVERALL APPROACH

The analysis, or design, of a rubble mound breakwater is complicated by difficulties in calculating or simulating some of the important structure responses. Few responses can be described analytically, as such methods are not able to describe the fluid behaviour at and beyond the point of wave breaking. Some parameters can however be estimated using simple empirical methods. Some of the processes of wave/structure interaction can be simulated in a physical model without significant scale effects, but others are less amenable to this approach.

Numerical models of wave/structure interactions, and of mound stability, have therefore been developed to aid analysis and design. Many of the models have been reviewed by Allsop & Wood (Ref 1), who identified methods available to predict hydrodynamic responses and/or mound stability. The work described here follows directly from that review.

The principal hydraulic responses of concern to the designer may be described at various levels of accuracy and/or detail. At the simplest level, termed here Level 1, estimates of the principal hydraulic response parameters of run-up levels and/or overtopping discharge; coefficient of reflection; and coefficient of wave transmission will often suffice. For small rubble structures, the pore pressures induced by wave action are generally low, and side slopes are relatively shallow. The geotechnical stability of these mounds will therefore be of little concern.

For larger structures, the design of elements of the structure may require significantly more information on the velocities and pressures of water on and in the mound. At Level 2, peak or "worst case" values for pore pressures and/or flow velocities may be estimated for "typical" wave conditions and an idealised cross-section. At a more comprehensive level, Level 3, calculations or measurements will be made to give

pressures and velocities in time and space for a range of extreme and service states.

The tools available to describe performance and stability (excluding armour layers which have been addressed elsewhere, eg. Refs 2-4) are summarised below:

a) Empirical data and/or formulae;
b) Physical modelling methods;
c) Numerical models.

Generally solutions at Level 1 will be derived using empirical methods and/or simple physical model tests. Solutions at Levels 2 or 3 will usually require numerical models of flows within the structure, supported by data on hydraulic boundary conditions derived from physical model tests. The development and application of numerical models is described in Chapter 5.

The geotechnical stability of a rubble mound structure is generally determined using analytical or numerical modelling methods. Example methods used in this study are described in Chapter 6.

Work on this project to develop and apply new techniques may be considered under five main headings:

a) Wave flume experiments, necessary to define the limiting hydraulic gradients required in any study of hydraulic conductivity or permeability;
b) Permeameter tests to describe the flow properties of rubble materials, giving input data for all three methods above, but particularly for the numerical models;
c) Field measurements of flows/pressures, intended to derive calibration data for numerical models;
d) Preliminary numerical models of wave flows/pressures;
e) Stability calculations for rubble slopes.

Results of work under each of these headings is described in this report, and in other papers or reports prepared during the course of the studies, References 12, 17, 22, 31, 34, 40, 41 and 42.

3. PERMEABILITY OF RUBBLE MATERIAL

3.1 Study design

The flow of water through the pores of rubble mound breakwaters has two effects upon the breakwater's performance. The pore pressures generated within the breakwater will effect the stability of the mound. The flow of water in and out of the pores plays a critical part in the dissipation of wave energy. To understand these actions it is necessary to know the permeability within the rubble mound.

The permeability of granular materials has been the subject of a great deal of study. However an inspection of the existing literature only demonstrates the difficulties involved. The wide range of results produced by different studies indicates that permeability depends on a complex interaction between both grain size distribution and some measure of the grain shape.

Den Adel (Ref 5) has collected some existing results together to obtain an analysis based on a wide range of experimental conditions. While such an analysis is useful, it does not provide the quality of information that is required for the breakwater problem. In order to obtain this information a full set of consistent experiments is required, conducted under controlled conditions and under hydraulic gradients that are relevant to rubble mound breakwaters.

Initially a set of wave flume tests were required to provide the information on the hydraulic gradients prevalent within the rubble mound. Once these gradients were obtained, then a full and consistent series of permeameter tests could be conducted.

3.2 Initial wave flume tests

Introduction

The range of hydraulic gradients experienced by a breakwater core are not well understood. Large hydraulic gradients may cause damage to the core through local instabilities. It is therefore important to quantify the range of gradients likely to occur, in order to reproduce these gradients in numerical models and also to test them in a permeameter. To this end the following tests were made on a model breakwater in the wave flume.

Model design and testing

A simplified rubble mound was constructed from 10-14 mm angular limestone in the large wave flume at HR. The mound had a slope angle of 1:2 and a porosity of approximately 40%. It had no armour or filter layers and was protected from wave attack by a sheet of expanded aluminium mesh of high porosity held rigidly by wires through the front face of the structure. Incorporated either side of the centre line of the mound were two rows of vertical wells. Each well was made of a perforated metal tube, with a similar porosity to that of the mound, extending from the front face to the base of the structure. Inserted in the wells were capacitance wave probes designed to measure the water surface elevation within the core. Capacitance probes, although not as intrinsically accurate, were favoured over resistance type probes because they are unaffected by changes in water salinity caused by salts washing off the core material. A wide range of regular wave tests were completed, monitoring the output from the wave gauges using a Compaq micro-computer. Each test used only a short series of waves, thus ensuring that only incident wave conditions were measured and there were no-reflections from the paddle.

Observations and results

A glass window along the side of the wave flume enabled the phreatic surface in the mound to be observed as well as measured by the wave probes in the wells. The effect of wave action on the rubble core is illustrated in Plate 1-5. Near vertical hydraulic gradients (in the order of 10:1) were observed in the mound for the complete range of tests as the waves permeated into the structure. This contrasts with the work of Hall (Ref 6) who only observed near vertical hydraulic gradients for very large waves. The position of these large gradients did not vary appreciably between each incoming wave. The spacing of the wave probes (100mm) was too large to place or measure accurately these large hydraulic gradients, but they did enable the set-up and and envelope of water surface elevations in the core to be determined. The magnitude of the mean set-up was found to exhibit little variability through the mound. The position of the largest reductions in the amplitude of the envelope (ie the position of the largest hydraulic gradients) exhibited a dependence on both wave height and wave period. The large gradients moved deeper into the mound as wave heights and periods increased and exhibited maximum penetration for a combination of the largest wave height and longest period.

The wave probe wells within the structure form preferential flow paths and hence introduces errors in the determination of the phreatic surface. It is recommended that any future tests of a similar nature should incorporate more instrumentation in order to give a better description of the water surface elevation within the mound.

3.3 Permeameter design

During the design of the permeameter which was constructed especially for the present study, the following points were considered:

(i) The main body should be sufficiently large to test material of characteristic diameters up to 50 mm. It has been suggested that the permeameter diameter should be at least ten times the diameter of the largest material to be tested (Refs 7-8).

(ii) The design should minimise the potential of air entrainment in the material sample.

(iii) The supply should be capable of generating a flow velocity through the sample of at least 0.1 m/s.

(iv) The measured pressure head loss should be representative of the complete sample cross-section.

(v) The sample should be constrained to retain constant porosity throughout a test without significant dilation or loss of fines.

(vi) The equipment should be manageable by one person without protracted setting-up procedure before each test.

(vii) The inflow discharge should be measured precisely.

(viii) The system should be capable of reproducing and measuring hydraulic gradients in the range 0.01 to 5.

It was decided that a bottom water entry would be most appropriate. This would allow the majority of air entrained in voids between particles to be eliminated by running water through the system for a few minutes before commencement of the test. Consideration was given to the type of outlet arrangements as described by Dudgeon (Refs 7-8), in which water flowing through the central core of the sample is separated from that

flowing through the outer annulus. This would have permitted the accurate gauging of flow velocity through the central portion of the sample, eliminating errors due to increased velocity in the high porosity outer annulus. However, such a design would have required an elaborate arrangement of large measurement tanks to gauge flow rate; this was considered inappropriate due to difficulties of construction and operation.

The design solution is presented in Figures 3.1 and 3.2. The permeameter is cylindrical in shape with overall height and internal diameter equal to 1.45m and 0.6m respectively. Flexible PVC tubes 9 mm in diameter were used to allow measurement of a representative pressure head loss at a separation of 0.5m across the entire sample cross-section. A rigid perforated steel plate was incorporated to contain the sample at both top and bottom. Water was pumped into the permeameter through a 0.3 metre baffled inlet section, and allowed to flow freely out over the upper rim. The system operating a flow velocity up to approximately 0.1m/s. The pumped water flow was gauged using an orifice plate meter in the supply pipe. This was later replaced by an electromagnetic flow meter logging to a chart recorder, and digital readout. The discharge water from the permeameter was allowed to drain back freely into the reservoir, within which the pump intake was located, thus providing continuous water cycling.

3.4 Permeameter tests

The testing procedure

The testing procedure is represented by a flow chart in Figure 3.3.

The permeameter was assembled as shown in Figure 3.1. During assembly, care was taken to ensure that all flanges, gaskets, bolt holes etc, were clear of stray particles which might prevent a water tight seal, or allow air into the system.

Once the permeameter was assembled it was filled with water to check for any leakage.

Pressure measurement

Pressures were measured at two levels, 0.5m apart, inside the permeameter. At each level, the measurement arrangement consisted of a pair of tapping tubes running perpendicularly across the inside diameters of the permeameter. These tubes were made of flexible PVC tubes 9 mm in diameter, with

perforations at 40 mm intervals. The open ends of these two tapping tubes were connected outside the permeameater via a looped PVC tube. The single outlet from this looped tube was connected to a manometer to provide a representative measurement of pressure at that particular level. This was later replaced by using a differential pressure transducer connected to the two sets of tappings.

Preparation of samples

The main samples used in the tests were generally limestone with density equal to 2.76 gm/cm^3. Before use each sample was sieved to produce the required size bands. They were then washed to eliminate fine material which might be washed away during the test, and hence affect the porosity.

Difficulty was experienced in cleaning the smallest size samples with D_{15} = 1.49 mm. Loss in total weight was found after the test, and the porosity was expected to have been underestimated by 6 to 9%.

Loading samples

Samples, in small quantities, were carefully loaded into the permeameter. The weight of each sack was recorded so that the total quantity in the permeameter could be determined.

When samples were filled up to the levels of each of the perforated tube tapping, the test material was distributed by hand to surround each of the tapping tubes. This ensured that their whole lengths were evenly supported.

The loading was carried on until the top of the sample was 100 mm from the top of the chamber. The surface of the sample was then levelled by rotating the perforated covering lid forwards and backwards. After a level surface had been achieved, the covering lid was clamped in position. The volume of the sample in the permeameter was therefore fixed between the upper and lower perforated plates.

Porosity of the test specimen

Before starting a new series of tests, water was pumped through the sample for 10 minutes at the highest discharge to allow natural settlement to take place. The porosity obtained at the end of this period was defined as the highest porosity that the sample could achieve.

Lower porosities were obtained by compacting the sample with a vibrating poker. This was done by following the procedures below:

(i) The permeameter was filled with water to the top surface of the sample.

(ii) A fixed amount of material was added onto the surface and smoothed by hand.

(iii) The vibrating poker was used until the water surface just covered the samples.

In cases of high porosities, the poker was only required to be inserted to a depth of about 150 mm at two locations. As the samples became more compact, the poker had to be inserted to a greater depth and at more locations. In general, six to eight different porosities were achieved in a series of tests.

Porosity measurements

Porosity measurements can be made in two ways:

i) By calculation from the weight of the samples loaded, the gross volume of the samples when stabilised, and the specific gravity of the samples. This method was subject to error due to greater porosity effect in the wall zone.

ii) By measuring the volume of water drained from the voids between the levels of the upper and lower head loss tappings. This method was subject to error caused by water retention on the particle surfaces, particularly in the contact regions.

Method i) has been used throughout this analysis.

Flow conditions

For each porosity, up to nine different flow rates were used, increasing regularly from approximately 0.01 m/s to 0.10 m/s.

The tests conducted

The test samples were initially produced as a range of single size classes, and mixtures later derived from them. Each single size class was initially referred to by its nominal upper sieve size expressed in millimetres, generally significantly greater than either D_{50} or D_{85}. As well as these narrow size classes, three types of mixed material were used.

Five mixtures were made up by blending two single sizes equally by weight. One mixture of 6 equal proportions, and two of 7 equal proportions were made up. All of these classes used crushed limestone. It is useful in considering the test results later to note that the D_{15} size for the gap graded mixtures remained essentially constant, but that D_{85}, and hence the ratio D_{85}/D_{15} increased 4-fold between the 6/10 mixture and 6/40. In addition two sizes of rounded pea shingle were included to explore the influence of particle shape on permeability.

In each series of tests a systematic variation of porosity was sought, although the range achieved was limited for some samples, particularly single sizes, by the degree of compaction work possible. Each test was run over the full range of flow conditions possible. In general up to 9 flow conditions were used at each of around 7 porosities for each of the samples tested. The full range of tests conducted are summarised in Table 3.1 with their sieve curves given in Figures 3.4 a-o.

3.5 Analysis of test results

Flow equations

The simplest description of the flow through a porous medium is given by Darcy's law.

$$u = ki \qquad 3.1$$

where u is the discharge velocity
k is the effective permeability
and i is the hydraulic gradient.

Darcy's law works well for low water velocities (ie low Reynolds Numbers) when the flow is lamina. However at higher velocities (Reynolds number >5) the flow becomes turbulent and a more complex flow equation is required.

In 1901 Forchhiemer suggested an equation to describe hydraulic resistance as a gradient, i, in terms of the superficial velocity, u, over the laminar to turbulent transition regime:

$$i = au + bu^2 \qquad 3.2$$

The problem now reduces to finding values for the coefficients a and b.

Englelund (Ref 9) conducted an extensive study of laminar and turbulent flow through homogeneous sand sized particles. From experimental results and

consideration of previous work, Engelund proposed a formula incorporating the material porosity, n, and a representative particle diameter, D:

$$i = \frac{\alpha_o (1-n)^3 \nu u}{n^2 gD^2} + \frac{\beta_o (1-n)}{n^3 gD} u^2 \qquad 3.3$$

with appropriate coefficient values:

(i) uniform spherical particles $\alpha_o \simeq 780$, $\beta_o \simeq 1.8$;

(ii) uniform rounded sand grains $\alpha_o \simeq 1000$, $\beta_o \simeq 2.8$;

(iii) irregular angular grains α_o up to 1500 or more, β_o up to 3.6 or more.

The above values were determined for materials of characteristic diameter less than 10 mm. The Engelund formulation using α_o and β_o values quoted for irregular angular grains has been used to consider flow through prototype coastal structure rubble mounds.

Similar relationships for a and b in equation 3.2 have been proposed recently by den Adel (Ref 5).

$$a = C_0 (1-n)^2 \frac{\nu}{gn^2 D_{15}^2} \qquad 3.4$$

$$b = \frac{C_7}{gn^2 D_{15}} \qquad 3.5$$

For granular material , mean, upper and lower bound values are given:

$C_0 = 160$ (75 to 350)

$C_7 = 2.2$ (0.9 to 5.3)

The wide ranges of values suggested for these coefficients gives an indication of the problem at hand. Particle size distribution and particle shape both seem to play complex roles in determining the values of the coefficients.

Gupta (Ref 10) has described the results of a series of tests for a somewhat random selection of graded and small size materials. He attempted to describe the particle shape influence on hydraulic resistance in terms of the rather empirical angularity parameter.

A more rigorous technique for the description of particle shape, using a spectral description of surface irregularities, has been described by Latham at Queen Mary College, (Ref 11). This type of

quantitative shape description has not yet been used in the context of hydraulic resistance in porous media.

Analysis of results

In considering the large amounts of data produced, it has proved to be convenient to describe the flow/resistance relationship for each test in terms of the Forchheimer equation. Values of a and b in equation 3.2 have been calculated for each sample at each porosity tested. These results are summarised for the 3 classes of sample:

(i) single size, in Figures 3.5. a,b
(ii) gap graded mixtures, in Figures 3.5. c,d
(iii) wide graded mixtures, in Figures 3.5.e,f.

For the single size classes, it is immediately clear that only a limited range of porosities were covered. The range covered is however still regarded as realistic, as single size material will generally require significantly more effort to compact to a given porosity than wide graded materials. Within the range studied, the values of a and b show a logical progression of increasing hydraulic resistance with decreasing porosity, and with decreasing particle size.

In general, the gap graded materials can be compacted to significantly lower porosities, for a given level of compaction effort. The test results for the gap graded samples, (Figs 3.5. c,d) follow similar trends as for single size materials over the upper range of porosities studied. At lower porosities the trends for coefficients a and b diverge. In more turbulent flow conditions, when the term bu^2 in the Forchheimer equation dominates the total hydraulic resistance (Fig 3.5 d), the value of b increases steadily but slowly as the porosity is reduced. Only when the maximum level of compaction is approached, does the hydraulic resistance increase more significantly.

Under conditions of less turbulent flow, when the term au in equation 3.2 has greater influence on the total resistance force, a more complex form for the coefficients a and b emerges, (Fig 3.5 c). Again, over most of the range studied, the resistance force for each sample increases steadily. At the lower porosities achieved, however, the resistance given by au reduces. For each sample this change occurs at approximately the same condition for which the value of b increases in Figure 3.5 d. This apparent

conundrum may well be rooted in the derivation of values of coefficients a and b from the measurements, and cannot be resolved without further analysis. It may be noted that the reduction of the laminar coefficient, a, at low values of porosity will only significantly influence the total resistance force at very low flow velocities, a condition of less concern in this study.

The wide graded samples, for which results are shown in Figures 3.5 e and 3.5 f, show trends for a and b more in line with those expected, and reasonably consistent with those of the gap graded mixtures.

Comparison of test results with prediction formulae

For the single size samples, with characteristic diameter given by D_{15}, the agreement between the coefficients derived from the measured data and the predicted values are generally reasonable. Engelund's coefficients α_o = 780 to 1500 and β_o = 1.8 to 3.6 describe a narrower band, within which the test data falls for most samples. Den Adel's coefficients reflect a wide band of uncertainty.

A very simple assessment of the values of coefficients α_o, β_o and C_o, C_7 is shown in Table 3.1. Within the central range of materials tested the coefficients are reasonably stable and supported by the data. For the larger size material the turbulent coefficients, β_o or C_7, are better described by the published methods than are the laminar coefficients, a_o or C_o. There are however some indications that the general trend for the larger size material is away from that shown by the smaller material.

Further Analysis

In addition to the comparison of the results with Engelund's and Den Adel's formulae, a further analysis was made to see if the coefficients α_o and β_o are dependent on grain size.

The results of this analysis were published by Shih (Ref 12), however a close inspection of the results has raised doubts about the conclusions.

A regression analysis was performed based on Engelund's formula, (Eq 3.2), and any dependence on grain size (D_{15}) was investigated using.

$$\frac{i}{u}\frac{gD_{15}^2}{\nu}\frac{n^3}{(1-n)^3} = \alpha_o + \beta_o \frac{1}{n(1-n)^2}\left(\frac{uD_{15}}{\nu}\right) \qquad (3.6)$$

The linear relations in Figures 3.6 a to g were

observed. The laminar constant (α_o) was found to increase in proportion to D_{15}^2. Its lower limit coincided with the upper limit suggested by Engelund (see Fig 3.6 a). The turbulent constant (β_o) was found to decrease exponentially with D_{15} (see Fig 3.6 b). These results suggest that Engelund's expressions for a and b will need to be modified to represent flow in material larger than 10 mm. At its simplest this may be given for formulae for a_o and β_o.
The permeability relationship for <u>single size materials</u> is therefore given by $i = au + bu^2$, where i = hydraulic gradient, u = superficial velocity and

$$a = \left[\alpha_1 + \alpha_2 \left(\frac{g}{\nu^2} \right)^{2/3} D_{15}^2 \right] \frac{(1-n^3)}{n^2} \frac{\nu}{g} \frac{1}{D_{15}^2} \qquad (3.7a)$$

$$b = \left\{ \beta_1 + \beta_2 \exp \left[\beta_3 \left(\frac{g}{\nu^2} \right)^{1/3} D_{15} \right] \right\} \times \frac{(1-n)}{n^3} \frac{1}{gD_{15}} \qquad (3.7b)$$

where

n = porosity
α_1 = 1683.71, α_2 = 3.12 x 10^{-3}
β_1 = 1.72, β_2 = 1.57, β_3 = -5.10 x 10^{-3}
ν = kinematic viscosity of water
= 1.14 x 10^{-6} m^2/s
g = gravitational acceleration = 9.81 m/s^2

For wide graded samples, the same permeability relationship for single size samples was adopted with D_{15} replaced by D_* where

$$D_* = D_{15} \left(\frac{D_{15}}{D_{50}} \right)^{c_1} \left(\frac{D_{50}}{D_{85}} \right)^{c_2} \qquad 3.8$$

so as to include the effect due to the grading of the material. Coefficients c_1 and c_2 were determined such that the total square errors in hydraulic gradient, $(i_{predicted} - i_{observed})^2$, was minimum. This gave $c_1 = -1.11$ and $c_2 = 0.52$.

The permeability relationship for <u>wide graded materials</u> is therefore given by:

$$i = au + bu^2$$

where

i = hydraulic gradient, u = superficial velocity

and

$$a = \left[\alpha_1 + \alpha_2 \left(\frac{g}{\nu^2} \right)^{2/3} D_* \right] \frac{(1-n^3)}{n^2} \frac{\nu}{g} \frac{1}{D_*^2}$$

$$b = \left\{ \beta_1 + \beta_2 \exp \left[\beta_3 \left(\frac{g}{\nu^2} \right)^{1/3} D_* \right] \right\} \frac{(1-n)}{n^3} \frac{1}{gD_*}$$

$$D_* = D_{15} \left(\frac{D_{15}}{D_{50}} \right)^{-1.11} \left(\frac{D_{50}}{D_{85}} \right)^{0.52} \qquad 3.9$$

where

n = porosity
$\alpha_1 = 1683.71$, $\alpha_2 = 3.12 \times 10^{-3}$
$\beta_1 = 1.72$, $\beta_2 = 1.57$, $\beta_3 = -5.10 \times 10^{-3}$
ν = kinematic viscosity of water
$= 1.14 \times 10^{-6}$ m²/s
g = gravitational acceleration = 9.81 m/s²

At first sight these results appear very promising in that they provide a set of formulae that should allow small scale laboratory tests to be scaled up to prototype size. However two criticisms must be made.

(i) Shih failed to make a full error analysis of his results. A close inspection of Figures 3.5.2a-f reveals that the expected error in β_o decreases with D_{15}. These trends in the errors may explain any observed variation in α_o and β_o as a function of D_{15}.

(ii) Shih's choice of function is not physically realistic. In order to keep α_o and β_o dimensionless whilst making them a function of D_{15} it was necessary to introduce factors of $(g/\nu^2)^{2/3}$ and $(g/\nu^2)^{1/3}$ into equations 3.7a and b. The introduction of these factors is highly artificial. Altering the strength or direction of the gravitational field would change the behaviour of α_o and β_o as functions of D_{15}.

In the light of these criticisms it is felt that Shih's new formulae should not be used to scale small laboratory permeameter tests to prototype sizes.

If we accept that there is no evidence to suggest that Engelund's coefficients have any dependence on particle size then we can only draw the following conclusions.

Since the error in α_o is smallest for small particle diameters, then from Figure 3.6 the most probable value for α_o lies in the upper region suggested by Engelund.

$\alpha_o \sim 1500$

If the error in β_o is least for large particle diameters, then we may expect a value for β_o close to the lower limit set by Engelund.

$\beta_o \sim 1.8$

It should be noted that these values correspond to the limestone gravel used in our tests. It is felt that values for α_o and β_o may well be dependent on particle shape. Some more work is required in order to investigate any such effect.

3.6 Effects of entrained air

The mechanics of the flow of liquid-gas mixtures has been the subject of much study. Even in the relatively simple situation of flow through pipes, the resulting flow patterns appear to be complex and are often unstable. However, here we are not so much interested in the exact details of the flow on a microscopic scale, as how the presence of entrained air effects the overall permeability of the granular medium within the breakwater.

The first question to be addressed is, does the entrained air penetrate the breakwater sufficiently deeply to significantly effect the performance? Hall (Ref 13) has made observations in a wave flume, with material of various sizes and shapes. He found that the depth of penetration increased considerably with the material size. While it is unclear how Hall's results might be scaled up to full size, his results indicate that the effect of entrained air within the breakwater may not be neglected.

Some experimental work on the effects of entrained air on the permeability of granular media have been carried out by Hannoura and McCorquodale (Ref 14). They investigated the suitability of existing two phase flow models derived from flow through pipes. They found the slug flow form of the drift-flux model matched their test data most accurately.

Changes in the permeability of the breakwater are not the only effects of entrained air. The presence of air greatly effects the compliance of the fluid within the breakwater. Any numerical model of the action of waves upon the breakwater should include a modification for the compliance of the air-water mixture. Much work in this area has been done by Barends (Ref 15 and 16). The situation is complex involving the two way transfer of air between solution

and the bubbles, free bubbles and bubbles which are held within the pores of the medium by surface tension. However Barends does produce an expression for the overall compliance of the combined system, which it should be possible to incorporate into a numerical model of the breakwater.

3.7 Conclusions and recommendations

The results of the permeameter performed in this study tests are consistent with both Engelund's and Den Adel's ranges for the Forchhiemer coefficients. The tests would appear to narrow down the considerable range of uncertainty in these coefficients, however the full effects of material shape are not understood at this stage.

Shih (Ref 12) has reported on a variation of Engelund's coefficients with particle size. It appears however that this observed variation may well be the result of the inherent experimental error. The new formulae proposed by Shih should not be used to scale up small scale permeability tests.

Some work has been done on the effects of air entrainment within the breakwater. Air entrainment effects both the permeability of the granular medium and the compliance of the fluid. More work needs to be done in both these areas, especially on the effects on the permeability. These effects may then be incorporated into existing numerical models of the breakwaters.

Little is known about the effects of particle shape on permeability. It is recommended that a study be made on the most effective way of classifying particle shape. Once this is done a set of permeameter tests may be carried out to investigate this effect.

4. FIELD DATA COLLECTION

4.1 Study design

The accuracy with which physical and numerical models can reproduce wave/structure interactions is limited. Some of the flow processes and forces reproduced in a physical model at small scale will suffer from scale effects. These generally include viscous drag forces; surface tension, and hence bubble size and air content; and particle surface strength, hence shear strength.

Numerical models are limited to simulating the physical processes described by the fundamental hydrodynamic equations used. Even when a (relatively) complete set of equations is used, practical aspects of computer storage and run time will place limits on the capabilities and accuracy of such a model.

All analysis techniques developed to describe the hydrodynamic processes of wave/structure interaction therefore require validation. Some validation of numerical models is possible using physical models at small scale, but experimental results are still then needed at, or near, prototype scale to remove any influence of scale effects.

Controlled experiments on wave/structure interactions at large scale require a very large wave facility. Two large wave flumes are available in Europe: the Delta flume at Delft Hydraulics in the North-East Polder in the Netherlands; and the Grosser Wellenkanal (GWK) operated by institutes within the Universities of Hannover and Braunschweig in Germany. The Delta flume is available for hire at commercial rates, but the costs of the construction and testing of a rubble mound section were outside the resources of this project. The GWK is committed to a programme of studies on the performance of a range of coastal structures including beaches; sloping sea dykes; vertical caisson walls; and rubble breakwaters. Early in this project, one of the HR team visited the Franzius Institute at Hannover to discuss exchange of information and collaboration (Ref 17). It was clear that some very relevant studies were being conducted in the GWK, but that results from those studies would not be available until after the completion of this project. The study team at Hannover were willing to discuss details of their work, and the study advice was used in the design of field and laboratory data collection.

Data collected on a prototype structure may offer alternatives to the large scale laboratory data. It is generally accepted that a high priority should be given to the collection and analysis of field data on the performance of coastal structures. However only on a few occasions has it been possible to install instruments in a rubble structure.

The new outer breakwater at Zeebrugge was instrumented during construction under a major programme supported by the Ministry of Public Works of the Belgian Government (Ref 18). The breakwater is formed by a rubble mound armoured with 25 tonne antifer cubes. The measurement equipment installed was based around a

purpose built jetty, to which wave probes and other measurement devices were attached. Other devices installed within the breakwater during and after construction include six 140 mm diameter tube wells bored down through the seaward slope, and a number of pore water pressure cells installed within the underblanket and sand core. Data was intended to be collected during the winters of 1988/89 and 1989/90, but was not analysed during the course of this project.

Few new breakwaters have been constructed in the UK recently. During the period of this project, one such was the Pickie breakwater at Bangor, County Down. This breakwater completes the protection of the harbour at Bangor. Both breakwaters are armoured with hollow cube Shed units laid in a single layer to a regular pattern. Following close contacts between HR and the designers of the new breakwaters, Kirk, McClure & Morton (KMM), it was agreed that field instruments could be deployed to measure pressures and water levels within this breakwater. Travel distances from Wallingford to Bangor could have restricted the operation of these instruments, but assistance in deploying the equipment was offered by Dr Trevor Whittaker of Queen's University of Belfast (QUB).

4.2 Development of instrumentation

Instrument design

The major area of interest in this part of the project was the transmission of wave pressures through the outer layers of the armoured slope to the core. It will be seen in Chapter 5 that this area is least well represented by the numerical models available, and remains one of the main areas of uncertainty.

At a point within the breakwater, the total pressure P_{total} may be given as the sum of the hydrostatic part P_{stat}, given by the height of the phreatic surface, and the hydrodynamic part P_{dyn}, due to flow velocities and accelerations. A pressure cell in the mound will measure P_{total}, whilst a level gauge in a tubewell will measure only the hydrostatic element, P_{stat}. Both measurements are needed to identify the contribution of the hydrodynamic part, P_{dyn}, to the internal flow field. Two devices were therefore needed at each point of interest to measure P_{total} and P_{stat}.

It would have been ideal if it had been possible to plan the installation of measurement equipment during the design of the breakwater. This would then have

allowed the installation of each measurement device to be carefully planned for the correct phase of construction. The timescale for the research project did not allow this. At a late stage in the construction of the breakwater six large perforated tubewells were installed in Pickie breakwater, see Figure 4.1. These were formed from 0.3m diameter plastic pipe, perforated by frequent saw cuts of about 6 mm by 80 mm. Each pipe was installed down to around lowest astronomical tide, -2.0m Ordnance Datum Belfast (ODB). Four pipes were installed in the front face seaward of the breakwater crown wall, termed wells A to D. Well E was installed through the crown wall slab against the parapet wall upstand, and well F at the crest of the rear armour.

Careful consideration was given to the use of these wells. A numerical model of flow within a porous mound was used to explore possible conditions within the breakwater (Ref 19). Example results are shown in Figure 4.2. During consideration of these results, it became clear that the large wells would probably provide a preferential flow path within the breakwater. All dynamic components of the internal flows would therefore be lost in driving water up or down the well.

A variety of ways of overcoming this problem were considered. Initially the preferred solution used a measurement staff lowered into each well. The staff would be equiped with inflatable pipe stoppers to inhibit flow up and down the well, thereby constraining flow into the porous core itself. The staff was intended to be formed from lengths of galvanised steel conduit, with the instrument cables passing up the pipes. On deployment the sections of conduit would be screwed together, and the device lowered into the measurement well. This solution was rather complex, and would have been very difficult to operate on the breakwater in storm conditions.

The solution adopted required the installation of much smaller diameter spiral wound steel tubewells within the plastic pipes, and backfilling the annular space with 20-50 mm aggregate. This reduced significantly the preferential flow path. A composite pressure and level measuring device was then lowered on cables down the inner tubewell. The pressure sensor used was a PSM borehole level transmitter, series 700. The pressure transmitter was coupled with a capacitance water level gauge produced at HR. The cables for the pressure transmitter and the capacitance water level gauge were held together at frequent intervals by small cable ties. A lead weight was attached to the lower end of each pair of devices to ensure that the

water level gauge was straight and vertical within the tubewell.

Equipment testing

Three measurement systems were assembled and tested at HR for linearity and calibration, and responded well for wave periods down to 3.5 seconds. It was however noted that the responses of the pressure transducers were not linear below about 3.5 seconds. Simple calibration graphs are suggested in Figure 4.3 for the 3 transducers. The three measurement systems were then shipped out to QUB for further testing, and deployment at Bangor.

The equipment was first used in a trial in March 1990. Staff from HR, QUB, and KMM assisted in the deployment. The measurement systems were connected to an Omnibus 286 PC via a National Instrumentation A/D data aquisition board, model ATMIO 16 AL. Lotus Measure was used to acquire the signals and write data files to Lotus 123, allowing simple scaling and plotting of results. Each set of transducers were checked. After some initial problems with zero levels which were overcome, sample results were logged for each set, see Figure 4.4.

Wave action during the trial was insignificant, and the tide was low when other problems had been resolved, so wave action was simulated by moving the instruments up and down in the wells. The equipment was then recovered and returned to Belfast. Setting up the equipment had taken around an hour, so it was concluded that it constituted a practical system.

4.3 Discussion

It was agreed with QUB that they would monitor the weather forecast for Belfast loch and the area seawards. Bangor harbour is only exposed to large waves from the north-east, so it was not expected that storms other than those from north to east would be of any interest. Deployment of the measurement device was therefore limited to periods of strong winds from that sector. Unusually this event only occured for a single period, less than 12 hours, between March 1990 and February 1991. At the time the QUB team were fully committed to similar work contracted by the Department of Energy on the Islay wave power device. No useful field data was therefore captured at Bangor before completion of these studies. The equipment remains available, and could gather useful data in a relatively short deployment.

5 NUMERICAL MODELLING OF WAVE ACTION

5.1 Study design

The main numerical modelling problem involves the action of waves on the outside of a permeable breakwater and subsequent movement of water through the core. Of importance is the degree of wave transmission through the breakwater and the amount of reflection. In order to make assessments of the geotechnical stability of the breakwater we also need to know the flow rates and subsequent pore water pressures within the structure.

The problem breaks down into two parts:

i) How does the wave behave on the outside of the breakwater?

ii) Given the external water pressures from (i), how does the water within the breakwater behave?

Models involving waves on impermeable surfaces already exist. The problem however is significantly more difficult for those cases in which the surface is permeable. In order to solve the equations that describe the behaviour of the wave, certain boundary conditions are required. For impermeable surfaces this presents few problems as we know that the water velocities through these surfaces must be zero. However the motion of water through the permeable surface of the breakwater makes the conditions more difficult to specify.

Once the external conditions acting upon the breakwater are given, it is possible if time consuming to describe the behaviour of the water within it. Here the problem is not so much to do with the calculation of the flow pattern, as determining the permeability of the breakwater material. Much work has been carried out in this area, including experiments described in Chapter 3.

Existing models

Initially, three models developed elsewhere were studied, and are described briefly to illustrate the problems involved. All the models require certain assumptions or approximations, such as long waves lengths or rectangular geometry of the breakwater. Whilst these models are of use in some instances, the limitations arising from these approximations should be well understood.

Madsen & White

This is a program developed by Madsen and co-authors (Refs 20-21) following work carried out over a number of years, involving calculations and measurement of the wave energy dissipated in wave run up and wave action within the core. Initial analytical models involved approximating trapezoidal breakwaters to a "hydraulically equivalent" rectangular breakwater.

The final model breaks up the problem into the domains shown in Figure 5.1. The equations that govern the motion in these regions are the continuity equation for incompressible flow,

$$\frac{\partial \eta}{\partial t} + \frac{\partial (h_1 u_1)}{\partial x} + \frac{\partial (h_2 u_2)}{\partial x} = 0 \qquad (5.1)$$

where h_1, h_2 and u_1, u_2 refer to the depths and discharge velocities respectively
and η is the free surface elevation

and the momentum balance equation.

$$\frac{\partial u_1}{\partial t} + \frac{g \partial \eta}{\partial x} + \frac{\tau_b}{\rho h_1} = 0$$

in which g is the acceleration due to gravity,
ρ is the fluid density,
and τ_b the bottom shear stress.

General solutions can be found to these equations of motion in each domain. The reflection and transmission coefficients at each interface and the energies dissipated in each region must be supplied. The only remaining boundary conditions required may be obtained by matching conditions at the boundaries between regions. The coefficients can be evaluated by assuming a linearized form for all frictional effects. Initally values for the linearized friction factors are estimated and then recalculated from the resulting flow. The process is iterated until the solution converges, which in most cases requires five or six iterations.

The full solutions are finally provided by use of the matching conditions at the boundaries of the sections. These conditions are those of the free surface elevation and the discharge at these points.

Along with the approximations that must be made to find the energy dissipation during run up, inherent within the model are the assumptions that the waves are linear, of long wave length and small amplitude.

The model was tested against a series of experiments made at MIT (Ref 21). These experiments found that the model produces good results for the important transmission coefficient, but a poorer match for the reflection coefficient. The predicted reflection coefficient was below that obtain empirically, with the discrepancy increasing with decreasing front slope.

Despite the limitations outlined above, the Madsen & White model has proved to be of use. At Hydraulics Research it has been used to estimate the wave transmission coefficients of the new breakwater at Peterhead. (Ref 22).

Sollitt & Cross.

Sollitt & Cross (Ref 23) developed a model that is almost totally analytical. To do this they used several sweeping approximations, but the introduction of compensatory factors does go some way to correcting for the errors.

They start from the usual incompressible equations of fluid motion.

$$\frac{\partial U}{\partial t} = -\frac{1}{\rho}\nabla(\rho + \gamma Z) + \text{resistance forces} \qquad (5.3)$$

$$\nabla u = 0 \qquad (5.4)$$

The difficult term here is the non-linear resistance term. The steady state resistance term developed by Ward (Ref 24) is introduced, along with a term for the additional inertial damping involved with unsteady flows.

A problem now arises due to the non-linear form of the resistance term, this must be linearised to solve this set of equations. This is done by invoking Lorentz's principal that the total amount of energy dissipated must be the same however the damping is expressed. This results in a complicated but easily calculated term for the linearised friction factor F_R. However in the resulting form f is now a function of the local discharge q and an iterative technique involving successive estimates of f are required.

The irrotational nature of the flow field allows the equations to be expressed in terms of a velocity potential. Boundary conditions at the sea bed and the free surface are now specified. The sea bed is assumed impermeable, while the surface is assumed to be at atmospheric pressure. Here the assumption of

low amplitude waves is made by approximating the surface to be at a constant height.

The resulting velocity potential may then be found as the summation of a series of Eigen functions and the resulting unknown coefficients are provided from boundary conditions at the breakwater/sea interface. It has been found that only the first five terms of the Eigen series are required to give a better than 95% convergence.

One of the more serious limitations of this model is that the fitting of the boundary conditions across the breakwater/sea interface require that the breakwater faces are vertical. In order to deal with trapezoidal breakwaters, adjustments are made to the resistance factor in equation 5.3 to account for the effects such as energy dissipation during wave run up.

The resulting model predicts the correct behaviour for the reflection and transmission coefficients, with varying wave length. The transmission coefficient decreases with decreasing wave length, breakwater porosity and permeability, and increasing wave height and breakwater width. The reflection coefficient decreases with decreasing breakwater width and wave length, and increasing porosity and permeability.

The model has a tendency to over estimate the transmission coefficient and under estimate the reflection coefficient. Some of these errors may be due to the difficulty in determining a suitable value for the virtual mass coefficients, needed in the determination of the permeability for unsteady flows. There are also problems involved with the estimates of energy losses due to wave run up when dealing with trapezoidal breakwaters.

Nasser & McCorquodale

The model developed by Nasser & McCorquodale (Ref 25) is again analytical in its approach. The starting point is the equations of flow developed by Nasser (Ref 26)

$$\begin{bmatrix} \frac{h_o + \eta_n}{n} & 0 & \frac{U_n}{n} & 1 \\ \frac{U_n}{n} & 1 & gn & 0 \\ dx & dt & 0 & 0 \\ 0 & 0 & dx & dt \end{bmatrix} \begin{bmatrix} \frac{\partial U_n}{\partial x} \\ \frac{\partial U_n}{\partial t} \\ \frac{\partial \eta_n}{\partial x} \\ \frac{\partial \eta_n}{\partial t} \end{bmatrix} = \begin{bmatrix} 0 \\ -g\, n\, F_R U_n \\ dU_n \\ d\eta_n \end{bmatrix} \quad 5)$$

in which η_n = the perturbation of the free surface with respect to the still water level.
U_n = depth averaged horizontal velocity (bulk velocity)
h_o = mean water level;
n = porosity
and F_R = non-linear friction term

The first two rows of the system are the continuity and momentum equations. The third and fourth rows represent the total differentials of the dependant variables, h_n and η_n.

The resistance term is given by the Forchheimer equation for non-Darcy flow in a porous medium,

$$F_R = a + b\,|q| \qquad (5.6)$$

where the coefficients a and b must be derived empirically, see chapter 3.

The method of characteristics is used to partly solve the equations and then a finite difference method is used to complete the solution. The model was developed for breakwaters with an impermeable boundary, thus one boundary condition is supplied by the condition of no horizontal flow at this boundary. A second boundary condition is given by the flow from the incident wave.

In this way the phreatic surface within the breakwater can be calculated as waves act upon the outside face. As in the Sollitt & Cross model, only true solutions are found for rectangular breakwaters. Approximations must be made for the effects of wave run up onto the sloping face of a trapezoidal breakwater. To model the flow through entirely permeable breakwaters would require some modifications to the form of the relevant boundary condition. This model does have the

advantage over the Sollitt & Cross model in that it does not make the small wave amplitude approximation.

Since this model at present can only deal with breakwaters with an impermeable boundary, direct comparisons with the Madsen & White and the Sollitt & Cross models are not possible. Some physical modelling for comparison with this model was carried out by Nasser & McCorquodale (Ref 25). They report that the observed values for the transmission factor within the breakwater correspond to those of the numerical model to within about 15%.

To model the action of wave run up on the seaward face of the breakwater a program called BEMTOOL by Shih (Ref 27) has been further developed. BEMTOOL uses a boundary element method to model both the run up and breaking of waves upon a sloping surface. In its existing form BEMTOOL only works for impermeable slopes, so some modification will be necessary for its use with permeable breakwaters. BEMTOOL is described more fully below.

The flow of water within the breakwater may be modelled by use of the program BWATER. BWATER utilises a finite difference method to model water flow through porous media.

5.2 Wave action on the mound

BEMTOOL

Introduction

BEMTOOL uses a Boundary Element Method to solve a class of two-dimensional time varying flow problems. In the breakwater models described above, the waves are assumed to be of long wave length and any effect of wave breaking must be added to the model as an amendment to the energy dissipation terms. Such approximations allow the problem to be tackled as either steady-state or quasi steady-state. To understand fully the dynamics of the problem we require a model that includes the full behaviour of waves as they run up on to the sloping face of the breakwater.

For low amplitude long wavelength waves the problem is not so difficult as the relevant equations of motion are linear in form. This results in periodic waves and the system may be solved by separating the time domain from the spatial part of the problem. However such systems are of limited relevance if we wish to study a breakwater under realistic conditions.

For large amplitude waves the equations of motion become highly non-linear and as a result the waves are non-periodic. This makes the separation of the time variable impossible. BEMTOOL can be used to solve such non-linear systems and hence provide the external conditions which act upon the breakwater.

Mathematical Method

The flow region to be solved by BEMTOOL is shown in Figure 5.2. The right hand boundary could be an impermeable slope. The left hand boundary is given by the incoming waves (or the paddle of a wave machine).

The basis of the method, and the source of its efficiency, is that it only needs to compute values of the flow variable around the boundary and not throughout the flow region. It is possible to do this by use of Cauchy's integral. This relates the values of a function within a specified region R, to an integral around the boundary C of that region. In order to do this the two-dimensional field of the flow problem becomes the mathematical complex plane. Now a position within the flow field is described by the complex variable $z = x + yi$.

Cauchy's integral is:

$$f(z) = \frac{1}{2\pi i} \int_C \frac{f(z_k)}{z_k - z} \, dz \qquad (5.7)$$

where $f(z)$ is the function,
z is any point within the region,
and z_k is any point on the boundary.
(Note that $f(z)$ must be analytical at all points within the region R).

Taking the flow to be incompressible,

$$\nabla u = 0 \qquad (5.8)$$

and with the flow irrotational, the flow field can be described either by the velocity potential ϕ or by the stream function ψ.

$$\nabla^2 \phi = 0 \qquad (5.9)$$

For numerical purposes the boundaries are represented by discrete points at which the flow variables are to be computed (see Figure 5.2). The computation is carried out in time steps from an initial starting condition. The points on the free surface move with the flow (Lagrange points) so that the kinematic surface condition is automatically satisfied. The

solid boundaries are either impermeable so that ψ is constant, or as with a wave maker have a known normal flow distribution through them, thus fixing ψ as a known function. On the free surface ϕ is known from the previous time step.

The discrete version of Cauchy's integral gives a set of linear equations whose solution provides the unknown values of ψ and ϕ. Knowing these, the velocity can be computed at the free surface enabling the surface points to be advanced at the next time step. The dynamic boundary condition at the free surface is given by Bernoulli's equation and thus enables the surface values of ϕ to be advanced for the next time step. Hence starting with known flow conditions at the boundaries the whole evolution of the flow and of the free surface can be computed in a series of time steps.

Boundary Conditions

One of the more important aspects of any boundary element program is its versatility to handle a range of boundary conditions. It is the boundary conditions that define the problem to be solved. The wider the range of conditions that can be applied then the wider the range of problems that may be solved.

The boundary conditions that are presently available within BEMTOOL are outlined below.

a) Free surface boundary

The free surface boundary is governed by Bernoulli's equation along which the values of ϕ are determined by using a Hamming's fourth order predictor-corrector method.

The initial elevation and kinematic properties along the free surface can be defined freely. In most of the cases, it is defined either as still and flat or in a form of wave which has its kinematic properties evaluated by using an existing analytical solution.

Nodal points are distributed such that the separations between adjacent nodal points decrease as the nodal points are further away from the mid point of the control volume (see Fig 5.3). As a result, higher nodal point concentration is obtained at locations near to the LHS and RHS boundaries. This arrangement is considered to be necessary to ensure that wave generation and runup at the LHS and RHS boundaries are smooth.

b) Left hand side (LHS) boundary

Nodal points are evenly distributed along this boundary. Three different conditions are allowed.

i) Lateral periodicity

This is equivalent to saying that whatever moves out from the right boundary (RHS) will move into the LHS boundary. To do so, the LHS and RHS boundaries should consist of same number of nodal points distributed at same vertical levels. For the corresponding pair of nodal points along these boundaries, they should have the same ϕ and ψ values. This reduces the total number of unknowns along these boundaries by half. In addition, the value of $\phi(1)$ $(=\phi(NF))$ can be defined from the free surface boundary condition. As a result, the matrix to be solved has a size of (N3-1)*(N3-1). For definitions of NF and N3, see Fig 5.2.

ii) Vertical wall (ie., no flow condition)

No flow condition is achieved by assuming that the values of ψ along this boundary are the same and constant. In BEMTOOL, these values are set to zero.

iii) Wavemaker

In shallow water region where $k_w h < \pi/10$, a simple theory for the generation of waves by wavemakers was proposed by Galvin (Ref 28), who reasoned that the water displaced by the wavemaker should be equal to the crest volume of the propagating wave form. For a piston wavemaker with a stroke S which is constant over a depth h (Fig.5.4a), the volume of water displaced over a whole stroke is Sh. The volume of water in a wave crest is $\int_L^{\frac{H}{2}} \sin kx\,dx = H/k_w$. Equating the two volumes,

$$\frac{H}{s} = k_w h$$

For transitional and deep water regions, the wave height to stroke ratio versus relative depth ($k_w h$) for a piston wavemaker can be found in Figure 5.4b.

By using the above theoretical approach, better control over the properties of the numerically generated waves can be obtained.

Numerical formulation of the wavemaker is achieved by defining ψ values along it so that $\psi = u(y+h)$ where u, y and h are the horizontal velocity of the wavemaker,

the y coordinate of the nodal point and the water depth respectively. To improve the wave generation, nodal point NF is assumed to lie on both the wavemaker and the free surface. This is achieved by evaluating values of ψ(NF) and ϕ(NF) according to the motion of the wavemaker and the free surface respectively.

c) Bottom boundary

The bottom boundary can adopt any geometrical shape. The shape is defined by the locations at which changes in geometry occur and the number of points inserted in between the changes. No flow condition is applied along this boundary. This is achieved by assuming that the values of ψ along this boundary to be equal to zero. Topographies such as step, hump and semicircle can all be included easily.

d) Right hand side (RHS) boundary

Nodal points are evenly distributed along this boundary.

i) Lateral periodicity
It is same as that for LHS boundary.

ii) Vertical wall (ie., no flow condition)
It is same as that for LHS boundary.

iii) Slope
In the case of a slope, the intersecting location of the tip of the run up/down wave and the slope is first determined by using linear extrapolation based on nodal points 4 and 3 (Fig 5.5). Once the intersecting point is located, this is assumed to be the location for nodal point 1. Nodal point 2 is then determined by linear interpolation between nodal points 1 and 3.

It may be noted that at present the right hand boundary condition of BEMTOOL must be impermeable and thus unsuitable for calculating the run up onto rubble mound breakwaters. However, it should soon be possible to link BEMTOOL to a program to calculate the flow within the rubble mound breakwater and thus provide the required right hand boundary condition.

Applications of BEMTOOL.

BEMTOOL has been run at HR for a number of boundary conditions. Below are given some examples of these conditions and the resulting wave forms.

(1)
Description : Simulation of shallow water up to breaking (Fig 5.6)

```
Time step = 0.005 s
NF, N1, N2, N3 = 60, 70, 80, 89
Water depth = 0.15 m
Length of channel = 1.0 m (= wavelength)
Boundary conditions :
Free surface : Properties at location x,
               Elevation, y = 0.5*wh*cos(2.0*pi*x/wl)
                          ψ = 9.81*wh*sinh(wk*(y+wd))*cos(wk*x)/
                               (2.0*ww*cosh(wk*wd))
                          ϕ = 9.81*wh*cosh(wk*(y+wd))*sin(wk*x)/
                               (2.0*ww*cosh(wk*wd))
                          u = pi*wh*(ww*0.5/pi)*cosh(2.0*pi*(y+wd)/wl)*
                              cos(2.0*pi*x/wl)/sinh(2.0*pi*wd/wl)
                          v = pi*wh*(ww*0.5/pi)*sinh(2.0*pi*(y+wd)/wl)*
                              sin(2.0*pi*x/wl)/sinh(2.0*pi*wd/wl)
               where wh = 0.15 m
                     wl = 0.15 m
                     pi = 3.141592654
                     wk = 2*pi/wl
                     ww = 3.14
                     wd = 0.15 m
LHS            : Periodicity
Bottom         : Flat and impermeable
RHS            : Periodicity

(2)
Description : Simulation of deep water up to breaking (Fig 5.7)
Time step = 0.005 s
NF, N1, N2, N3 = 60, 70, 80, 89
Water depth = 0.53 m
Length of channel = 1.0 m (= wavelength)
Boundary conditions :
Free surface : Properties at location x,
               Elevation, y = 0.5*wh*cos(2.0*pi*x/wl)
                          ψ = 9.81*wh*sinh(wk*(y+wd))*cos(wk*x)/
                               (2.0*ww*cosh(wk*wd))
                          ϕ = 9.81*wh*cosh(wk*(y+wd))*sin(wk*x)/
                              (2.0*ww*cosh(wk*wd))
                          u = pi*wh*(ww*0.5/pi)*cosh(2.0*pi*(y+wd)/wl)*
                              cos(2.0*pi*x/wl)/sinh(2.0*pi*wd/wl)
                          v = pi*wh*(ww*0.5/pi)*sinh(2.0*pi*(y+wd)/wl)*
                              sin(2.0*pi*x/wl)/sinh(2.0*pi*wd/wl)
               where wh = 0.15 m
                     wl = 0.15 m
                     pi = 3.141592654
                     wk = 2*pi/wl
                     ww = 3.14
                     wd = 0.53 m
LHS            : Periodicity
Bottom         : Flat and impermeable
RHS            : Periodicity

(3)
Description : Generation of a solitary wave and its runup on a vertical wall
(Figs 5.8a to 5.8d and Figs 5.9a to 5.9c)
```

```
Time step = 0.05 s
NF, N1, N2, N3 = 61, 65, 85, 90
Water depth = 1.0 m
Length of channel = 20.0 m
Boundary conditions :
Free surface : Initially flat and still
             : Distribution factor = 1.2
LHS          : Piston wavemaker to generate solitary wave
             : Horizontal velocity (u) at time (t),
               tstop=10. s
               For 0 < t < tstop
               u = -x0*ww*4.0/((exp(dum)+exp(-dum))**2)
               where dum=ww*(t-tc)
                     ww=1.574 /s
                     tc=1.6 s
                     x0=0.6 m
               For t > tstop, u = 0
Bottom       : Flat and impermeable
RHS          : Impermeable vertical wall

(4)
Description : Generation of a solitary wave and its runup on a slope
(Figs 5.10a and 5.10b)
Time step = 0.025 s
NF, N1, N2, N3 = 31, 35, 55, 60
Water depth = 1.0 m
Length of channel = 8.0 m (up to toe of slope)
Boundary conditions :
Free surface : Initially flat and still
             : Distribution factor = 1.0
LHS          : Piston wavemaker to generate sinusoidal waves
             : Horizontal velocity (u) at time (t),
               tstop=10. s
               For 0 < t < tstop
               u = -x0*ww*4.0/((exp(dum)+exp(-dum))**2)
               where dum=ww*(t-tc)
                     ww=3.1416 /s
                     tc=1.6 s
                     x0=0.4 m
               For t > tstop, u = 0
Bottom       : Flat and impermeable
RHS          : Impermeable slope at 30 degree
```

Conclusions

BEMTOOL is useful for the calculation of waves running up on to the slope of a breakwater. At the moment it is of limited use for our application in that it is unable to model a permeable boundary to correspond with the slope of the breakwater. However it should be possible to link BEMTOOL to a model of the flow through the porous medium of the breakwater and thus obtain the missing boundary condition.

It should be noted that the Lagrangian modelling of the free surface breaks down as the wave begins to break. BEMTOOL can only model the wave run up to the point of wave breaking. The processes involved in breaking waves are complex as the free surface ceases to be well defined and should be the subject of further study.

5.3 Flow modelling within the mound

Flow equations

The simplest equation which describes the flow through a pores media is given by Darcy's law.

$$i = ku \tag{5.10}$$

This describes a simple linear relation between the discharge through the medium and the hydraulic gradient present in the medium. Such a description works well for cases in which the flow is laminar, but begins to breakdown as the flow moves into the turbulent regimes.

There are many equations which attempt to describe the turbulent flow through pores media. One of the most commonly used is that of Forchheimer.

$$i = au + bu^2 \tag{5.11}$$

Here the coefficients a and b are in some way a measure of the permeability of the medium and must be determined experimentally. The determination of these coefficients turns out to be more complicated than might be thought at first sight, since such complexities as particle size and shape may have a significant effect. Chapter 3 describes experiments to determine these coefficients and gives an indication of the complexities involved.

Ideally any model of the water flow through the breakwater mound should be based upon the Forchheimer equation, or a similar expression that takes into account the non-linear behaviour of any part of the flow. In practice this is difficult to implement and may in many cases be unnecessary as the whole system may be within the laminar flow regime, or only small parts of the system may be flowing sufficiently quickly to be turbulent.

BWATER

BWATER is a computer program developed to model the flow through the core of the breakwater under wave

action. The model must be able to cope with the rapidly changing external conditions which occur when a wave runs up on the seaward face of the breakwater. Due to the difficulties involved in modelling such a dynamic system the governing flow equation is the linear Darcy equation described above.

BWATER uses a finite difference method in order to calculate the required flow pattern. The flow region is divided up into a number of grid points and the flow at the grid points are calculated at each time step. Beginning with an initial starting condition the flow at these points is recalculated using the flow and pressure gradients from the five surrounding points. Once this has been done then the phreatic surface and pressure gradients at the grid points may be adjusted. The process continues in a step wise manner, constantly adjusting the phreatic surface.

In most previous models the boundary conditions were held constant. One such case may involve the constant supply of water to the face of the flow region so that the subsequent flow may be modelled throughout the system. In our case the situation is not so simple, as waves run up on the outside of the breakwater the boundary condition at the seepage face is constantly changing. BWATER differs from most finite difference models in that it allows this boundary condition to change.

Application

BWATER was used to model the flow within Pickie breakwater, Bangor, County Down as described in section 4.2. Typical model results of BWATER are shown in Figures 4.2a-c.

5.5 Discussion, conclusions and recommendations

The use and performance models by Madsen & White, Sollitt & Cross, Thompson, and Nasser & McCorquodale were investigated at HR. Whilst these programs have some applications, the approximations involved in their formulation places restrictions on their use. The greatest restriction is generally that only

rectangular breakwaters may be fully modelled. Most of the models suggest correction terms to allow the modelling of trapezoidal breakwaters, but these are inadequate to model the full effects of wave run up on the seaward slope of the breakwater.

The program BEMTOOL is a useful model for predicting wave run up on the slope of the breakwater. However significant development work must be done to allow the boundary condition of the slope to be of a permeable nature.

BWATER is capable of modelling the flow through the breakwater, provided it is supplied with the necessary boundary conditions at the seepage surface. In principle this boundary condition could be provided by BEMTOOL. It is not possible to run each of the programs separately since the conditions at the seepage boundary are constantly changing. The programs must be fully integrated together so that they may pass information to each other at each time step.

A further refinement of the modelling of the water flow within the breakwater would involve the incorporation of a non-linear flow equation for the porous medium.

When it is possible to integrate models like BEMTOOL and BWATER, and the suggested improvements have been made to the models, all the significant processes involved will be incorporated. The only factors not covered will be the effects of wave breaking upon the slope and the effects of entrained air. Whilst these processes play a small part in the total system, they are very complex to model fully. A more practical approach may be to include these effects as correction factors in the final model.

6. GEOTECHNICAL STABILITY

The results of this research project are intended to improve methods of analysis and/or prediction of the stability of rubble mound breakwaters and related structures. This chapter deals with aspects of the geotechnical stability of such structures.

Rubble mound breakwaters are themselves naturally stable under static conditions, but may fail when wave action increases the applied loads, and/or reduces the mound strength by increasing pore pressures. Geotechnical failures may also be precipitated by foundation failures, but this aspect is not dealt with explicitly in this project. Internal settlement is common with other mounds, and does not need to be

covered in this study. The two main failure modes considered here are:

(a) slip failure of the mound slope(s);
(b) internal erosion of core and/or underlayers.

6.1 Slope stability methods

The primary failure mode considered in geotechnical work is the slip failure. Many papers and textbooks describe methods of analysis for slip failures (eg Ref 29). Most methods are intended for material that is at least partially cohesive. Some methods are designed only for material that is fully cohesive, $\phi' = 0$. Rockfill is however usually taken as non-cohesive, $c' = 0$, although Simm & Hedges included an apparent cohesion to describe the interlock strength of the armour layer (Ref 30). Slope stability analysis methods are usually based on a static case with constant pore pressures. Methods described by Bromhead (Ref 29) include:

(a) Swedish slip circle, Fellenius' method;
(b) Bishop's simplified method;
(c) Spencer's method;
(d) Janbu's method of slices;
(e) Morgenstern & Price's procedure.

Methods derived principally for rock fill have been considered by Fung (Ref 31). These are also generally based on 2-dimensional continua models, despite the much greater relative particle size. Fung notes that recent research on the stability of rockfill structures has addressed them as 3-dimensional discontinuous media, but that this remains a research approach only.

Stability charts have been derived from Fellenius' and Bishop's methods for drained rockfill. Examples are given by Charles & Soares (Ref 32). These charts are however of relatively limited application. It is important that the variation of pore pressures within the mound, as calculated using methods outlined in Chapter 5, can be included. Many of these more complex analysis methods are now available in commercial computer software packages. An example package was made available to Hydraulics Research by Ove Arup Partnership through their computer software division, OASYS Ltd. Some simple trials were conducted with the SLOPE program from the GEO suite of programs.

6.2 Oasys programs

The version of SLOPE supplied by OASYS was intended to be run on an IBM compatible personal computer (PC). The program is divided into two parts. The first part handles input and output of data and results. The second part handles the slope stability calculations. The complete program contains over 10,000 lines in Fortran, and has a size on the PC of 3.5Mbyte. For development at HR the core elements of the program were transferred onto HR's networked SUN system, on which the wave programs BEMTOOL and BWATER were run.

The program is able to calculate slope stability using three alternative methods, based on:

(a) Swedish slip circle, Fellenius' method;
(b) Bishop's simplified method;
(c) Janbu's method of slices.

The section to be analysed is described by a series of soil strata defined on a co-ordinate grid. Pore pressures can be included as a simple hydrostatic pore pressure distribution beneath a phreatic surface, or by a "piezometric" pore pressure distribution. Both submerged or partially submerged slopes can be analysed. External forces can be included, such as wave loads on crown wall elements (see Ref 33), or down-rush shear forces acting on the armour (see Ref 34).

More complete details of the original programs are available in the program manual supplied by OASYS.

6.3 Initial tests

Three different cases were studied. The first two were example cases from the OASYS manual. These gave results in agreement with the original program. The third test used pore pressures calculated using Thompson's original program (Ref 19). A "model" breakwater configuration was simulated by a simple slope. Factors of safety were calculated by the slope stability program using pore pressures after every 50 time steps. Example results are shown in Figure 6.1. This test was run using the full pore pressures calculated by the wave model, and using the hydrostatic element only. Factors of safety calculated in the latter case were significantly greater than when the full hydrodynamic pressure was used.

6.4 Internal stability and suffusion

Internal stability of the core of a breakwater is of considerable importance to the overall stability. Material forming the core is often extracted from the quarry substantially "as blasted". The grading curve may therefore be wide, or even gap-graded. Under steady or non-steady flows, many wide graded mixtures can become unstable. The finer fractions may be sufficiently small, and/or the hydraulic forces sufficiently great, to allow fine material to pass through the pores formed by the coarse material. This process may occur without initially changing the structural properties of the primary fabric, and is often termed suffusion (Ref 35). The stability of such a mixture will depend on the geometric restrictions given by the grading curve, and by the hydraulic forces, generally given by the hydraulic gradient.

6.4.1 Prediction methods

Considering the geometric condition alone, Kovacs Ref 35) gives three conditions described simply by values of Hazen's uniformity coefficient, $U_c = D_{60} / D_{10}$:

No suffusion	$U_c < 10$
Transition	$10 \leqslant U_c \leqslant 20$
Probable suffusion	$20 < U_c$

This approach is highly simplistic, and does not represent well the situation considered here. A more complex approach is suggested, based on the work of Kenney & Lau (Ref 36), as extended by den Adel et al (Ref 37). This method assesses the differential gradient of the grading curve to produce an F-H diagram, based on the work of Lubochkov. The gradient of the size grading is calculated over a size ratio of 4. The F-H diagram is plotted over the range of sizes, D, in the grading for values of F, the fraction smaller than D, and H, the fraction with sizes between D and 4D. Low values of H indicate possible instability. Kenney argues that the limits of stability for the mixture are given by:

Stable	$H > 1.3F$
Semi-stable	$1.3F \geqslant H \geqslant 0.6F$
Unstable	$0.6F \geqslant H$

Kenney & Lau did not address in detail the hydraulic conditions at which suffusion can start. Den Adel et al (Ref 37) have extended this analysis using data on the onset of movement of fine material derived in

filter box tests. They suggest a tentative relationship between a minimum value derived from the F-H curve, $(H/F)_{min}$ and the critical hydraulic gradient for the onset of suffusion, i_{cr}:

$$i_{cr} = 0.5\ (H/F)_{min}$$

This may be illustrated by an example. The methods above were used in the Alderney breakwater project (Ref 34) to estimate the likely performance of composite gradings derived for the breakwater mound. Example F-H curves are given for gradings B1 and E1 in Figure 6.3. The grading curves themselves are shown in Figure 6.2. Grading B1 gives a F-H curve which lies well above the unstable zone, but E1 shows a clear minimum at F = 0.12. At this point $(H/F)_{min} = 0.12$, giving a suggested critical hydraulic gradient around 0.06. This gradient is less than had been indicated by the numerical modelling of flows within the mound, which gave estimates of hydraulic gradients around 0.1 to 0.2.

It should be noted that the methods used to calculate these critical conditions were not well supported. During the studies for the Alderney project, it was decided to conduct tests in a large laboratory permeameter, 0.6m diameter, to measure flow conditions at the onset of suffusion. This permeameter has been described in Chapter 3 of this report.

6.4.2 Steady state tests on internal stability

The size of the permeameter required that the larger sizes in the sample be restricted. The flow conditions would not be correct if all sizes above a given limit, say 0.25 of the permeameter diameter, D = 0.15m, were simply removed. The target grading, E1, was therefore steepened over the size range 0.08 - 0.15m to give E11, whilst keeping the lower part of the grading coincident with E1 (Fig 6.2). This grading was then tested for stability using the procedure outlined above to ensure that this adjustment to the grading would not of itself introduce an error. The F-H diagram was re-calculated for E11, and is also shown in Figure 6.3. The minimum of the diagram was not influenced by the change to the grading, suggesting that tests on grading E11 were valid for grading E1.

During the design of these experiments, it was argued that the influence of unsteady flows should also be explored. Previous work by de Graauw et al (Ref 38) had shown that unsteady flows could give more severe conditions. Two series of tests were therefore designed, using both steady and unsteady flows. In

each instance grading E11 was tested to identify the critical hydraulic gradient for suffusion.

The large permeameter described in Chapter 3 was used for the segregation studies. The test sample was restrained by braced perforated plates at top and bottom. The pressure drop between tappings 0.5m apart was recorded using a differential pressure transducer. The flow rate was measured using an electromagnetic flowmeter in the supply pipe to the permeameter. Outputs from both devices were logged onto a paper chart recorder.

Grading curve E11 was used for the testing (Fig 6.2). Material with effective diameters from 0.16mm to 6mm were produced from sharp sand. Materials from 6mm to 40mm were derived from crushed limestone used in previous tests. Materials from 40mm to 142mm were hand weighed rocks from stock. Materials from 142mm to 150mm were hand weighed rocks which were specially bought in for the study. All materials were washed before use.

Materials from 0.16mm to 40mm were well mixed in a large bucket, which was then hoisted up to the top of the permeameter. Materials from 40mm to 150mm were placed by hand in the permeameter in single or double layers, with the voids among the materials being filled with the 0.16mm to 40mm material. A vibrating poker was inserted to compact the materials to the lowest porosity achievable. The permeameter was filled in about ten layers to a porosity of 14%. The system was then filled with water. Considerable effort was required to get rid of the air in the tappings. Before conducting each test, the permeameter was run continuously at a low flow rate, around 0.5 l/s, for about two hours to remove any silt.

In the first test, the flow rate was increased gradually until suffusion took place. Both the pressure head drop (dh) and the flow rate (Q) were recorded on a paper chart recorder, and were then digitised. Three quantities were calculated based on the results: the hydraulic gradient,i; the superficial velocity, u; and the permeability, k, given by:

$$i = \frac{dh}{L_t}, \quad u = \frac{Q}{A}, \quad k = \frac{u}{i}$$

Results from the tests are summarised in Figure 6.4. Three stages were identified: stable; transition; and suffusion.

In the first stage, the sample remained stable for hydraulic gradients up to about i = 0.01, k = 10^{-4}m/s, and u = 10^{-6}m/s. At these flow rates it proved difficult to set and/or measure the flow accurately, and these values should not be regarded as correct to better than half an order of magnitude.

In the second stage, fine material started to wash out of the sample. During this test, the flow rate was increased from 10^{-6} to 10^{-3}m/s, and the permeability of the sample increased from 10^{-4}m/s to 2.5×10^{-2}m/s.

At higher flows the permeability of the sample was governed mainly by the sizes in the primary fabric, and remained at about 0.025 m/s.

A second test was conducted in 12 stages. The limiting hydraulic gradient for the onset of suffusion was between 0.03 and 0.04. Suffusion was rapid for steeper hydraulic gradients.

6.4.3 Un-steady tests on internal stability

Previous work in The Netherlands (Refs 37-38) had suggested that un-steady flows could cause instability at lower hydraulic gradients than steady flows. A brief set of tests were conducted with un-steady flows in the apparatus used above. For each test a period of oscillation of around 10 seconds was used. Three tests were run. The pressure loss and flow velocity were digitised as before, and example results are shown in Figure 6.5. Visual observations during testing, and inspection of the test results, suggested that the critical hydraulic gradient at which suffusion occurred was similar to that measured in the steady state tests. This agrees with work by Bezuijen et al (Ref 39) who tested the stability of filter layers under cyclic flows with a period around two seconds. Their results indicated that the critical filter velocity amplitude for cyclic flow was equal to the critical velocity for stationary flow.

6.5 Discussion, conclusions and recommendations

Two areas of mound stability have been addressed briefly in the course of this project: slope failure; and internal erosion. Simple analysis methods have been explored for each failure mode.

No laboratory work was conducted on slope stability, but well accepted slope stability calculation methods were used in conjunction with pore pressures derived by models covered in Chapter 5. The integration of

the models appeared to present no particular problems.

Internal erosion of a rubble mound was also studied. Prediction methods derived by Kenney & Lau, and den Adel et al, gave relatively good agreement with the results of a short series of suffusion tests in the large permeameter.

7. CONCLUSIONS AND RECOMMENDATIONS

7.1 Descriptions of permeability

A series of systematic tests have been run to quantify the permeability of narrow- and wide-graded rubble. These required the use of a large (0.6m diameter) laboratory permeameter.

It was intended that the flow conditions used in the tests would be typical of those found in rubble mound structures. Initial trials were run to identify the range of hydraulic gradients that should be used in permeameter testing. These wave flume tests suggested that hydraulic gradients in the underlayers and core of a rubble mound would seldom exceed i= 5 to 10.

Two series of permeameter tests were conducted using narrow- graded material, then wide- or gap-graded materials. Many relationships have been advanced to describe partially and fully turbulent flows in rubble material. Of these the most useful has generally proved to be Engelund's version of the Forchheimer equation. Data derived in this study has been compared with Engelund and den Adel's equations. Initial analysis suggested some new coefficients to be applied to Engelund's method to describe the influences of particle size and grading width. Further analysis suggested that these more complex equations were not fully justified, and simple engineering conclusions were drawn as to the appropriate values of the coefficients in Engelund's equations.

7.2 Numerical modelling of wave effects

This project was intended to develop only preliminary numerical models of wave/structure interactions. During the project the capabilities of 4 existing models were explored. A further 2 models were developed further during the study.

BEMTOOL may be used to calculate wave flows and pressures over an impermeable surface up to the point of wave breaking. The model was refined during the research project to the point where it was possible to use it in a site specific study to explore wave pressures and velocities over a large mound.

BWATER is capable of modelling the flows with a permeable mound, provided that the boundary conditions are known, and the permeability may be linearised. Again it was refined during this project to the state where it was possible to use it to give estimates of internal pressures in a sand-filled mound.

The limitations of the models available have been explored within
this project. The major weaknesses of all the models are in the descriptions of flows at and through the sloping surfaces of the structure. These are compounded by difficulties in describing internal flow conditions under non-linear and/or non-steady flows, the effects of entrained air in this zone, as well as inside the mound. Furthermore, none of the models developed to date can calculate beyond the point of wave breaking.

7.3 Geotechnical stability

Two areas of the geotechnical stability of rubble mound breakwaters and related structures have been addressed briefly in this project:

a) slip failure of the mound slope(s);
b) internal erosion of core and/or underlayers.

Slope stability analysis methods are usually based on a static case with constant pore pressures, and are intended for material that is at least partially cohesive. Methods derived for rock- fill have been described by Lee and Fung. These are generally based on 2-dimensional continua models, despite the relatively large particle sizes. In this study, trials were therefore conducted with existing slope stability calculation programs from the GEO suite by OASYS. Slope stability was calculated using three alternative methods, based on:

a) Swedish slip circle, Fellenius' method;
b) Bishop's simplified method;
c) Janbu's method of slices.

A "model" breakwater configuration was simulated. Factors of safety were calculated by the slope stability program using pore pressures calculated

after every 50 time steps using one of the models described in Chapter 5. This test was run using the full pore pressures calculated by the wave model, and using the hydrostatic element only. Factors of safety calculated in the latter case were significantly greater than when the full hydrodynamic pressure was used, confirming the need for a full description of internal pressures.

Internal stability of the core of a breakwater is of considerable importance to the overall stability. The stability of core and underlayers will depend on the geometric restrictions given by grading curves, and by the hydraulic forces, generally given by the hydraulic gradient. An approach to the calculation of internal stability has been suggested, based on the work of Kenney & Lau, Lubochkov and den Adel. The prediction method were not initially well supported, so a series of tests were conducted to measure conditions at the onset of suffusion. The prediction methods gave relatively good agreement with the test results.

8. ACKNOWLEDGEMENTS

The work reported here has been conducted principally by members of the Coastal Structures Section, assisted by other sections at Hydraulics Research. The permeameter tests were designed and initiated by RV Stephens, and conducted principally by AR Channell. The development of the numerical models and the field measurement equipment was by RWK Shih.

Hydraulics Research are grateful for the support of their collaborators in this research: Mr Lee, Mr Fung, Mr A Thompson, Dr I C Pyrah, and Dr W Anderson at the University of Sheffield; Dr T J T Whittaker and Mr A Thompson at Queen's University of Belfast; Professor H Peregrine and Mr R Tong at the University of Bristol; Dr ZC Sun and Mr HY Pan from Dalian University of Technology, China.

The support of Ove Arup Partnership and OASYS Ltd in the supply of computer software for slope stability calculation is gratefully acknowledged.

The support of the Technical Services Department of the States Board of Administration, States of Guernsey, in funding further development of models described here, and giving their permission to include results from studies conducted for them, is also gratefully acknowledged.

9. REFERENCES

1 Allsop NWH & Wood LA "Hydrogeotechnical performance of rubble mound breakwaters" Report SR 98, Hydraulics Research, Wallingford, March 1987

2 Allsop NWH "Concrete armour units for rubble mound breakwaters and sea walls" Report SR 100, Hydraulics Research, Wallingford, March 1988

3 Allsop NWH & Herbert DM "Single layer armour units for breakwaters" Report SR 259, Hydraulics Research, Wallingford, March 1991

4 Allsop NWH "Reflection performance of rock armoured slopes in random waves" proc 22nd ICCE, Delft, July 1990 (available as Hydraulics Research published paper no 37)

5 Adel H den. "Re-analysis of permeability measurements using Forchheimers equation". Report CO 272550/56, Delft Geotechnics, Delft, November 1987, (in Dutch).

6 Hall, K R. "A study of the stability of Rubble Mound Breakwaters". PhD Thesis, University of New South Wales, Australia, May 1987.

7 Dudgeon, C R. "Wall effects in permeameters". Proc ASCE Jo Hyd Div, HY5: 137-148. Paper No 5433. September 1967.

8 Dudgeon, C R. "An experimental study of the flow of water through coarse grandular media". L Houille Blanche No 7, 1966, pp 785-800.

9 Engelund, F. "On the laminar and turbulent flows of groundwater through homogenous sand". Trans Danish academy of technical sciences, Vo 3, 1953, No 3.

10 Gupta, R D. "Angularity of aggregate particles as a measure of their slope and hydraulic resistance". Proc Inst CW Engrs, Part 2, 1985, 79, December, pp 705-716.

11 Latham J-P, Mannion M B, Poole A B, Bradbury A P and Allsop N W H. "The influence of armour stone shape and roughness on the stability of breakwater armour layers". Coastal Eng Research Group, Queen Mary College, London, September 1988.

12 Shih, R W K. "Permeability Characteristics of Rubble Material - New Formula". Proc 22nd

ICCE, Delft, July 1990, available as HR Published Paper No 38 Hydraulics Research, Wallingford.

13 Hall, K R. "Aeration in Rubble-Mound Breakwater Models". Proc ASCE Jo Waterway, Port, Coastal, and Ocean Engineering, Vol 116, No 3, May/June 1990, page 400-405.

14 Hannoura, A A & McCorquodale J A. "Air-water flow in coarse Granular Media". Proc ASCE Jo Hydraulics Division, Vol 104, HY7, July 1978.

15 Barends, F B J. "Non-linearity in groundwater flow". Delft Soil Mech Lab LGM-Mededelingen, 21, No 1, April 1980.

16 Barends, F B J. "The compressibility of an air water mixture in a porous medium". Delft Soil Mech Lab LGM-Mededelingen, 20, No 2, August 1979.

17 Stephens RV "Notes on a visit to the Franzius Institute, Hannover, 30 September to 1 October 1987" Hydraulics Research, Wallingford, October 1987

18 van Damme L, Wens F & de St Aubain T "Outer harbour Zeebrugge: monitoring programme of the NW breakwater section" Proc 9th International Harbour Congress, KVIV, Antwerp, June 1989

19 Thompson AC "Numerical model of breakwater wave flows" Proc 21st ICCE, Malaga, June 1988

20 Madsen, O S, Shusang, P & Hanson S A. "Wave transmission through trapeziodal breakwaters." Proc 16th Coastal Engineering conference, 1978, Vol III, pp 2140-2152.

21 Madsen, O S & White A M. "Energy dissipation on a rough slope." Proc ASCE Jo Waterways, Harbours and Coastal Engineering, Vol 102, No WW1, 1976, pp 31-48.

22 Stephens, R V. "Peterhead South Bay Development Desk Study of proposed breakwater." Report EX 1752. Hydraulics Research, Wallingford, 1988.

23 Sollitt, C K, & Cross R H. "Wave transmission through permeable breakwaters." Proc 13th Coastal Engineering Conference, 1972.

24 Ward, J C. "Turbulent flow in pores media." Proc ASCE, Jo Hydraulics div, Vol 90, HY5.

25 Nasser, M S, & McCorquodale J A. "Wave Motion in Rockfill." Proc ASCE Jo Waterways, Harbours and Coastal Engineering, Vol 101, No WW2, 1975, pp 145-159.

26 Nasser, M A. "Theoretical and experimental analysis of wave motion in rock fill structures." PhD thesis, Univ Windsor, Windsor, Out.

27 Shih, R W K. "Wave induced uplift pressures acting on a horizontal platform." PhD thesis University of London, 1989.

28 Galvin, C J, Jr, "Wave height prediction for wave generators in shallow water". Tech Memo 4, US Army, Coastal Engineering Research Centre, March 1964

29 Bromhead EN "The stability of slopes" Surrey University Press, Blackie Group, London, 1988

30 Simm JD & Hedges TS "Pore pressure response and stability of rubble mound breakwaters" Proc Conf Breakwaters '88, ICE, Eastbourne, May 1988

31 Fung HW "Geotechnical stability of rockfill embankments and rubble mound breakwaters" MSc thesis, University of Sheffield, September 1989

32 Charles JA & Soares MM "Stability of compacted rockfill slopes" Geotechnique, Vol 34, 1984

33 Bradbury AP, Allsop NWH & Stephens RV "Hydraulic performance of breakwater crown walls" Report SR 146, Hydraulics Research, Wallingford, March 1988

34 Allsop NWH & Shih RWK "Alderney Breakwater: Phase 3, hydraulic model studies" Report EX 2231, Hydraulics Research, Wallingford, December 1990

35 Kovacs G "Seepage hydraulics" Developments in water science Volume 10, Elsevier, Amsterdam 1981

36 Kenney TC & Lau D "Internal stability of granular filters" Canadian Geotech Jo, Vol 22, 1985

37 den Adel H, Bakker KJ & Breteler MK "Internal stability of minestone" Modelling soil-water-structure interactions, SOWAS 88, Balkema, Rotterdam, 1988

38 de Graauw AF, van der Meulen T, & van der Does de Bye MR "Granular filters: design criteria"

Proc ASCE, Jo Waterway Port & Coastal Eng Div, Vol 110, February 1984

39 Bezuijen A, Klein Bretler M & Bakker KJ "Design criteria for placed block revetments and granular filters" Modelling soil-water-structure interaction, SOWAS 88, publ Balkema, Rotterdam, 1988

40 Allsop NWH & Shih RWK "Permeability of rubble mound coastal structures to wave action: laboratory and numerical modelling" Proc. 2nd nt. Symposium on Wave Research and Coastal Engineering, SFB 205, University of Hannover, October 1988

41 Lee KY "The engineering characteristics and behaviour of rockfill" MSc thesis, University of Sheffield, September 1988

42 Shih RWK "BEMTOOL A two-dimensional numerical program based on Boundary Element Method". Report IT 349, Hydraulics Research, Wallingford, November 1990.

Tables

TABLE 3.1 Summary of permeameter tests

Test Nos.	Material	Nominal Size (mm)	D_{15} (mm)	D_{50} (mm)	D_{85} (mm)
1-8	L"stone, single	4	1.49	2.13	2.76
9-13	" "	6	4.94	5.42	6.26
14-24	" "	10	7.22	8.65	9.74
25-29	" "	14	9.35	10.87	12.4
30-35	" "	20	12.72	14,65	17.39
36-44	" "	28	19.28	21.77	24.58
45-55	" "	40	27.61	33.23	37.77
56-59	" "	61	54.5	63.0	73.8
77-84	" "	6/10	5.1	6.7	9.2
85-92	" "	6/14	5.1	6.7	11.5
93-101	" "	6/20	5.1	6.7	15.6
102-107	" "	6/28	5.1	6.7	23.0
108-112	" "	6/40	5.1	6.7	35.5
113-119	" "	6/10/14/20/28/40	6.6	12.3	26.5
120-126	" "	4/6/10/14/20/28/40	4.8	10.8	25.0
127-131	" "	6/10/14/20/28/40/61	7.0	14.6	41.0
60.67	Shingle, Single	10	8.15	9.05	10.07
68-76	" ""	14	8.34	10.01	12.18

TABLE 3.2 Estimates of Engelund and den Adel coefficients from single size sample results

	D_{15} (mm)	Engelund α_o	Engelund β_o	den Adel C_o	den Adel C_7
Angular	4.9	1500	2.8	300	4.0
	7.2	1500	2.8	350	4.0
	9.4	1500	2.3	350	3.4
	12.7	1500	2.0	350	3.4
	19.3	~ 2000	2.0	~ 500	2.0
	27.6	~ 2000	1.8	~ 500	2.4
Rounded	8.2	1300	2.5	300	4.8
	8.3	1300	2.8	300	3.8

Figures

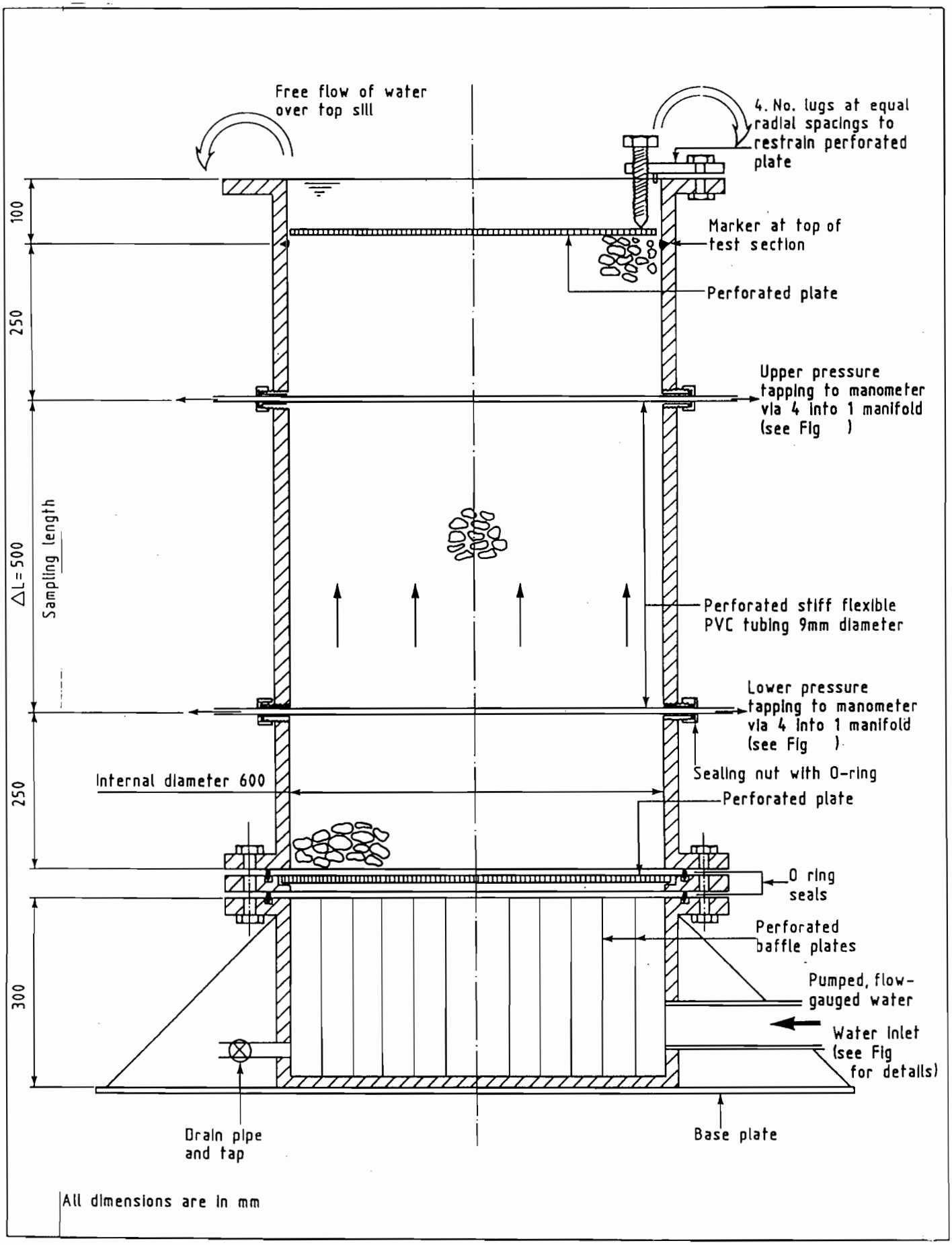

Fig 3.1 Schematic sectional view of permeameter.

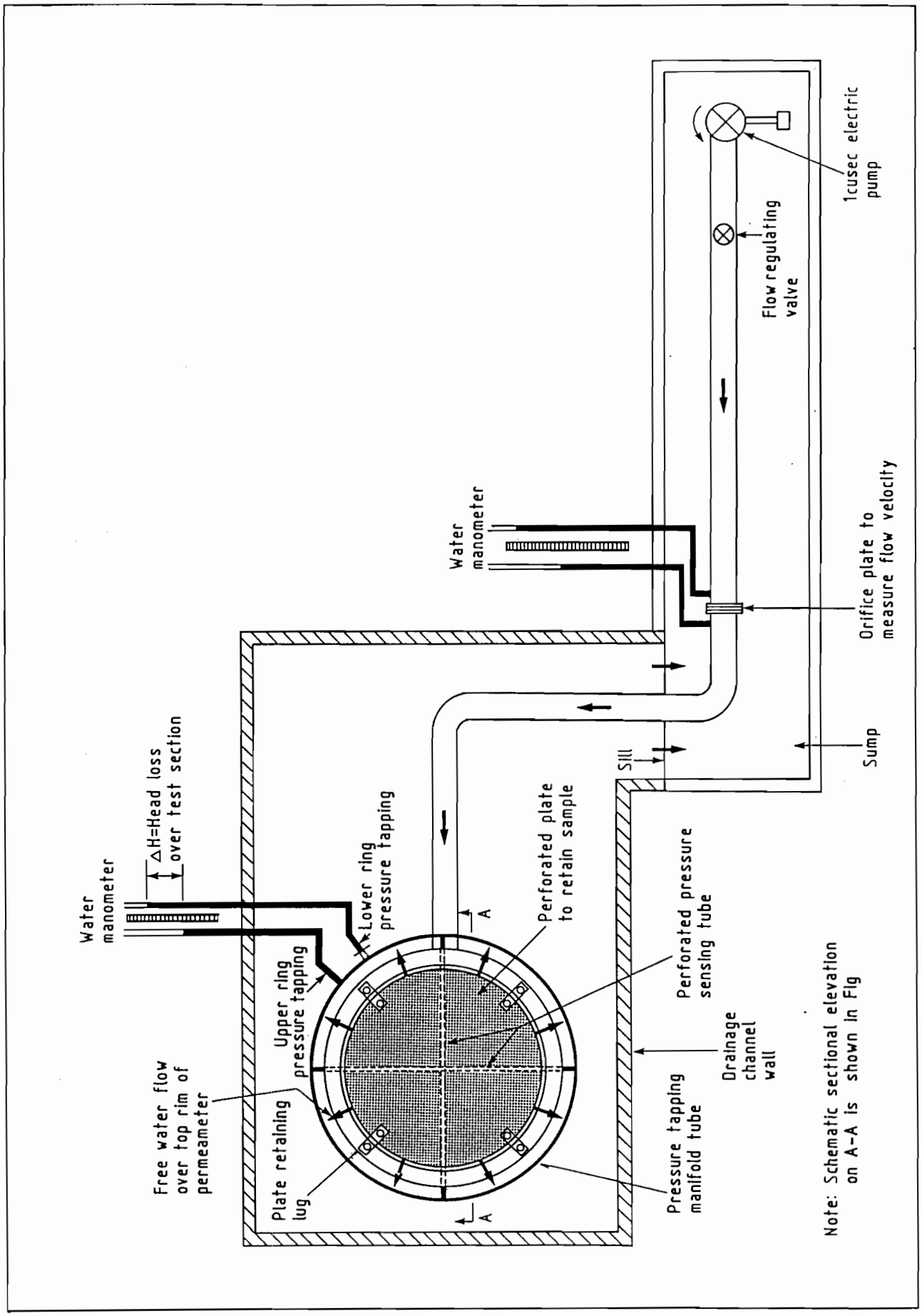

Fig 3.2 General layout of the measurement set-up.

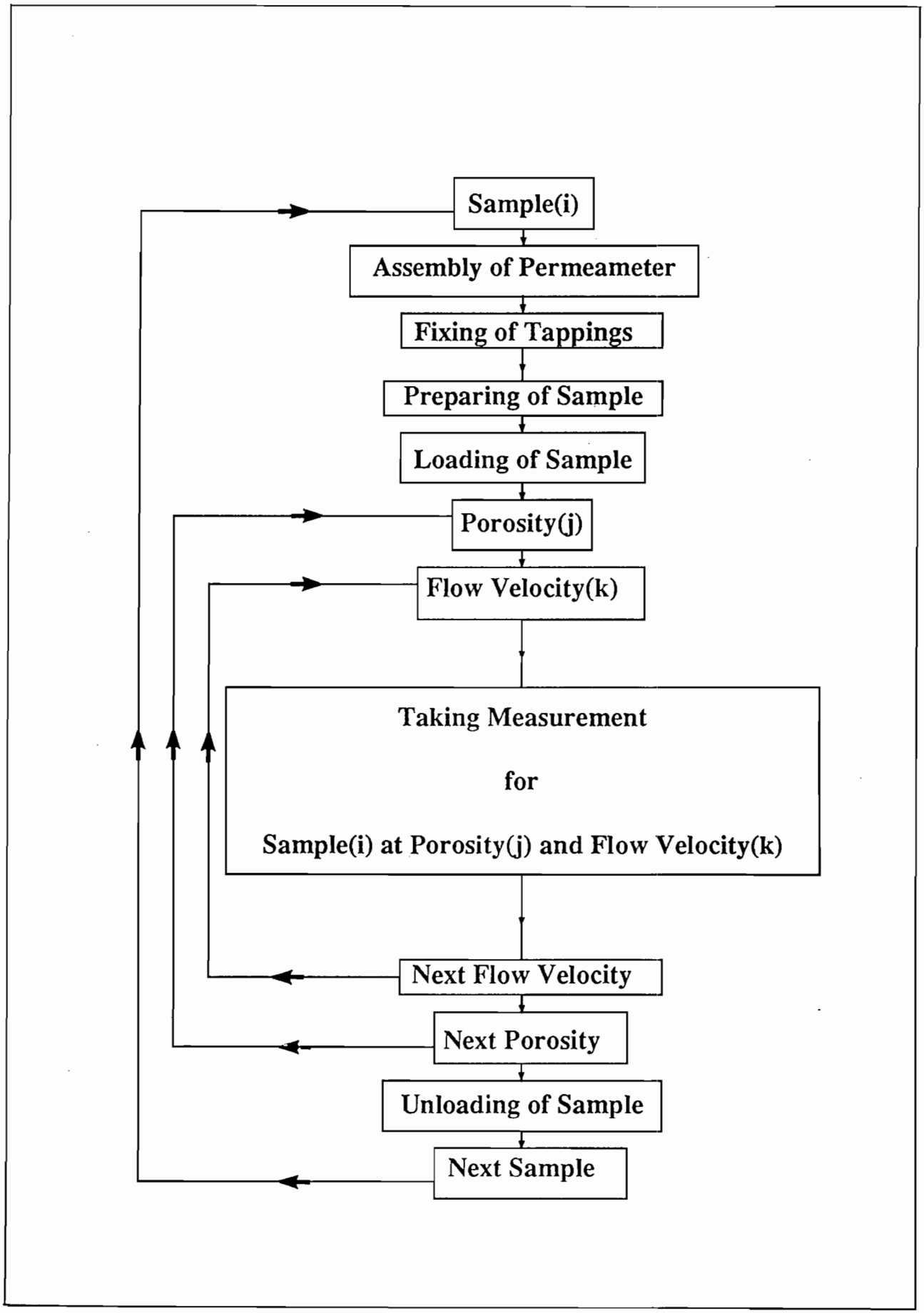

Fig 3.3 Flow chart of test procedures.

Fig 3.4 a-d Sieve curves for the testing samples.

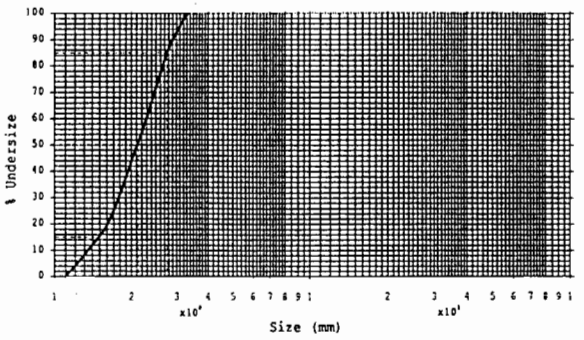

File Identity :regular (No. 1 of 8)
Number of different sizes : 1
Sizes of particles = 4 mm
d15 = 1.5 mm
d50 = 2.2 mm
d85 = 2.8 mm

(a)

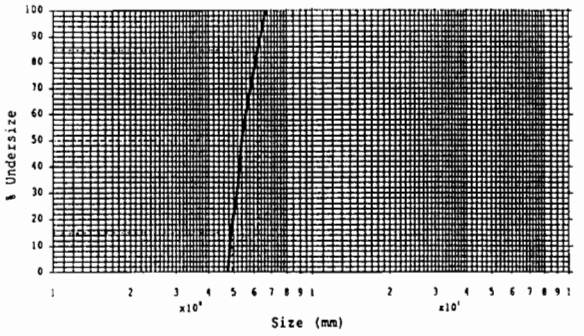

File Identity :regular (No. 2 of 8)
Number of different sizes : 1
Sizes of particles = 6 mm
d15 = 5.0 mm
d50 = 5.5 mm
d85 = 6.3 mm

(b)

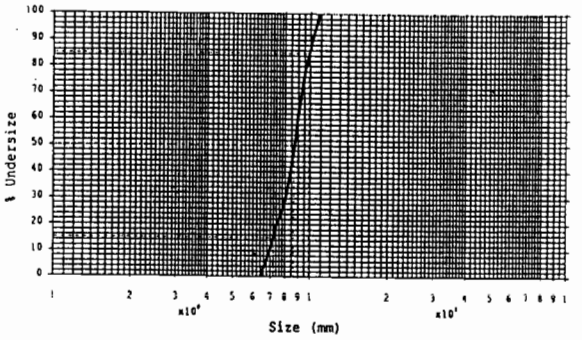

File Identity :regular (No. 3 of 8)
Number of different sizes : 1
Sizes of particles = 10 mm
d15 = 7.3 mm
d50 = 8.7 mm
d85 = 9.9 mm

(c)

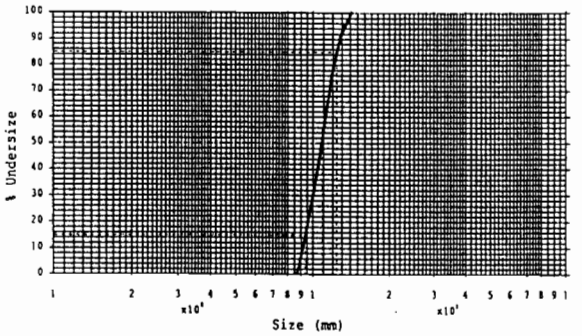

File Identity :regular (No. 4 of 8)
Number of different sizes : 1
Sizes of particles = 14 mm
d15 = 9.4 mm
d50 = 10.9 mm
d85 = 12.5 mm

(d)

Fig 3.4 e-h Sieve curves for the testing samples.

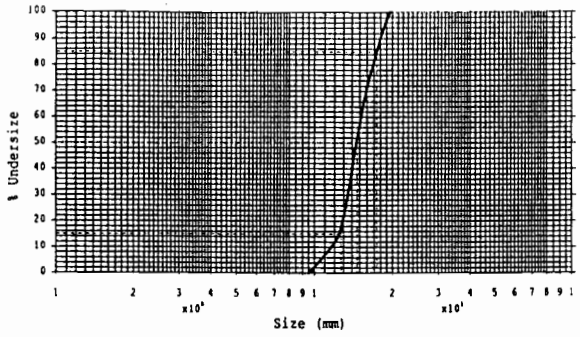

File Identity :regular (No. 5 of 8)
Number of different sizes : 1
Sizes of particles = 20 mm
d15 = 12.8 mm
d50 = 14.7 mm
d85 = 17.4 mm

(e)

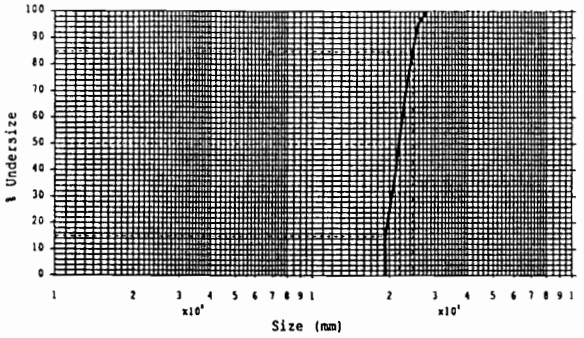

File Identity :regular (No. 6 of 8)
Number of different sizes : 1
Sizes of particles = 28 mm
d15 = 19.3 mm
d50 = 21.8 mm
d85 = 24.6 mm

(f)

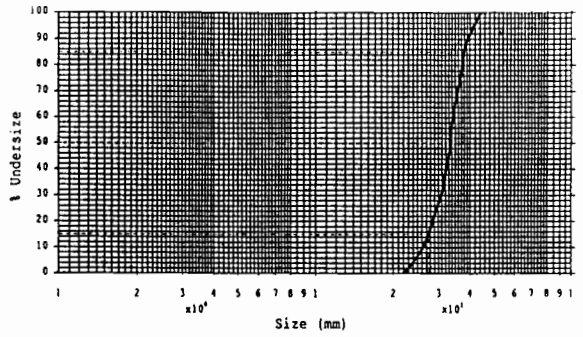

File Identity :regular (No. 7 of 8)
Number of different sizes : 1
Sizes of particles = 40 mm
d15 = 27.7 mm
d50 = 33.3 mm
d85 = 37.8 mm

(g)

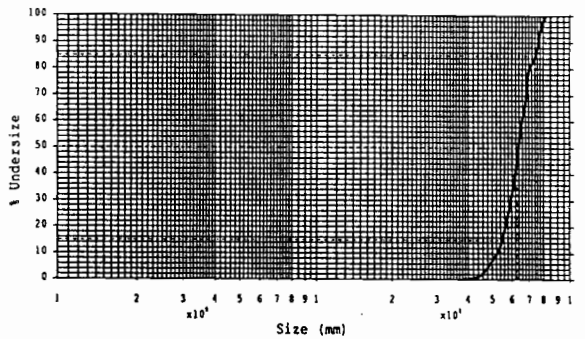

File Identity :regular (No. 8 of 8)
Number of different sizes : 1
Sizes of particles = 61 mm
d15 = 54.4 mm
d50 = 62.9 mm
d85 = 74.7 mm

(h)

Fig 3.4 i-l Sieve curves for the testing samples.

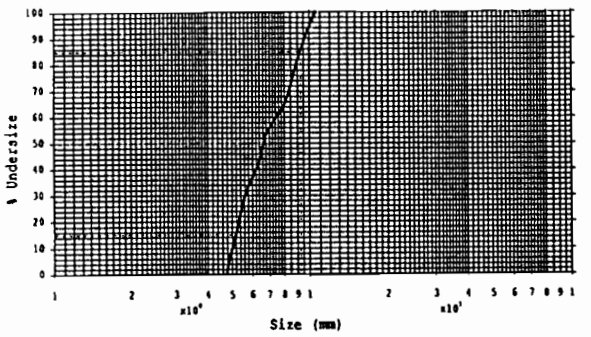

File Identity :gap_graded (No. 1 of 5)
Number of different sizes : 2
Sizes of particles = 6, 10 mm
d15 = 5.2 mm
d50 = 6.6 mm
d85 = 9.3 mm

(i)

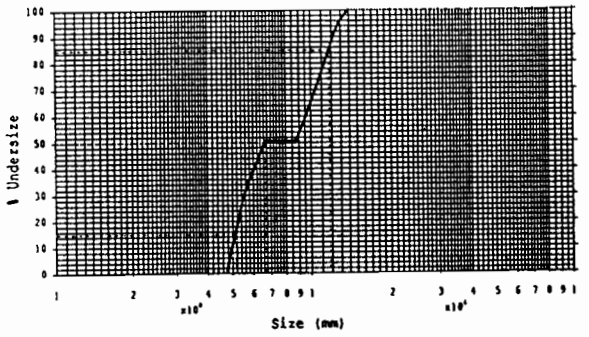

File Identity :gap_graded (No. 2 of 5)
Number of different sizes : 2
Sizes of particles = 6, 14 mm
d15 = 5.2 mm
d50 = 6.8 mm
d85 = 11.8 mm

(j)

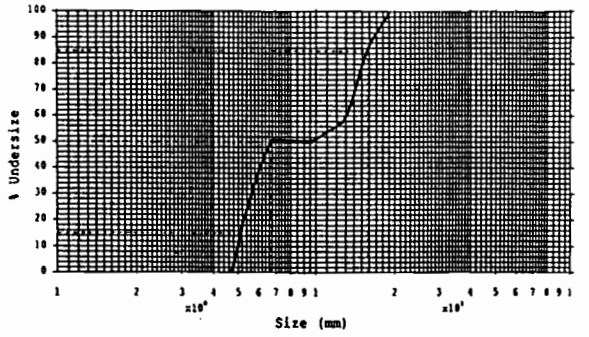

File Identity :gap_graded (No. 3 of 5)
Number of different sizes : 2
Sizes of particles = 6, 20 mm
d15 = 5.2 mm
d50 = 6.8 mm
d85 = 15.8 mm

(k)

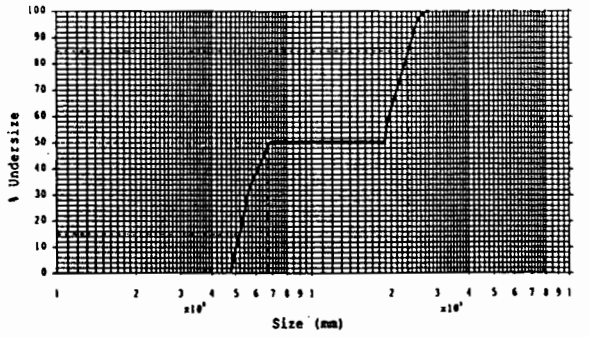

File Identity :gap_graded (No. 4 of 5)
Number of different sizes : 2
Sizes of particles = 6, 28 mm
d15 = 5.2 mm
d50 = 6.8 mm
d85 = 23.4 mm

(l)

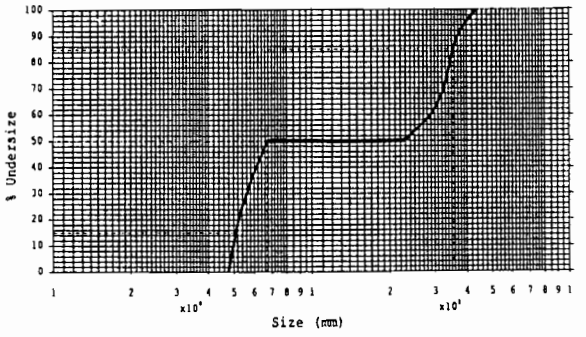

File Identity :gap_graded (No. 5 of 5)

Number of different sizes : 2

Sizes of particles = 6, 40 mm

d15 = 5.2 mm
d50 = 6.8 mm
d85 = 35.5 mm

(m)

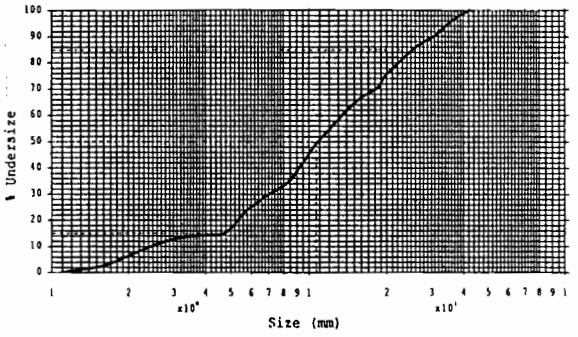

File Identity :wide_graded (No. 2 of 3)

Number of different sizes : 7

Sizes of particles = 4, 6, 10, 14, 20, 28, 40 mm

d15 = 4.9 mm
d50 = 10.7 mm
d85 = 25.0 mm

(o)

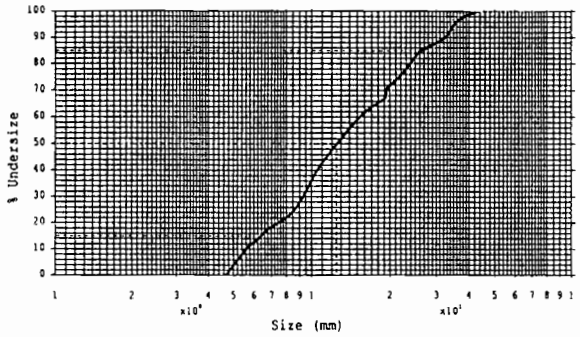

File Identity :wide_graded (No. 1 of 3)

Number of different sizes : 6

Sizes of particles = 6, 10, 14, 20, 28, 40 mm

d15 = 6.4 mm
d50 = 12.5 mm
d85 = 26.9 mm

(n)

Fig 3.4 m-o Sieve curves for the testing samples.

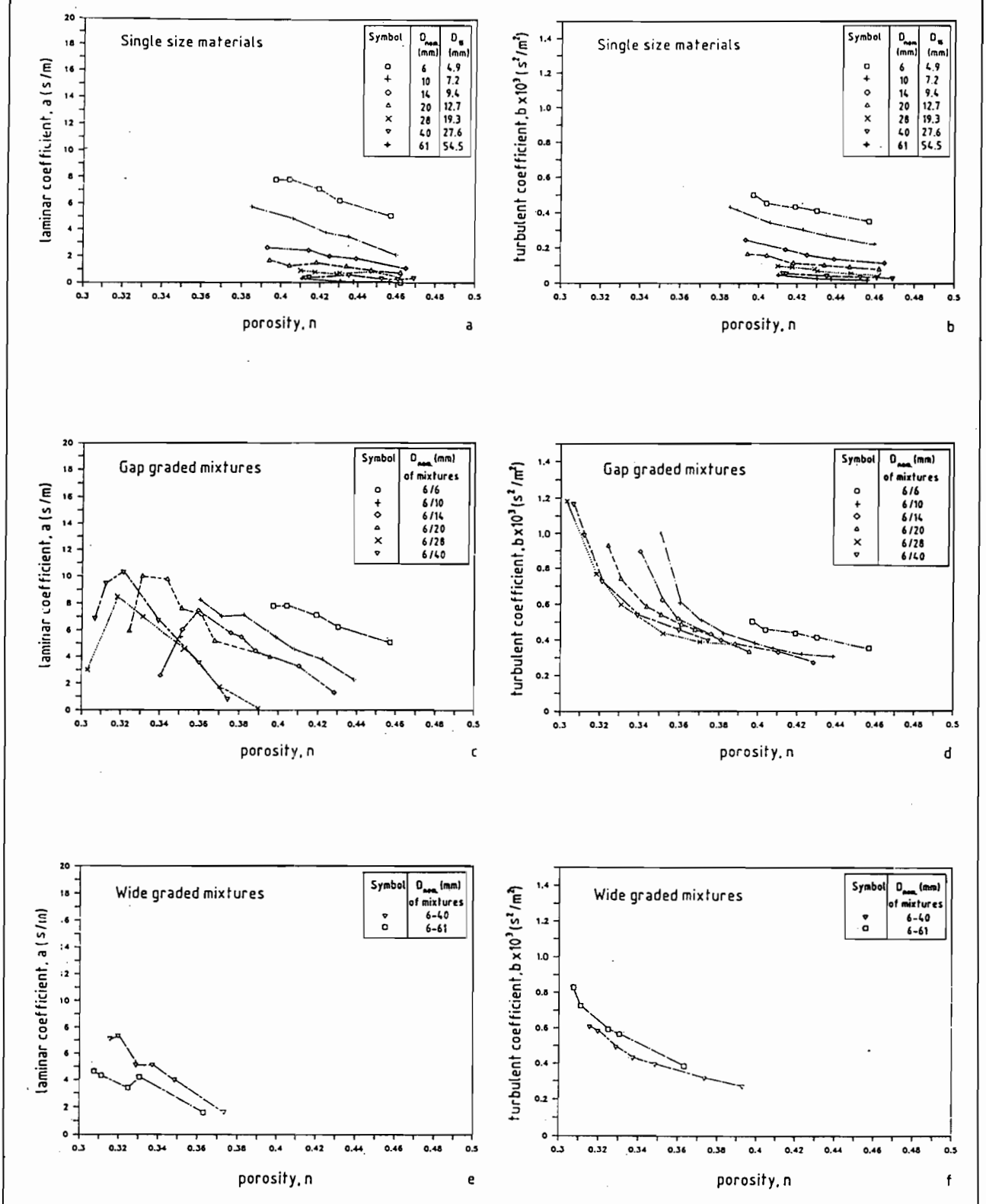

Fig 3.5 a-f Values of Forchheimer coefficients a and b.

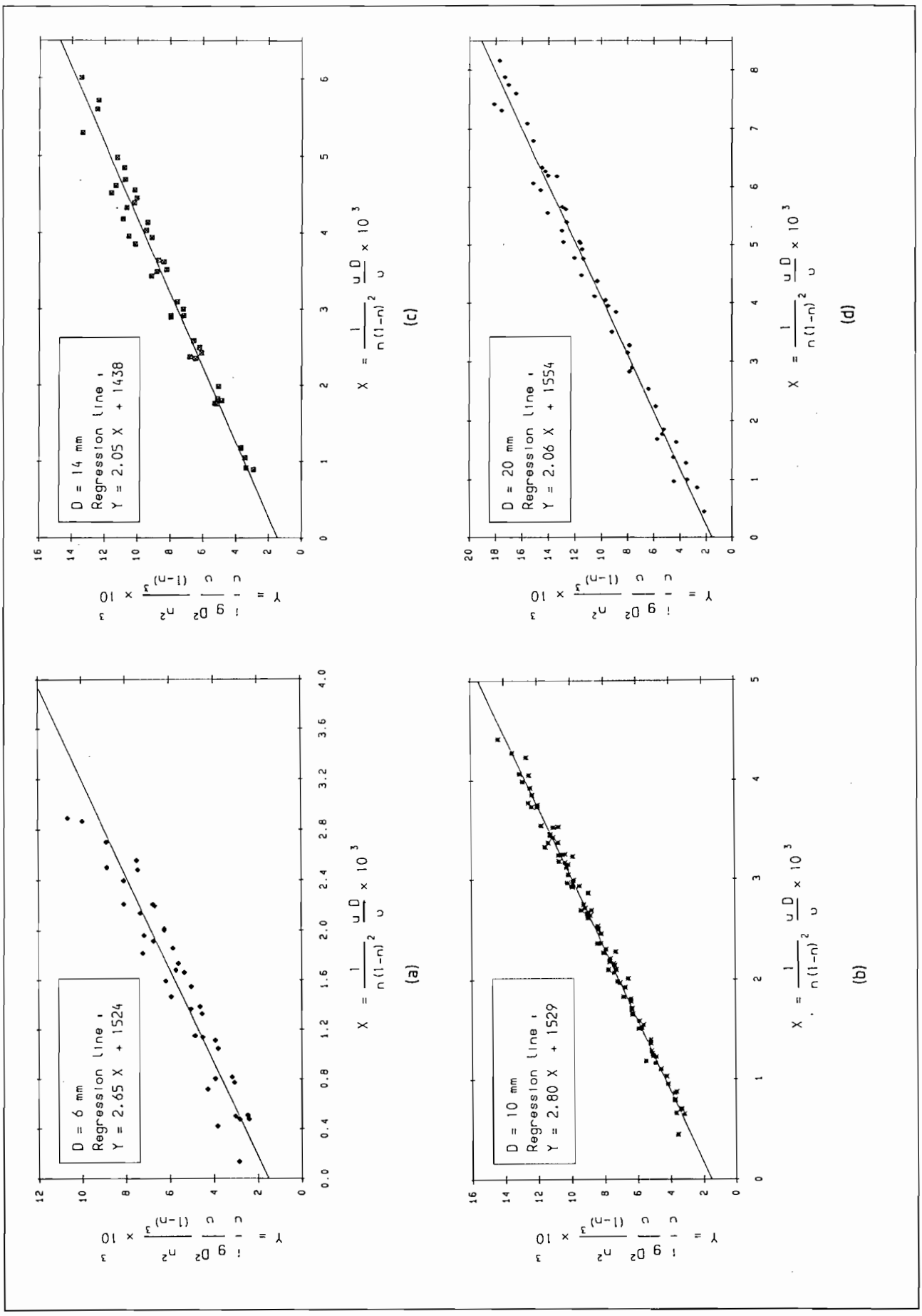

Fig 3.6 a-d Regression analysis for single size materials.

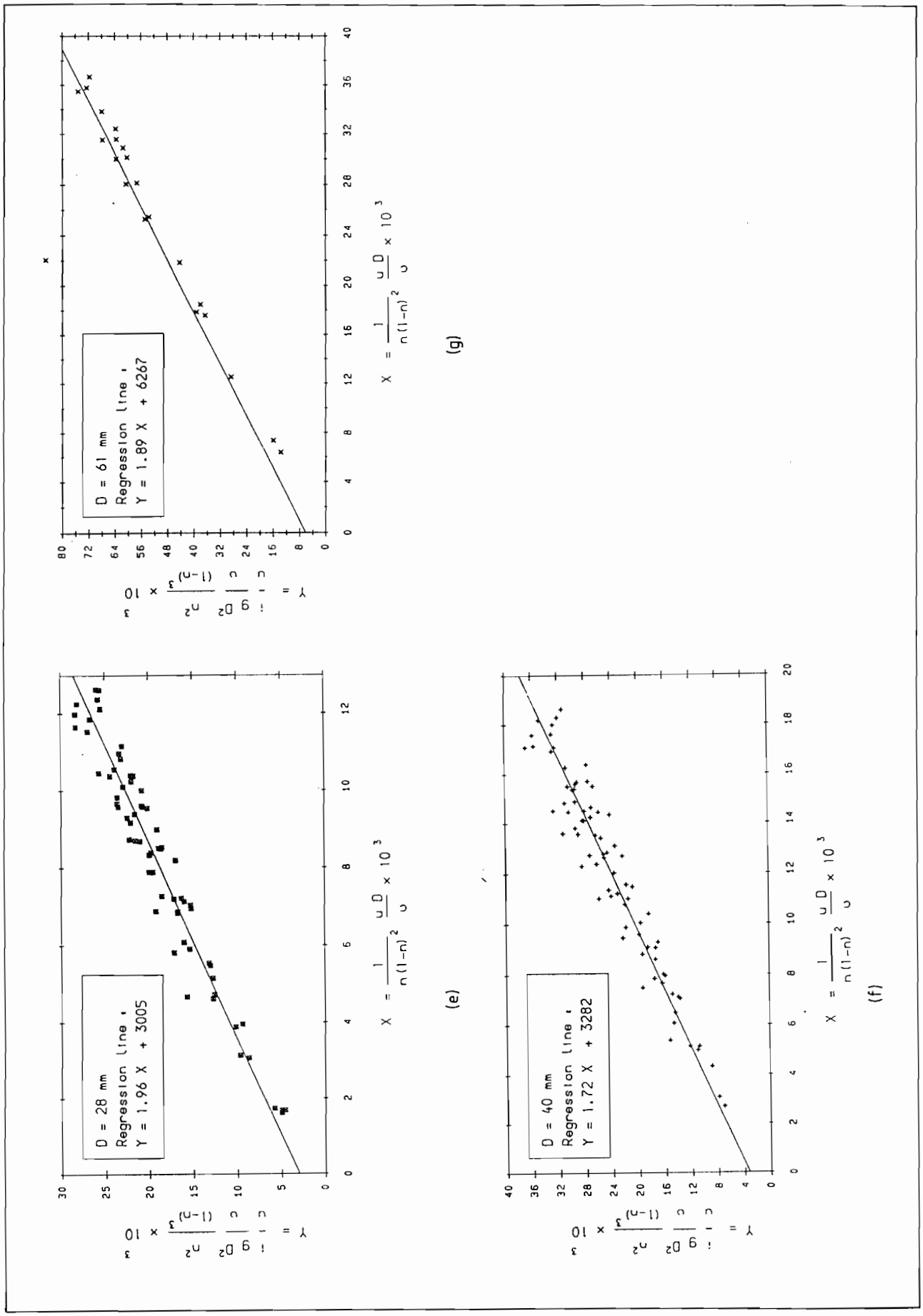

Fig 3.6 e-g Regression analysis for single size materials.

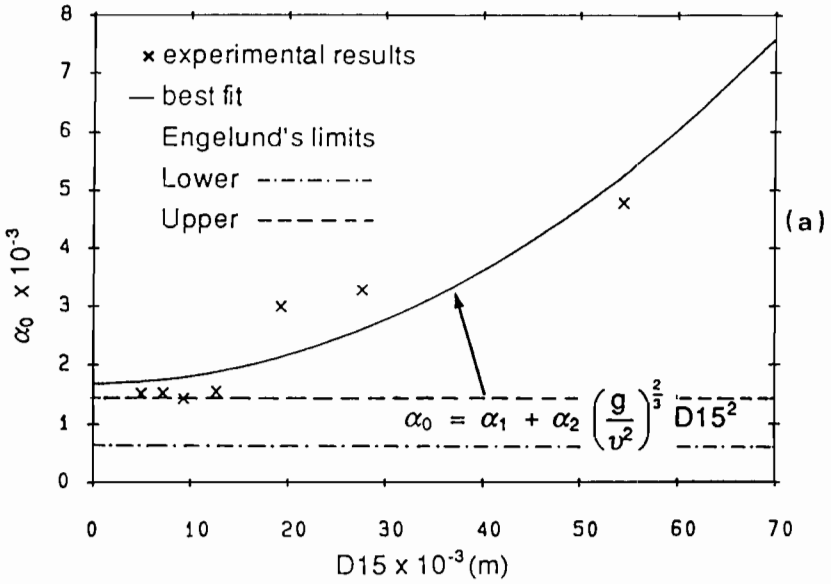

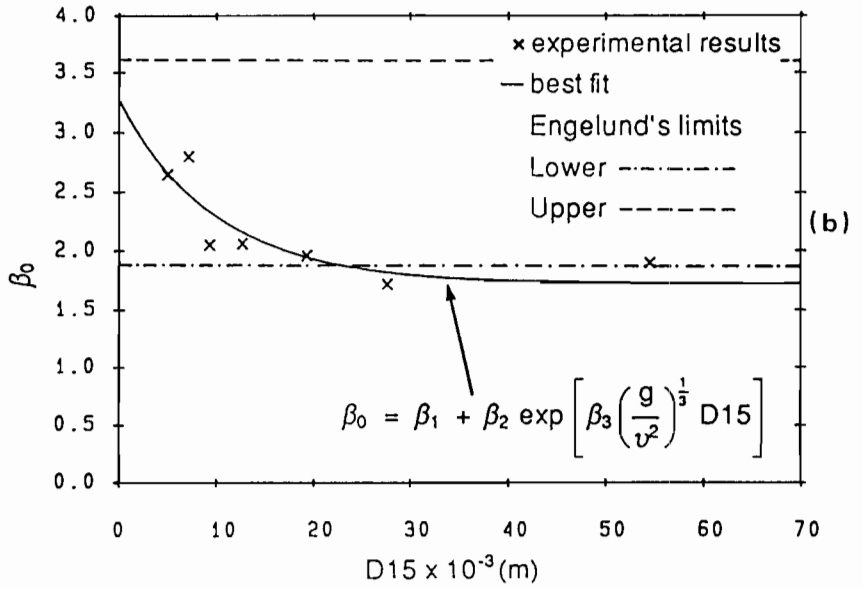

α_1 = 1683.71

α_2 = 3.12 x 10^{-3}

β_1 = 1.72

β_2 = 1.57

β_3 = -5.10 x 10^{-3}

υ = kinematic viscosity of water
= 1.14 x 10^{-6} m^2/s

g = gravitational acceleration = 9.81 m/s^2

Fig 3.7 Dependance of α_o and β_o on particle diameter D_{15} for single size materials.

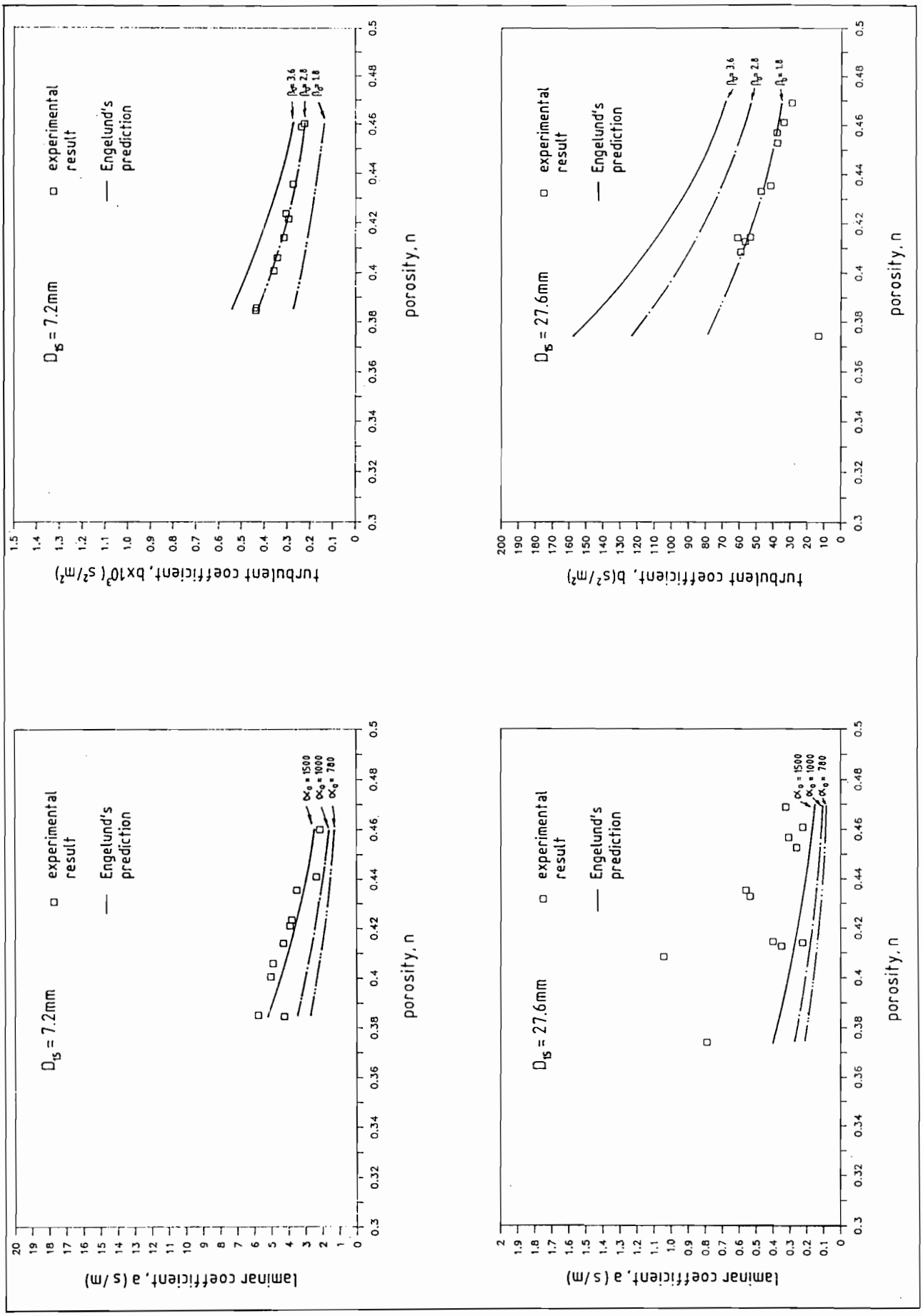

Fig 3.8 Comparison of test results with Engelunds method, D_{15} = 7.2 and 27.6mm.

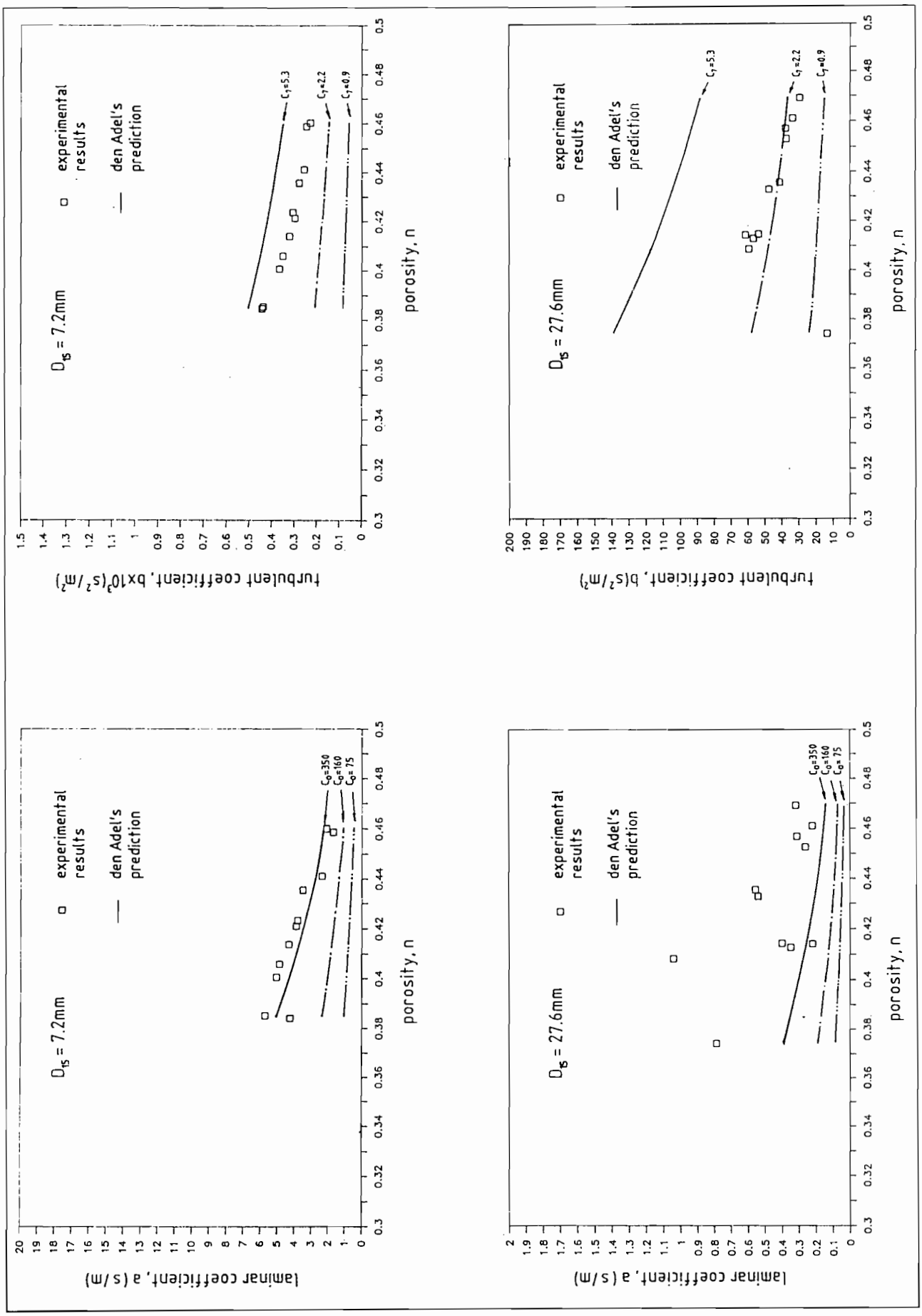

Fig 3.9 Comparison of test results with den Adel's method, D_{15} = 7.2 and 27.6mm.

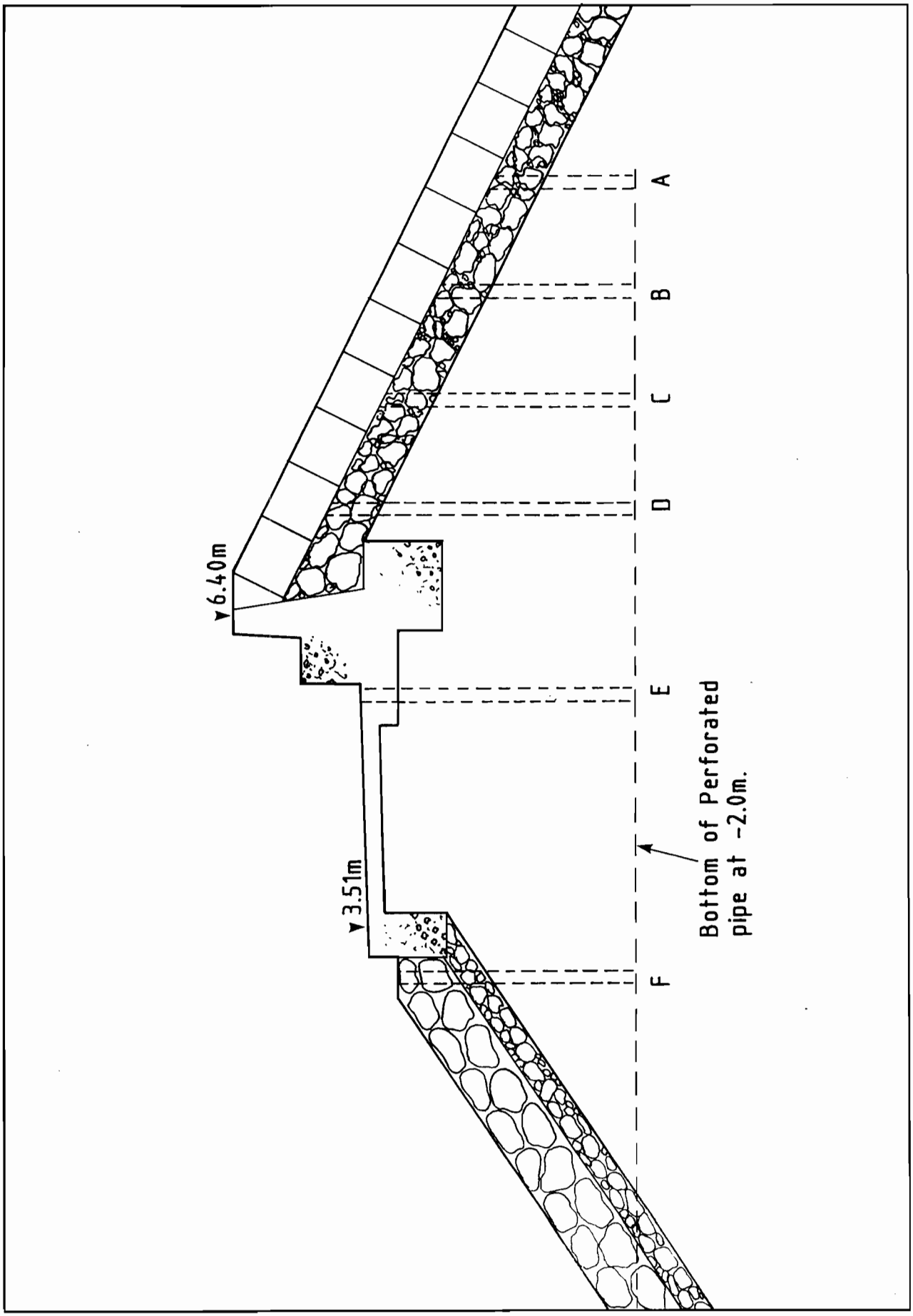

Fig 4.1 Cross-section of Pickie breakwater, showing instrumentation.

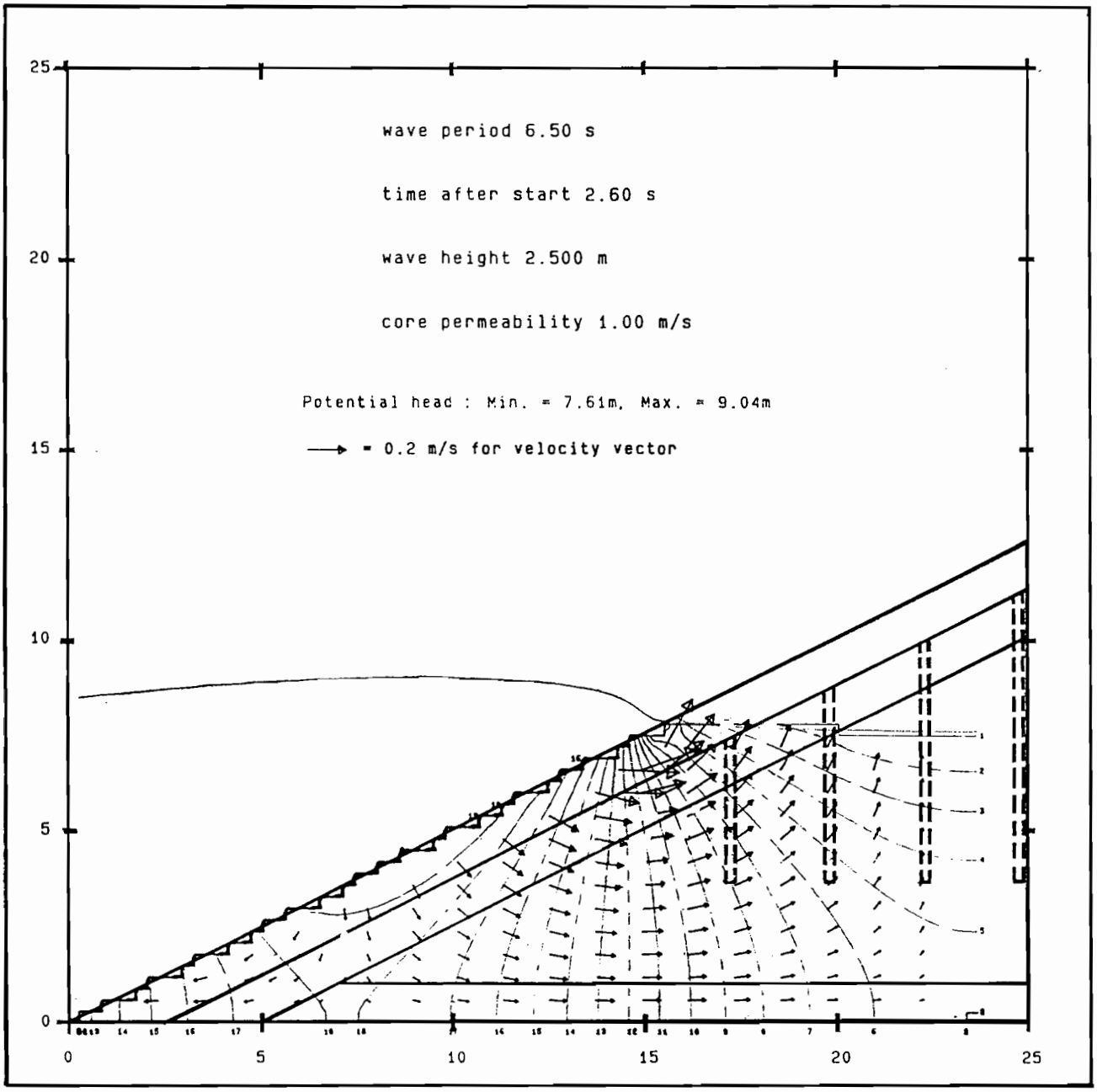

Fig 4.2 a Example results of calculations of flow conditions within Pickie breakwater.

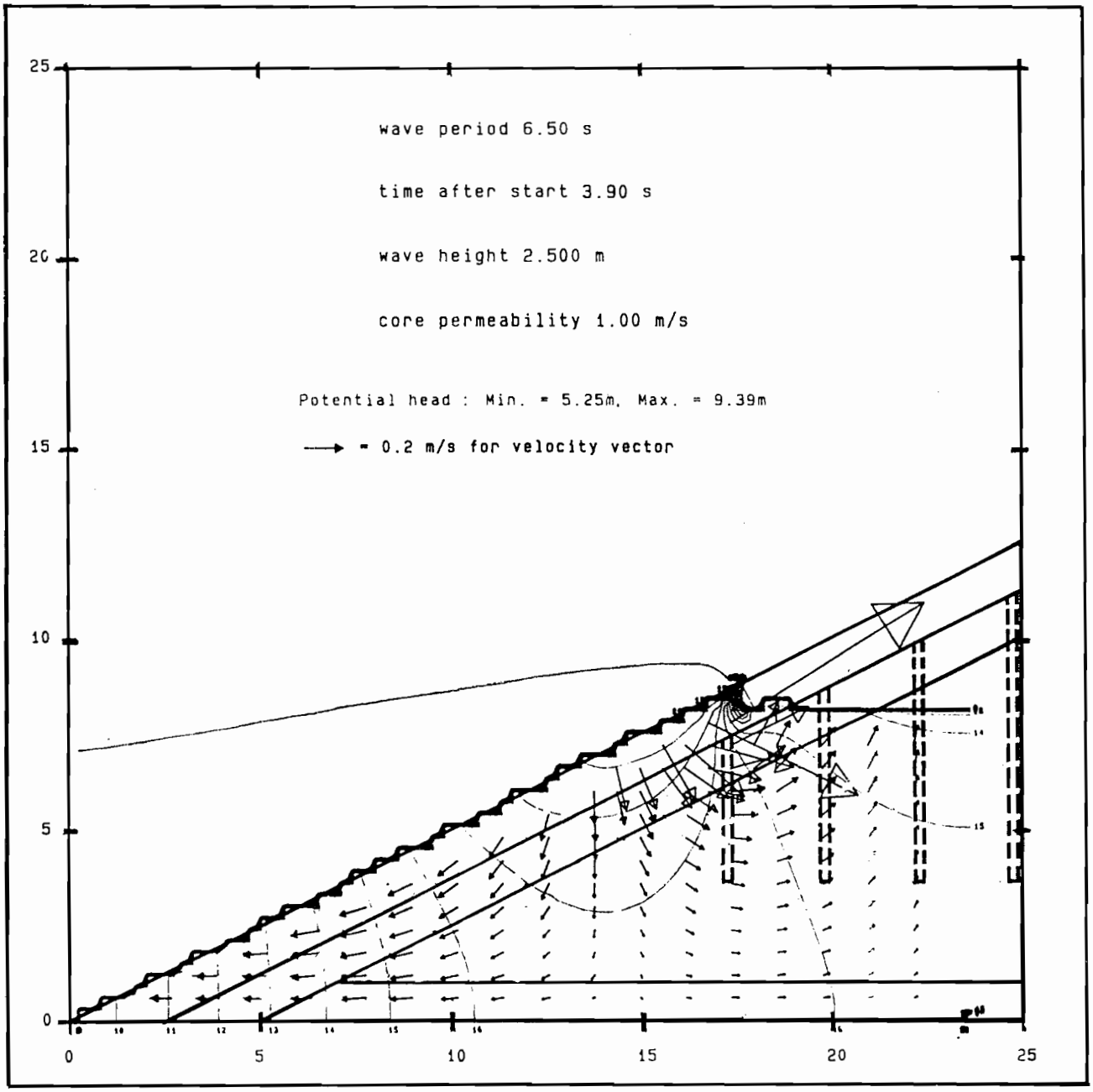

Fig 4.2 b Example results of calculations of flow conditions within Pickie breakwater.

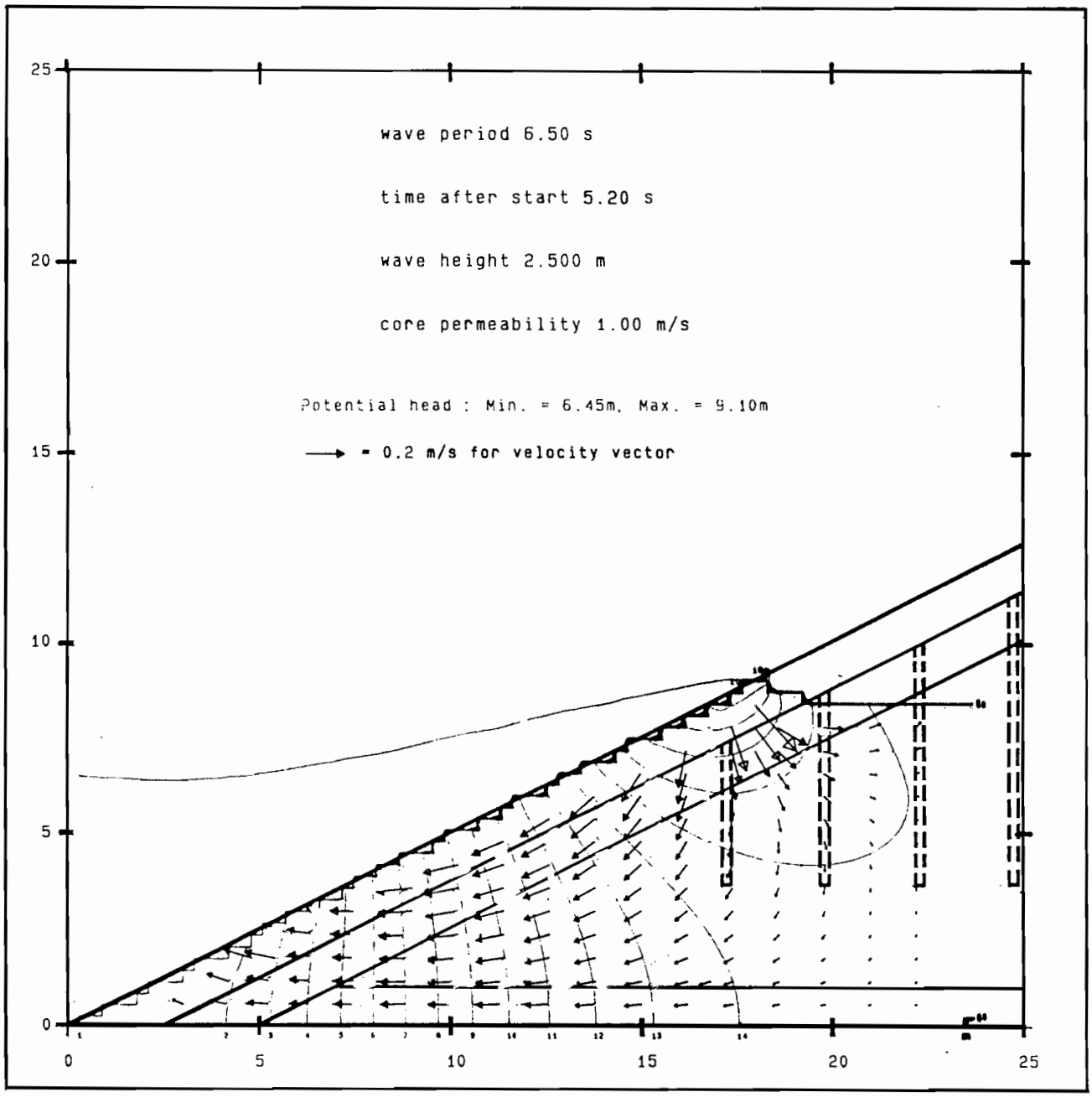

Fig 4.2 c Example results of calculations of flow conditions within Pickie breakwater.

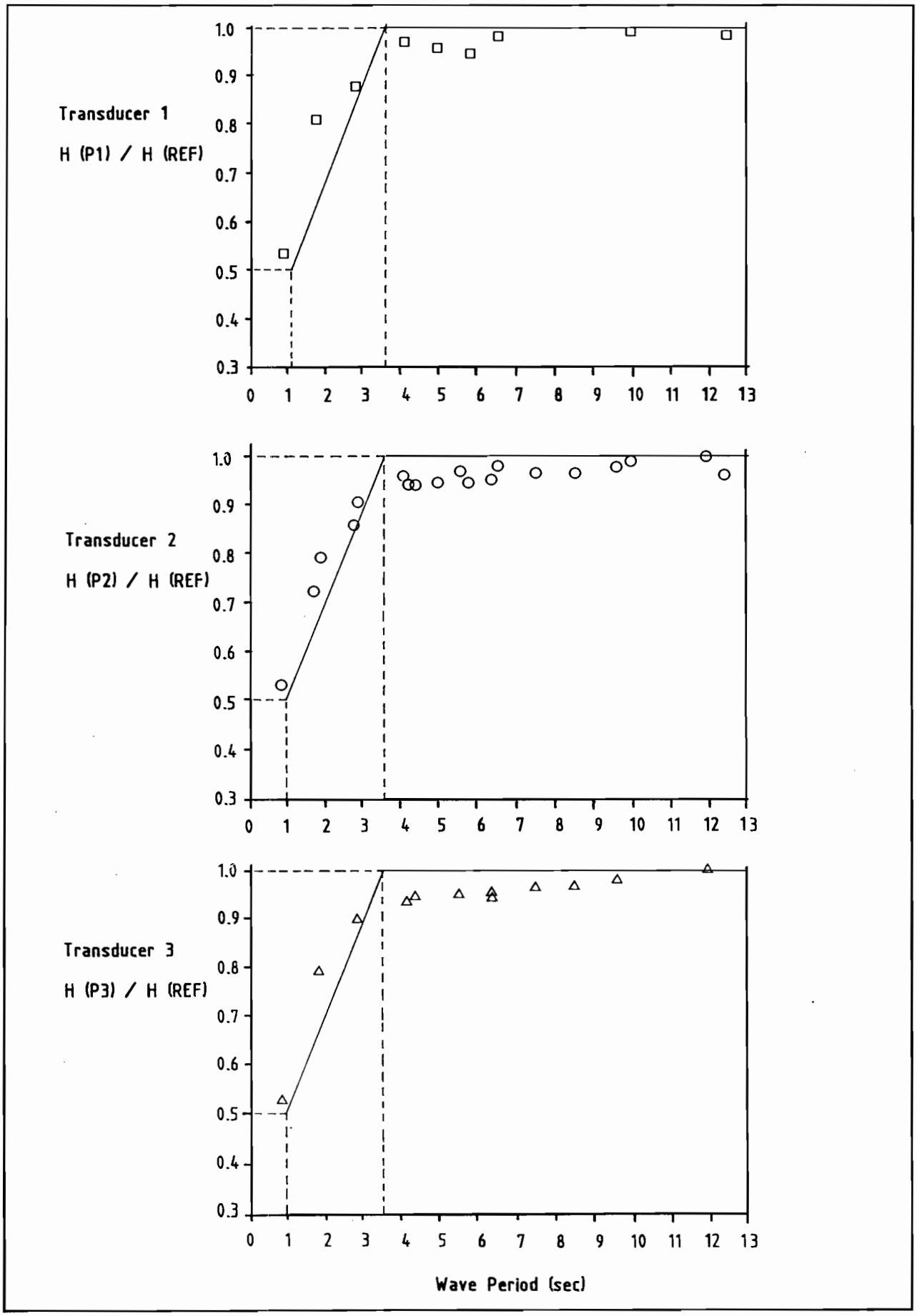

Fig 4.3 Calibration graphs for PSM transducers, wave periods 1-13 seconds.

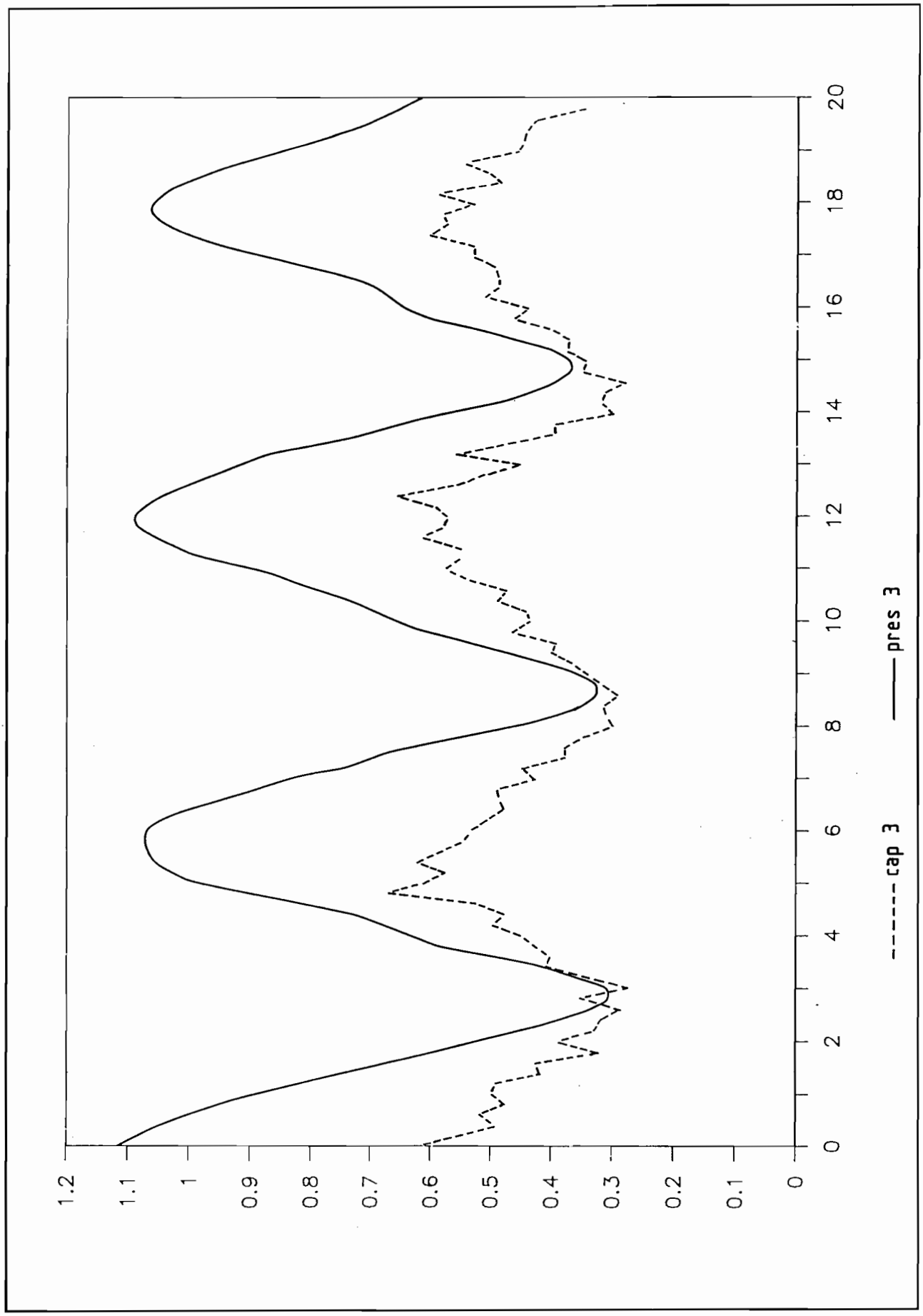

Fig 4.4 Example output from pressure transducer and capacitance gaauge, test at QUB.

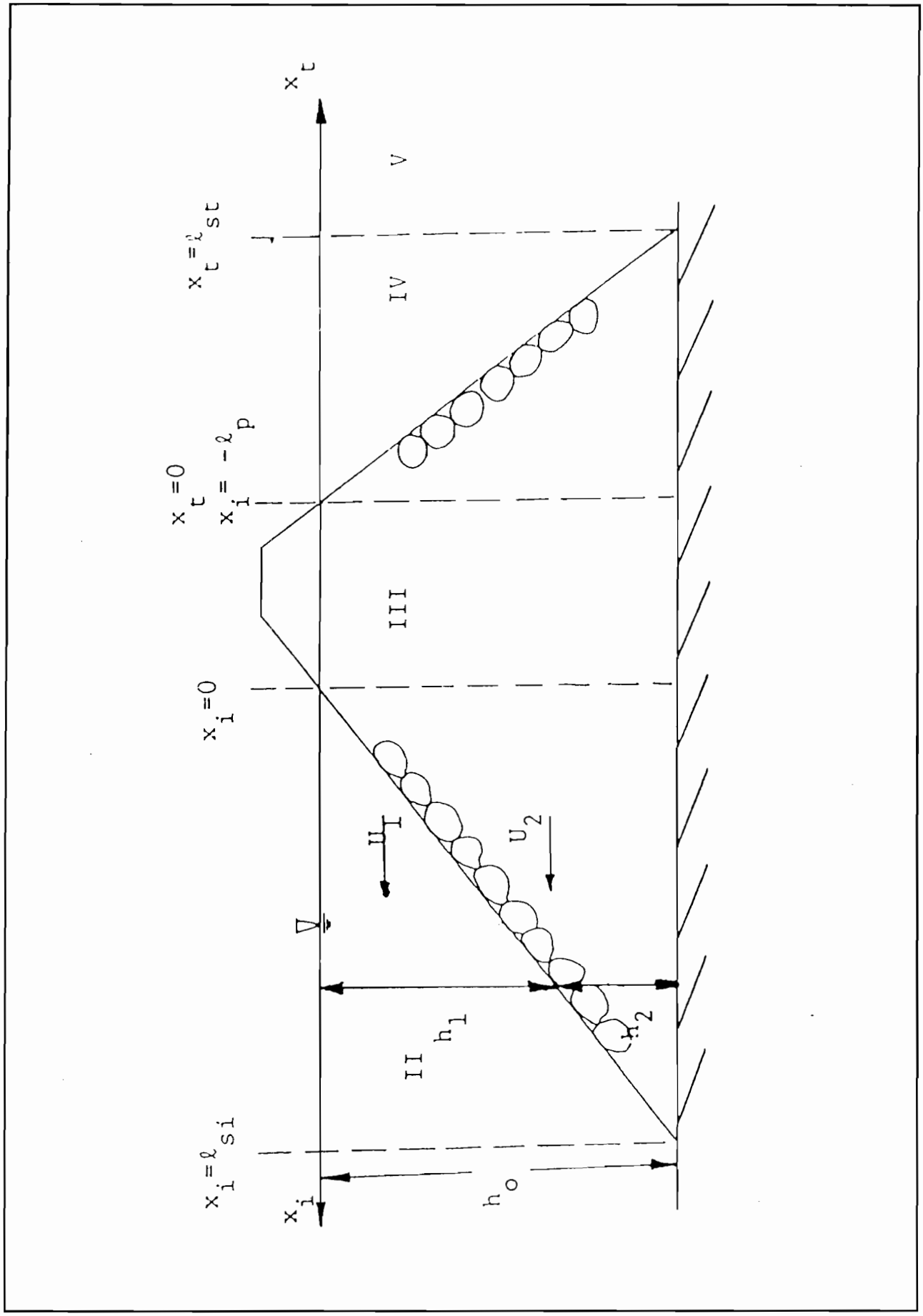

Fig 5.1 Trapezoidal breakwater for the Madsen & White model.

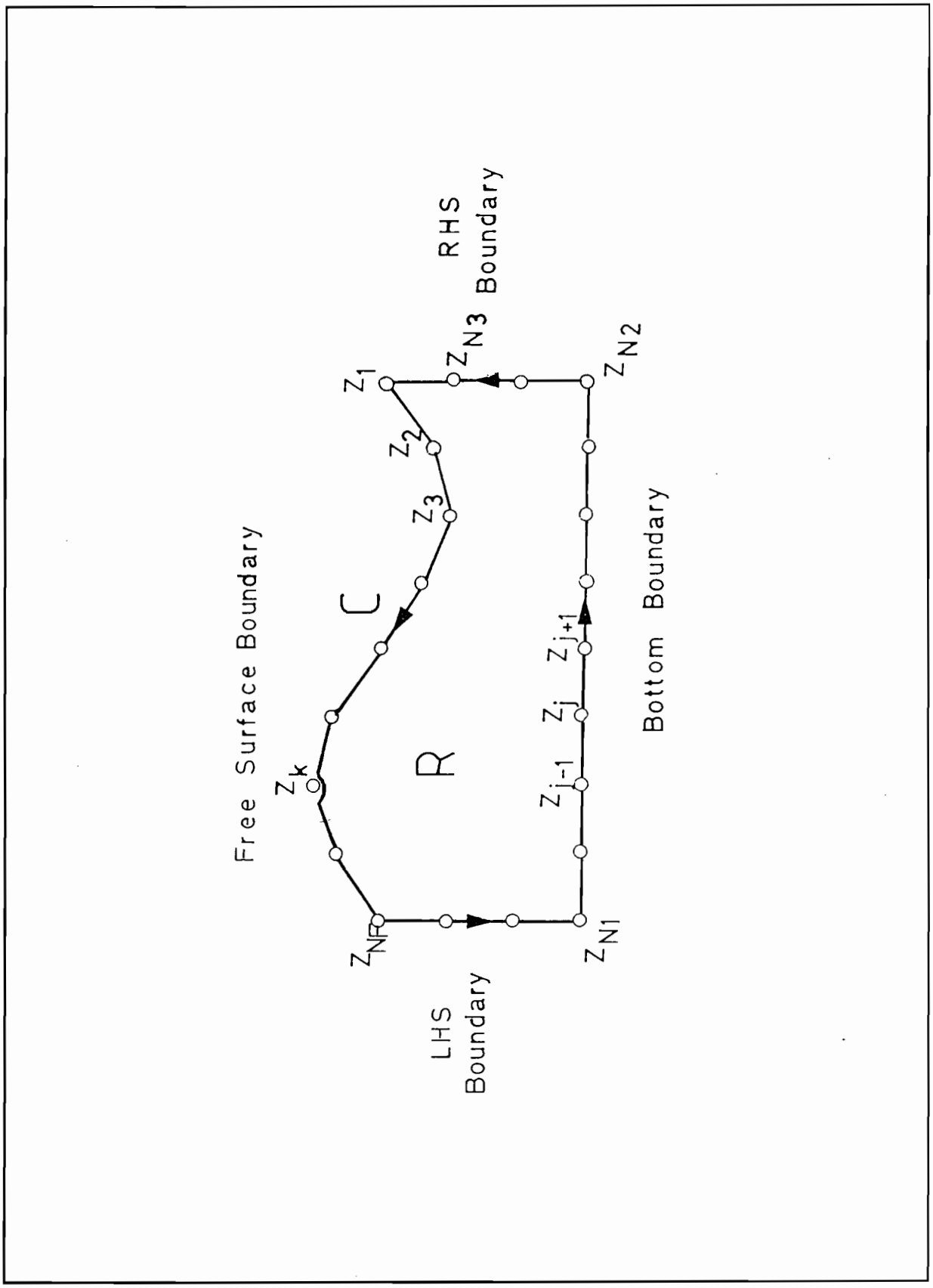

Fig 5.2 Schematic representation of the control volume.

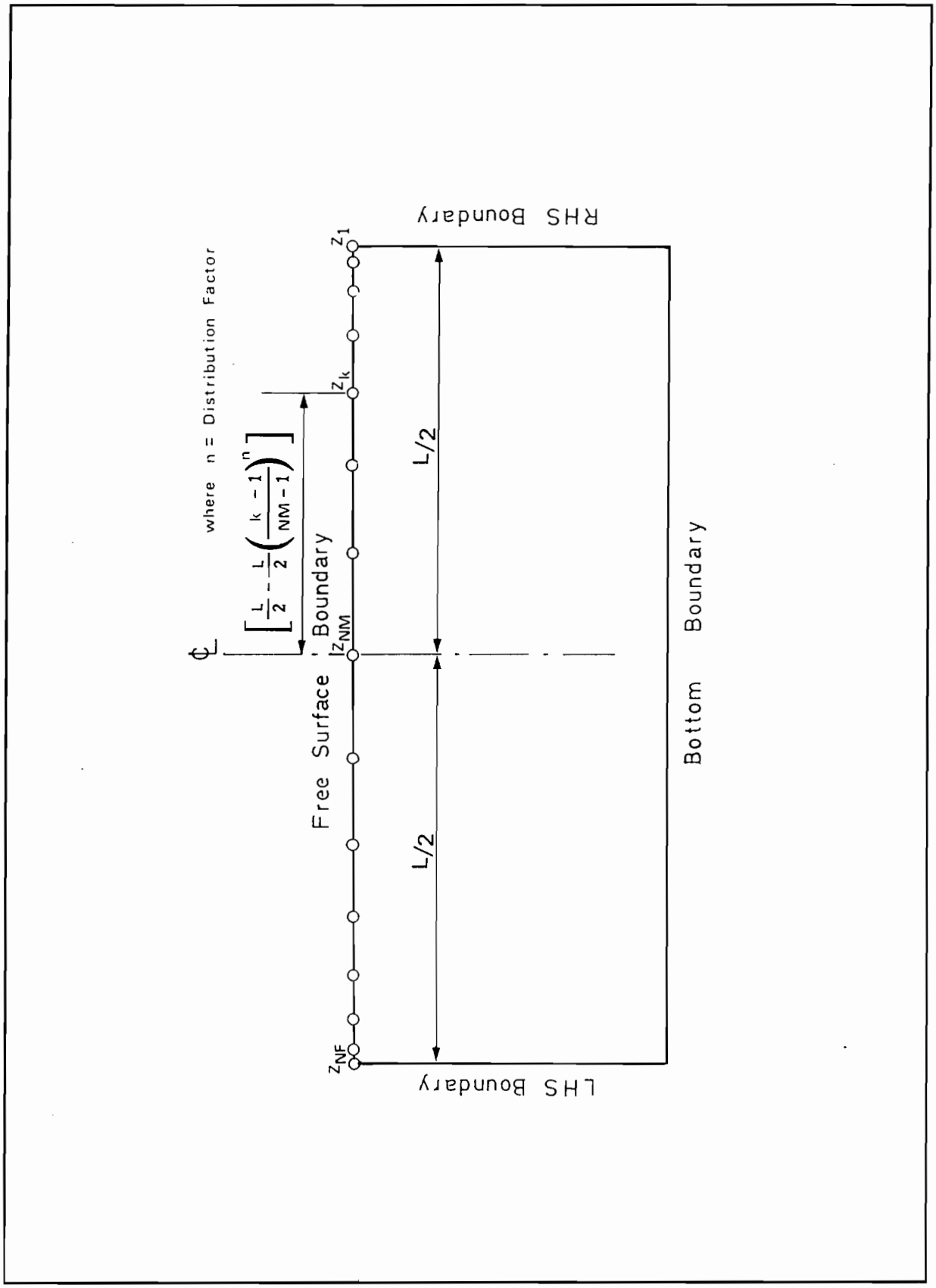

Fig 5.3 Distribution of nodal points along the free surface boundary.

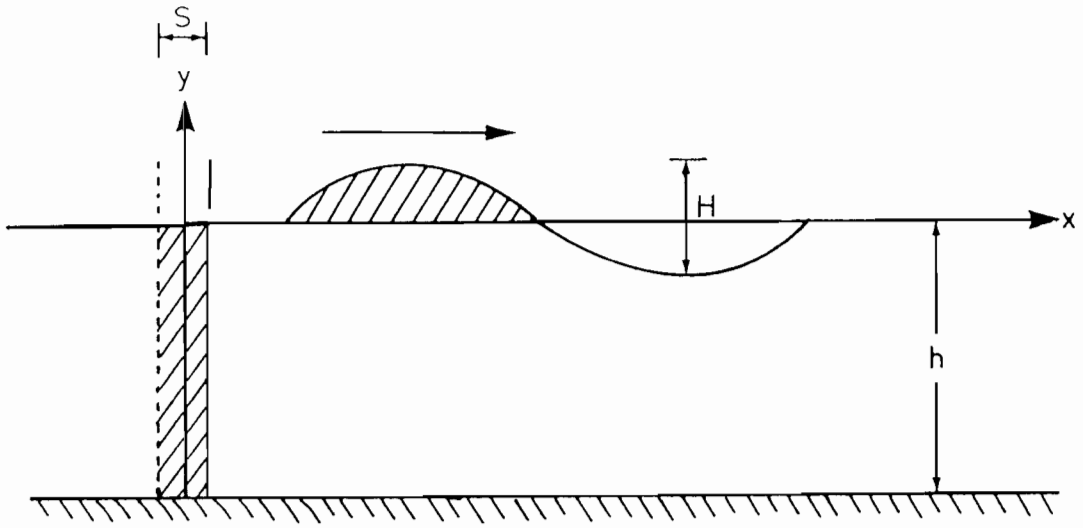

(a)

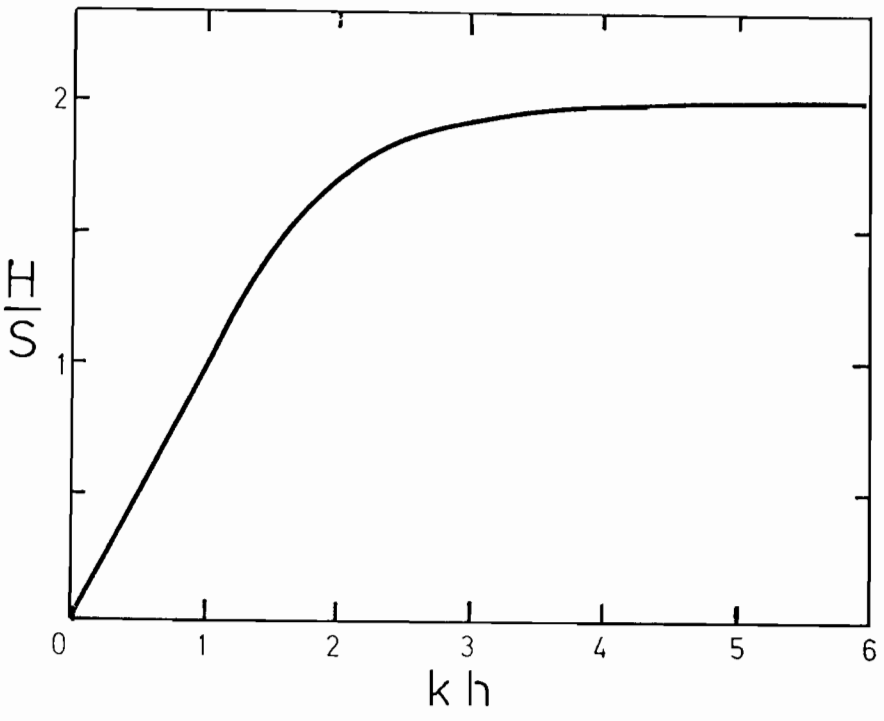

(b)

Fig 5.4 Correlation between a piston-type wavemaker and the wave it generates.

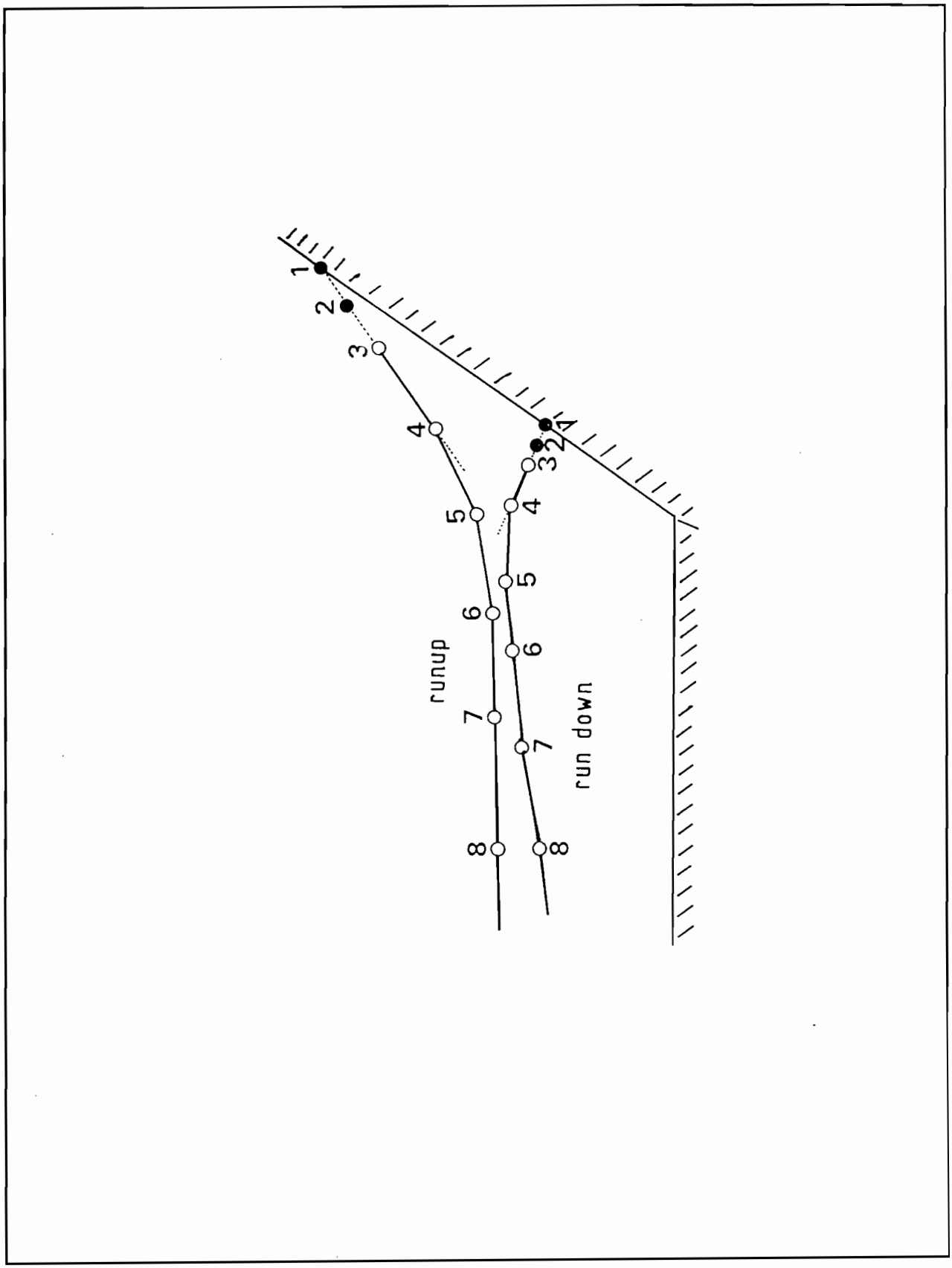

Fig 5.5 Numerical treatment for contact point during wave runup / down on a slope.

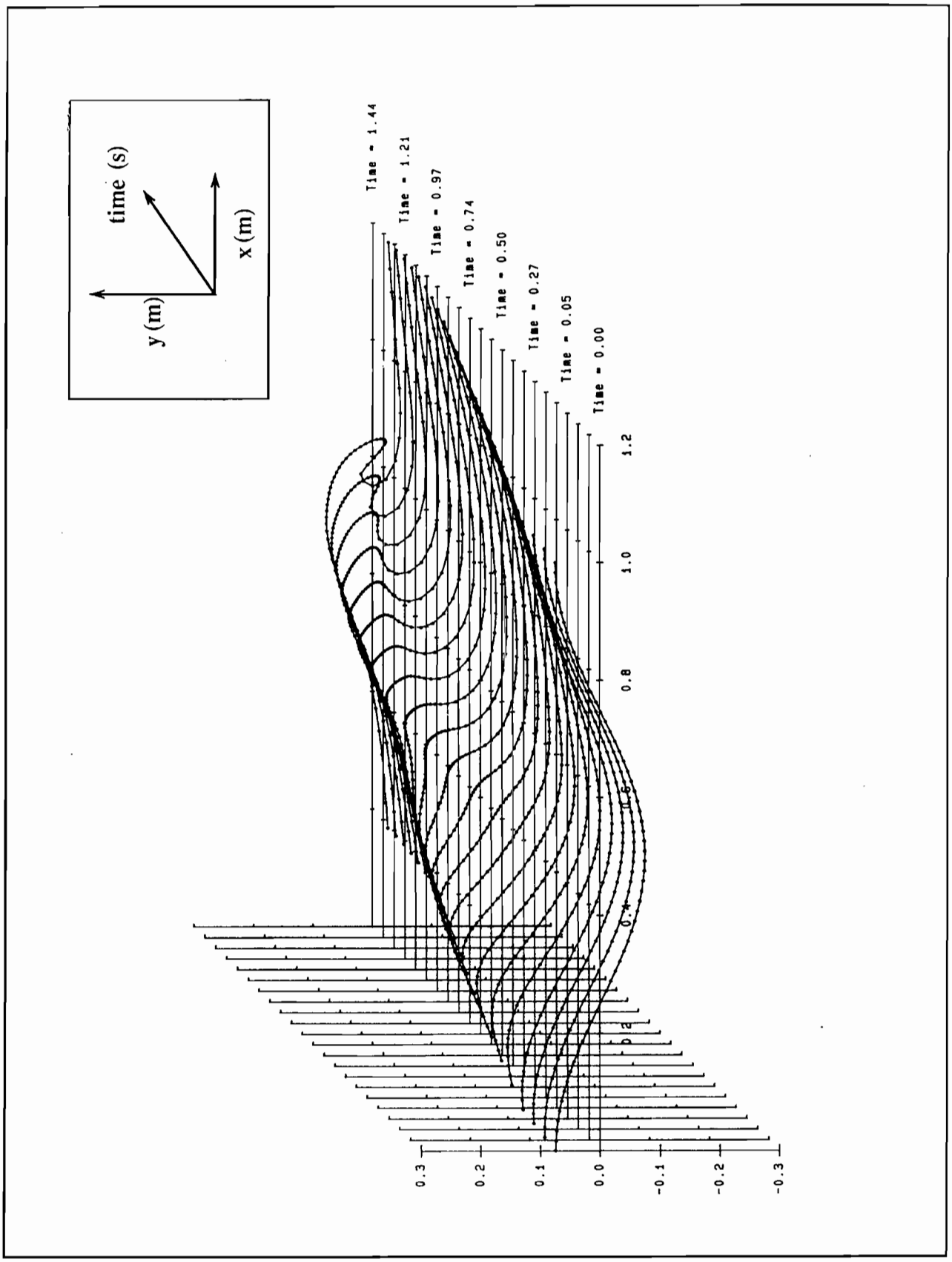

Fig 5.6 Simulation of shallow water wave.

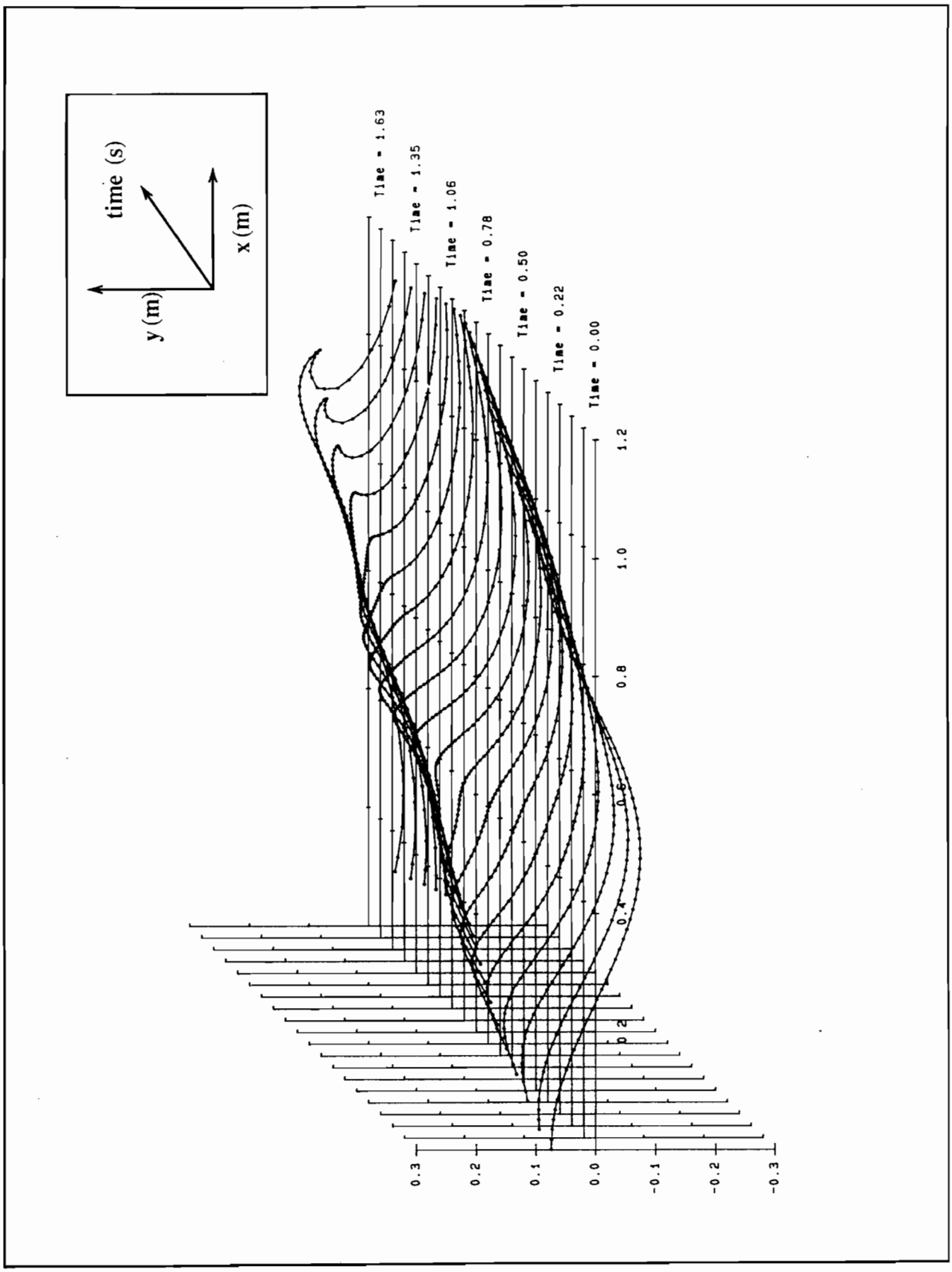

Fig 5.7 Simulation of deep water wave.

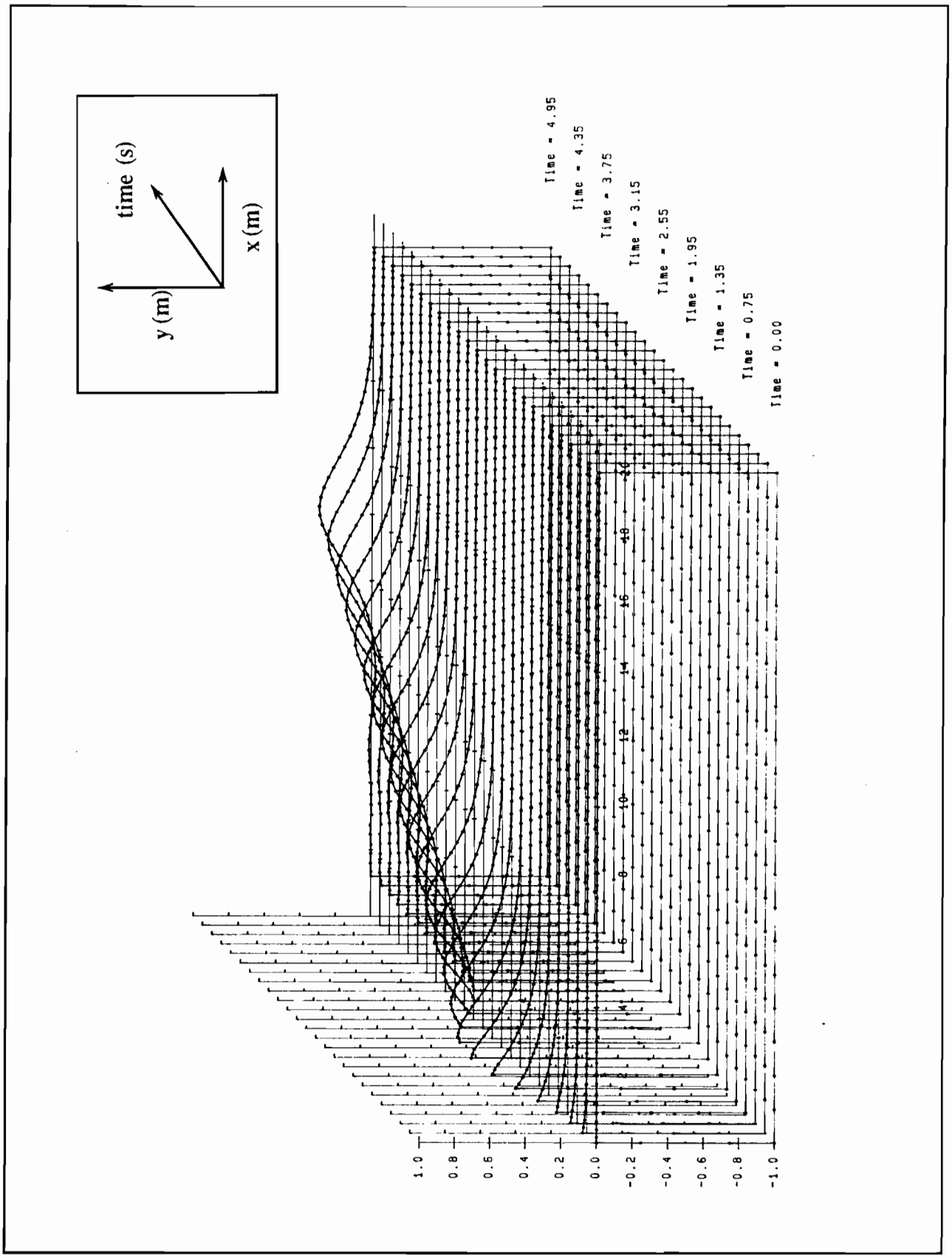

Fig 5.8 a Generation of a solitary wave and its runup on a vertical wall.

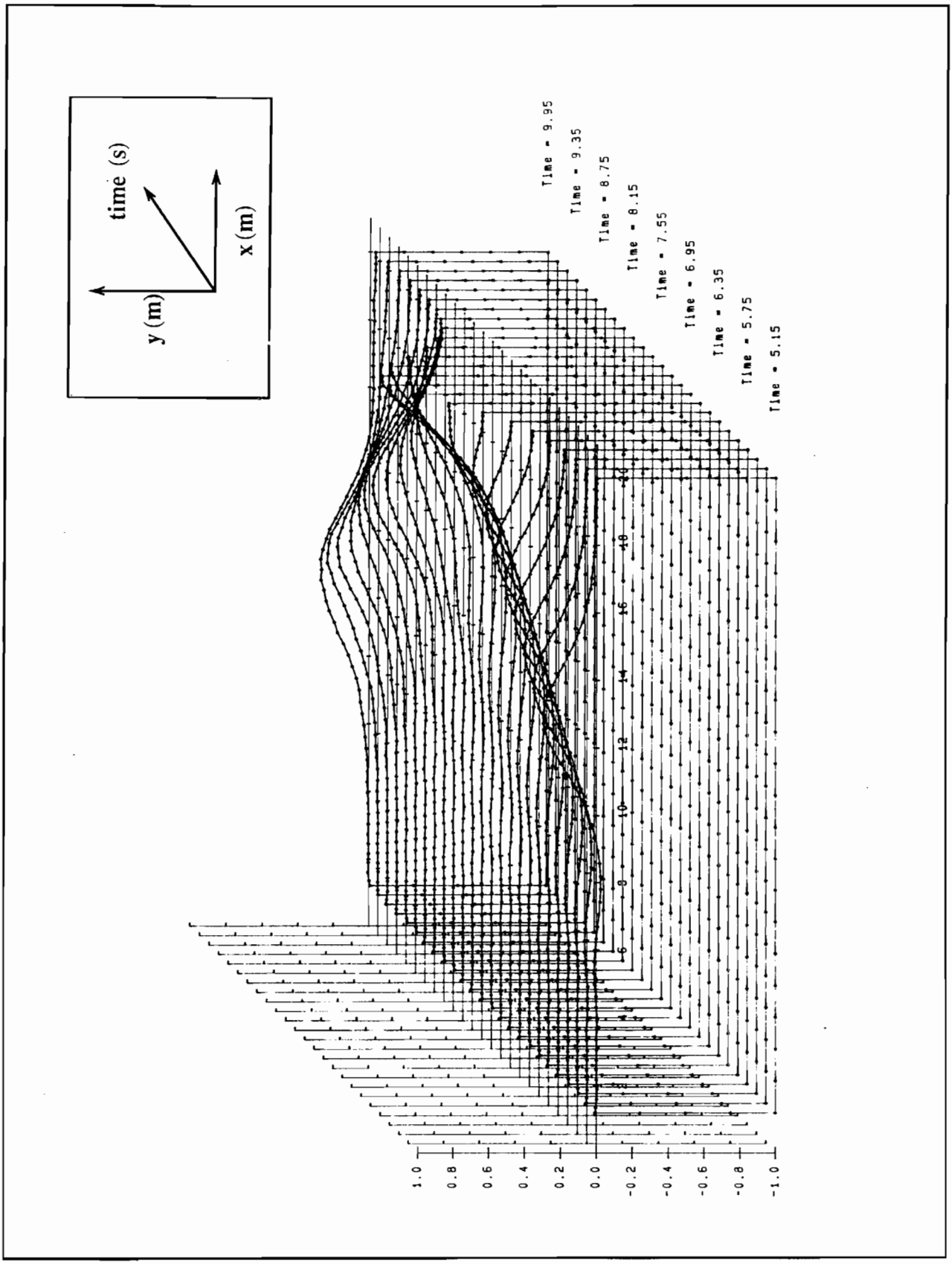

Fig 5.8 b Generation of a solitary wave and its runup on a vertical wall.

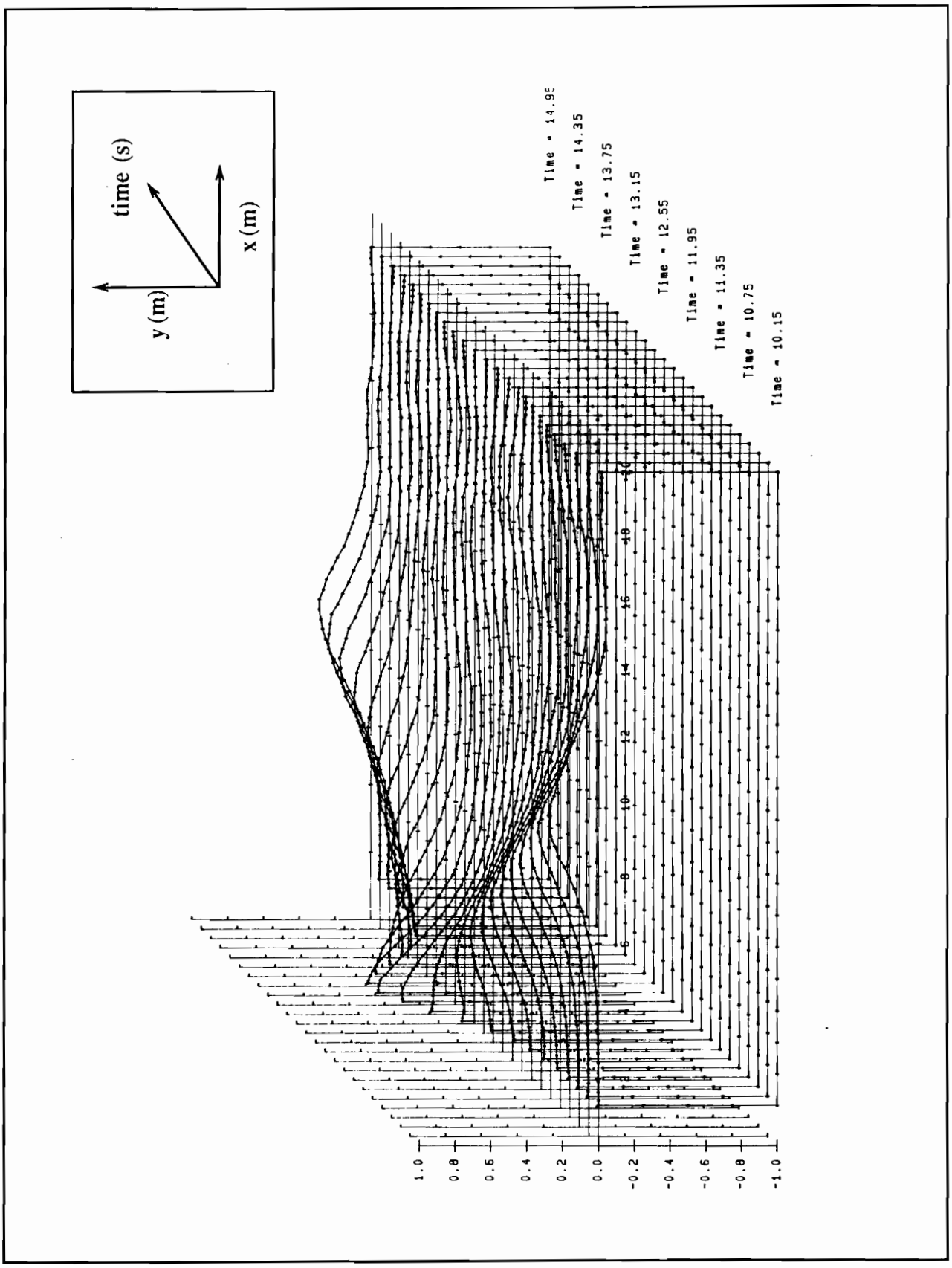

Fig 5.8 c Generation of a solitary wave and its runup on a vertical wall.

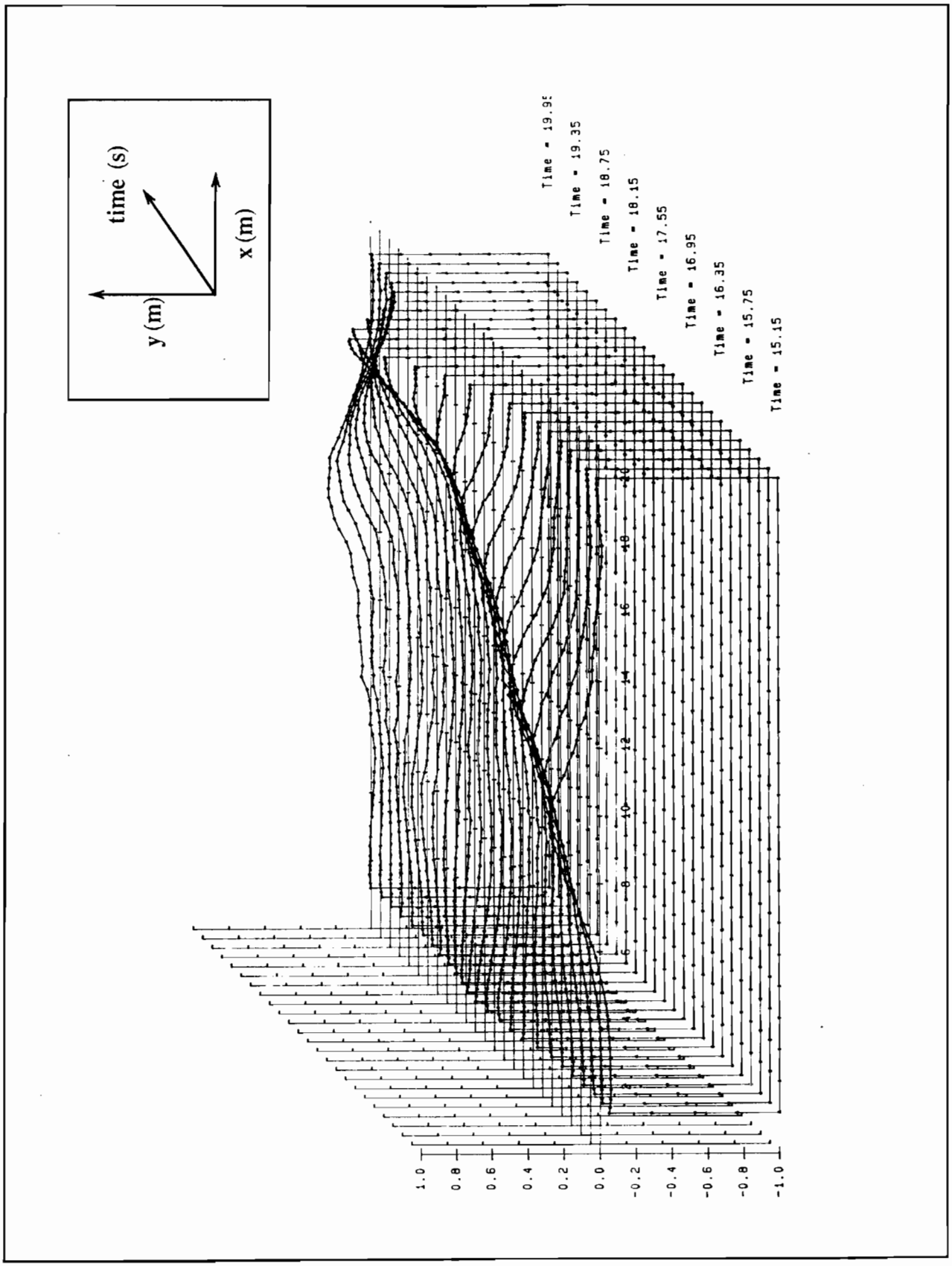

Fig 5.8 d Generation of a solitary wave and its runup on a vertical wall.

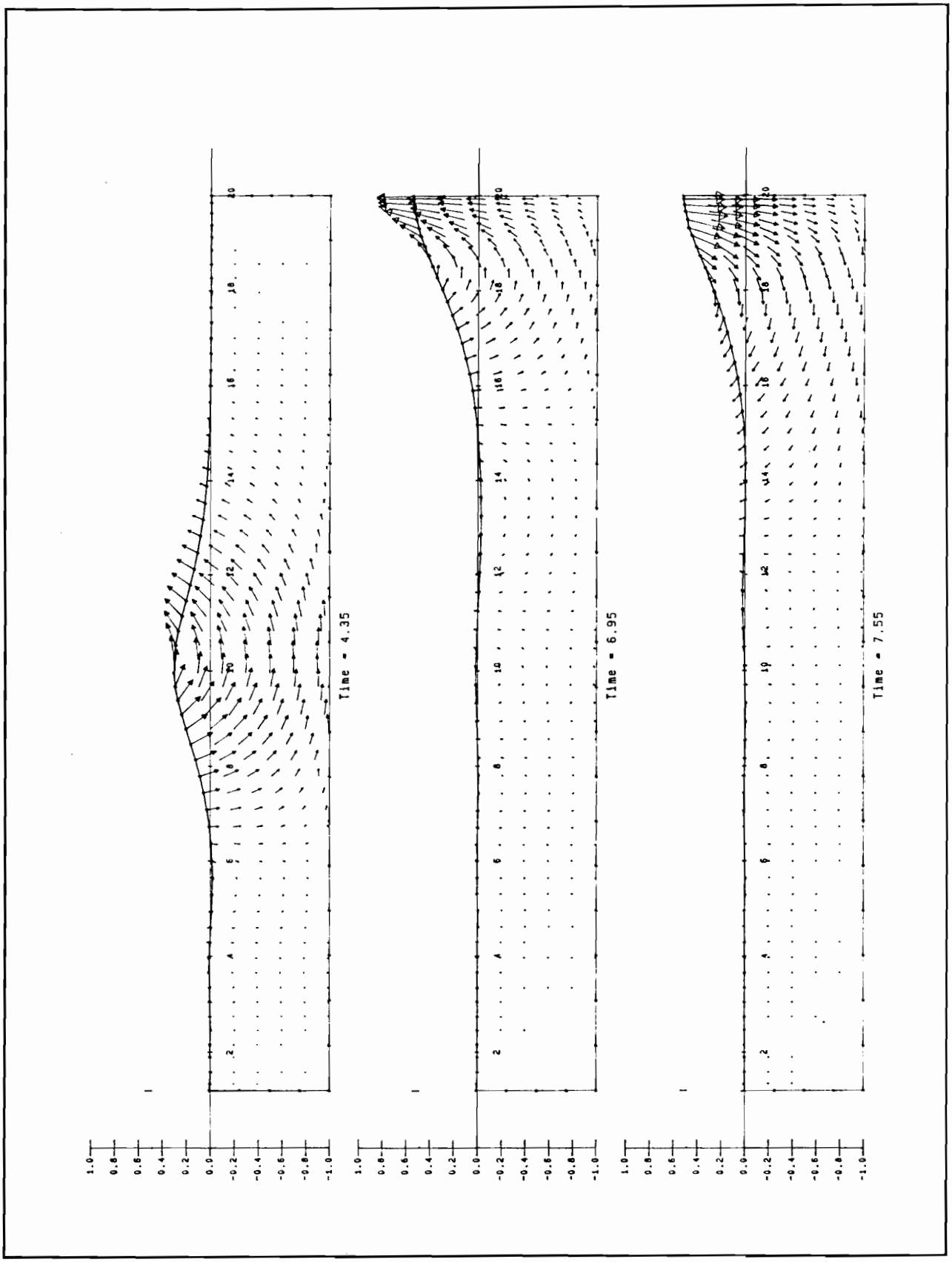

Fig 5.9 a Internal kinematic fields for Figs 5.8 a-d.

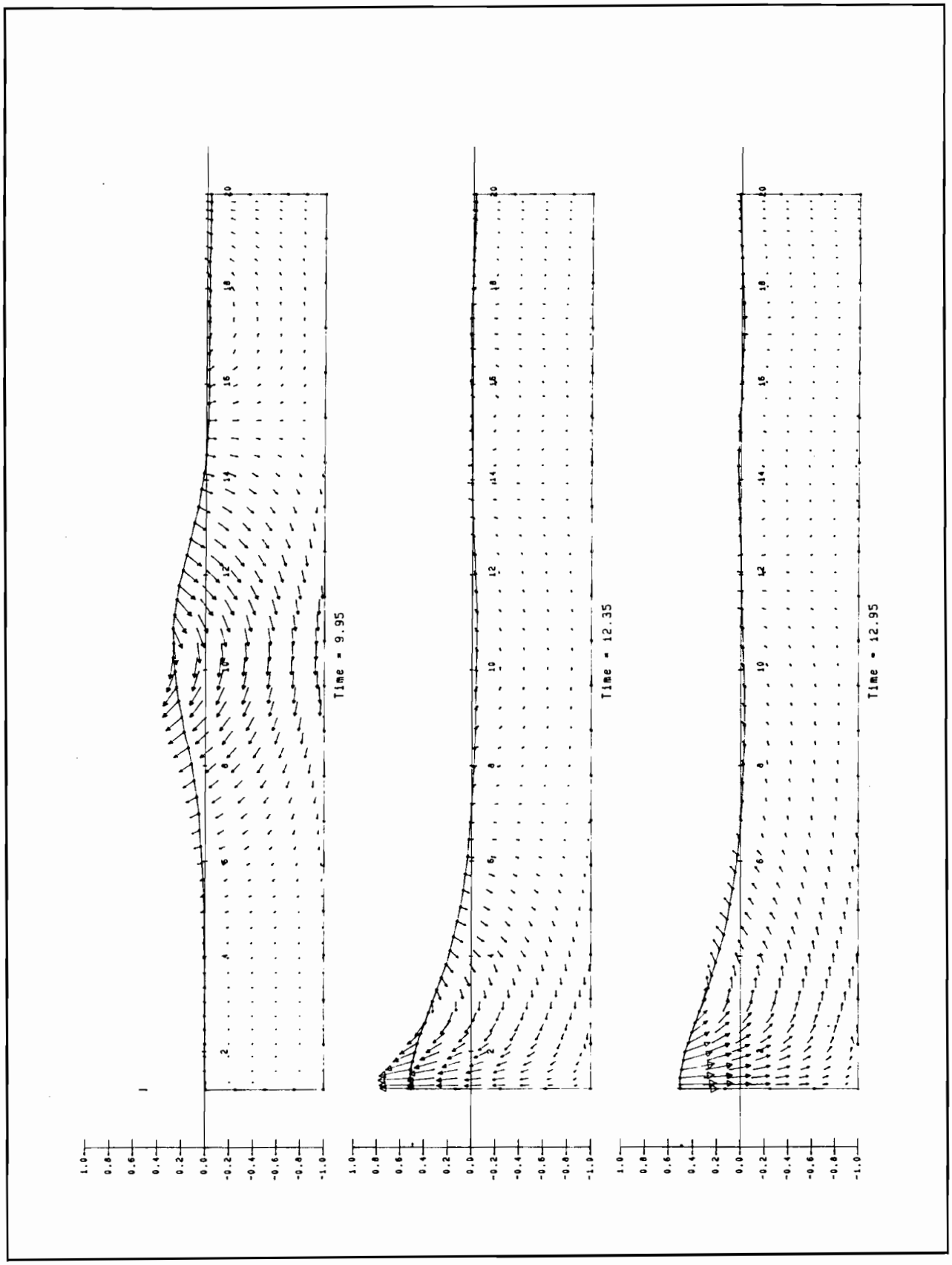

Fig 5.9 b Internal kinematic fields for Figs 5.8 a-d.

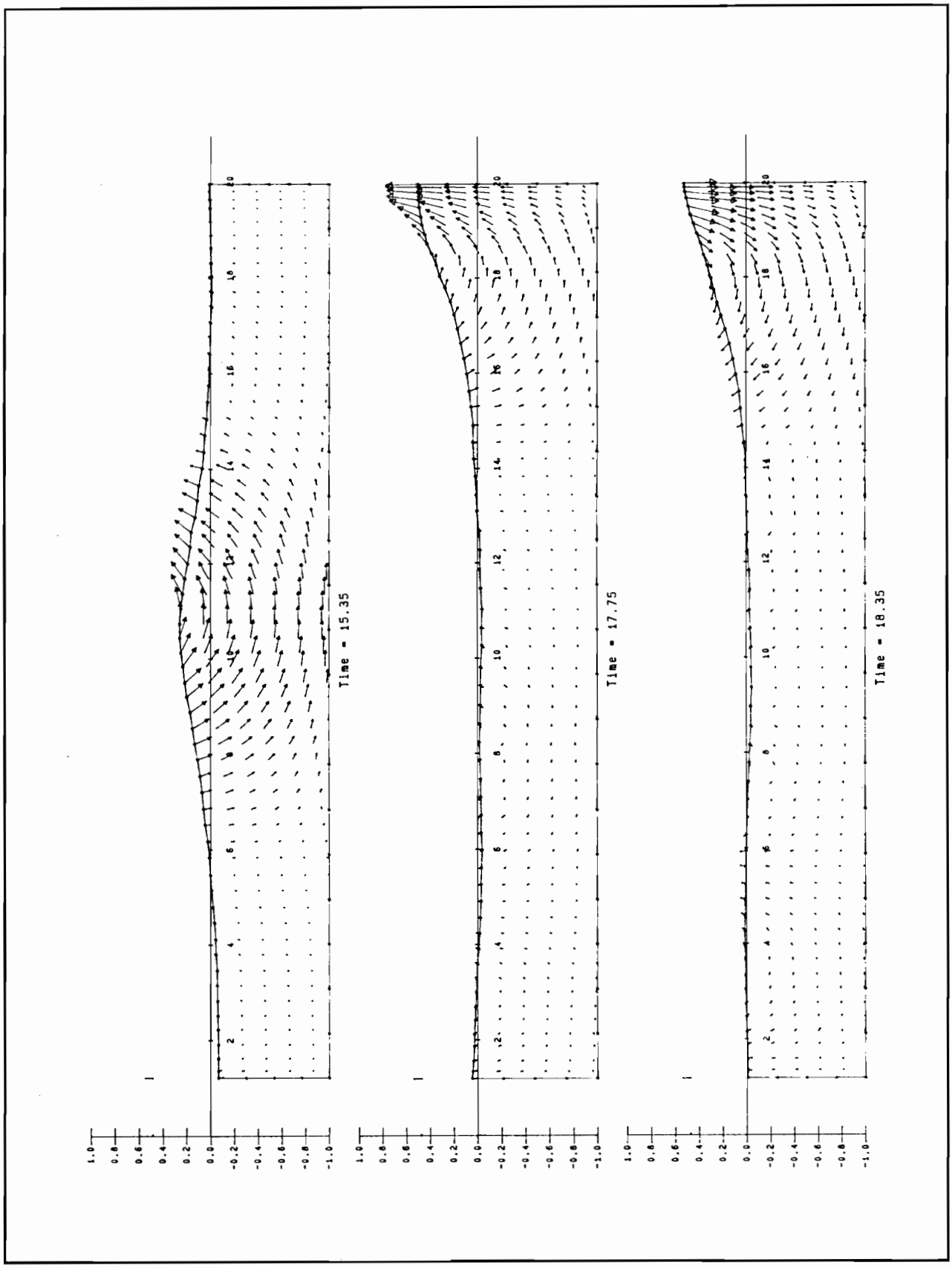

Fig 5.9 c Internal kinematic fields for Figs 5.8 a-d.

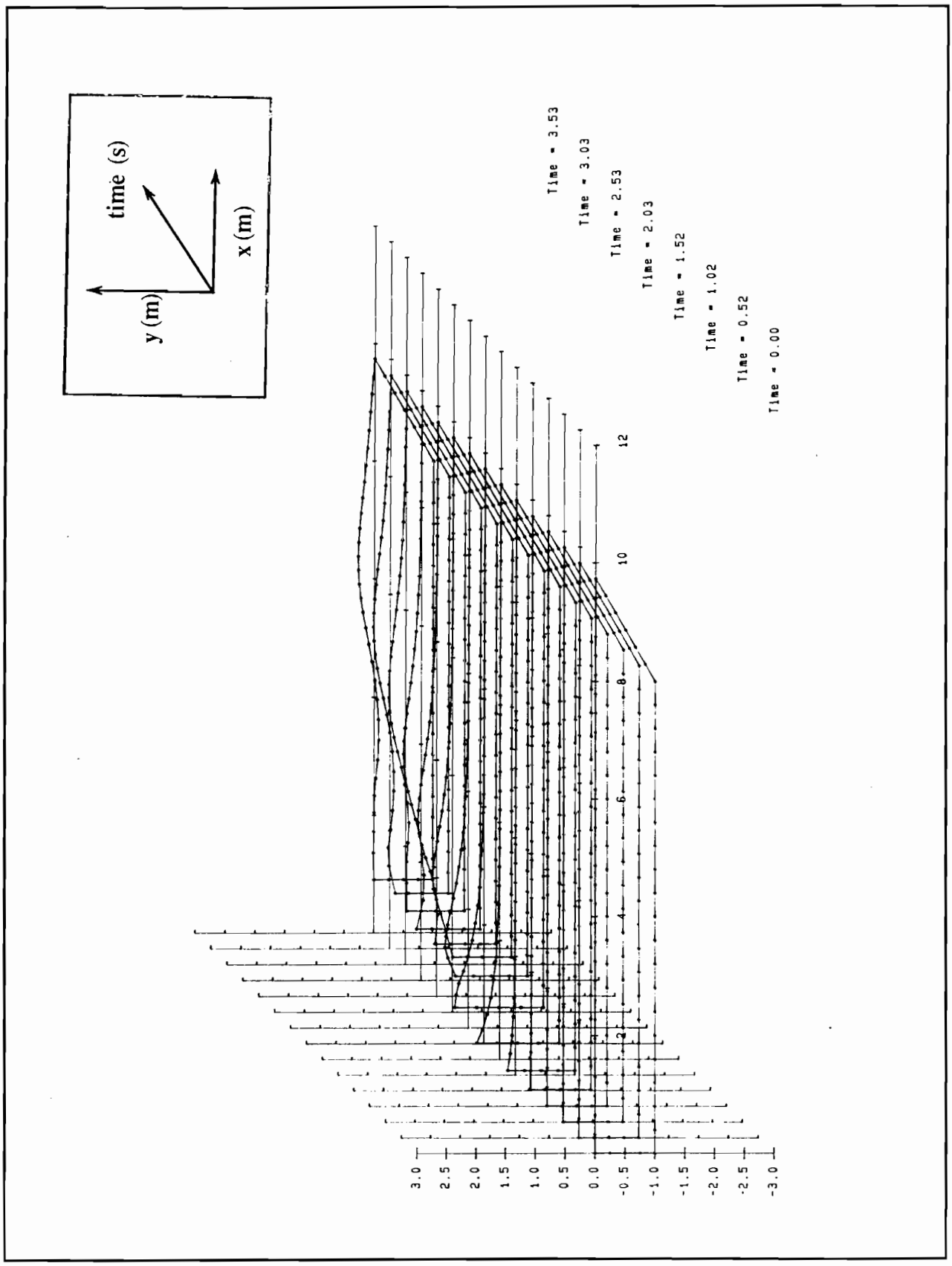

Fig 5.10 a Generation of a solitary wave and its runup on a slope.

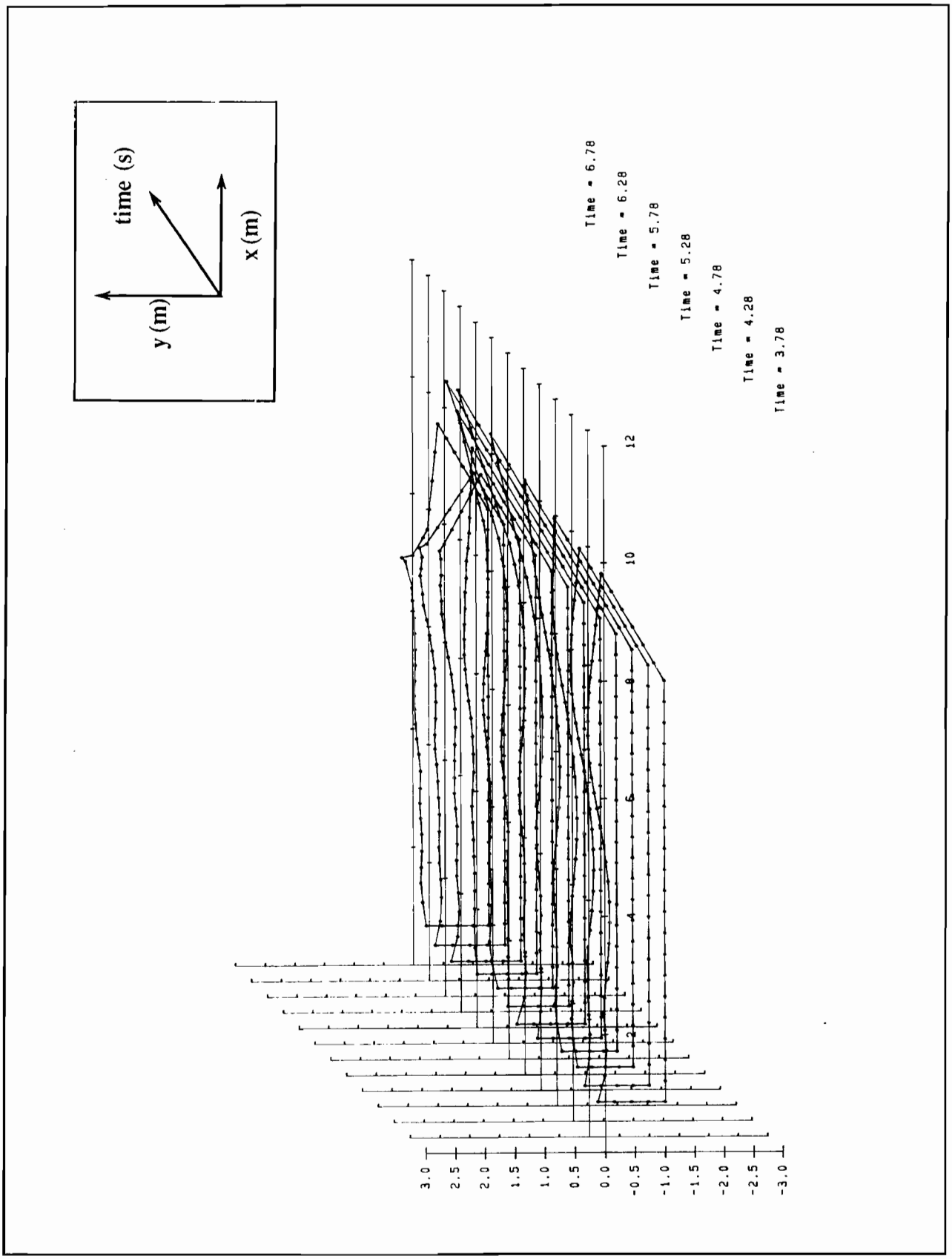

Fig 5.10 b Generation of a solitary wave and its runup on a slope.

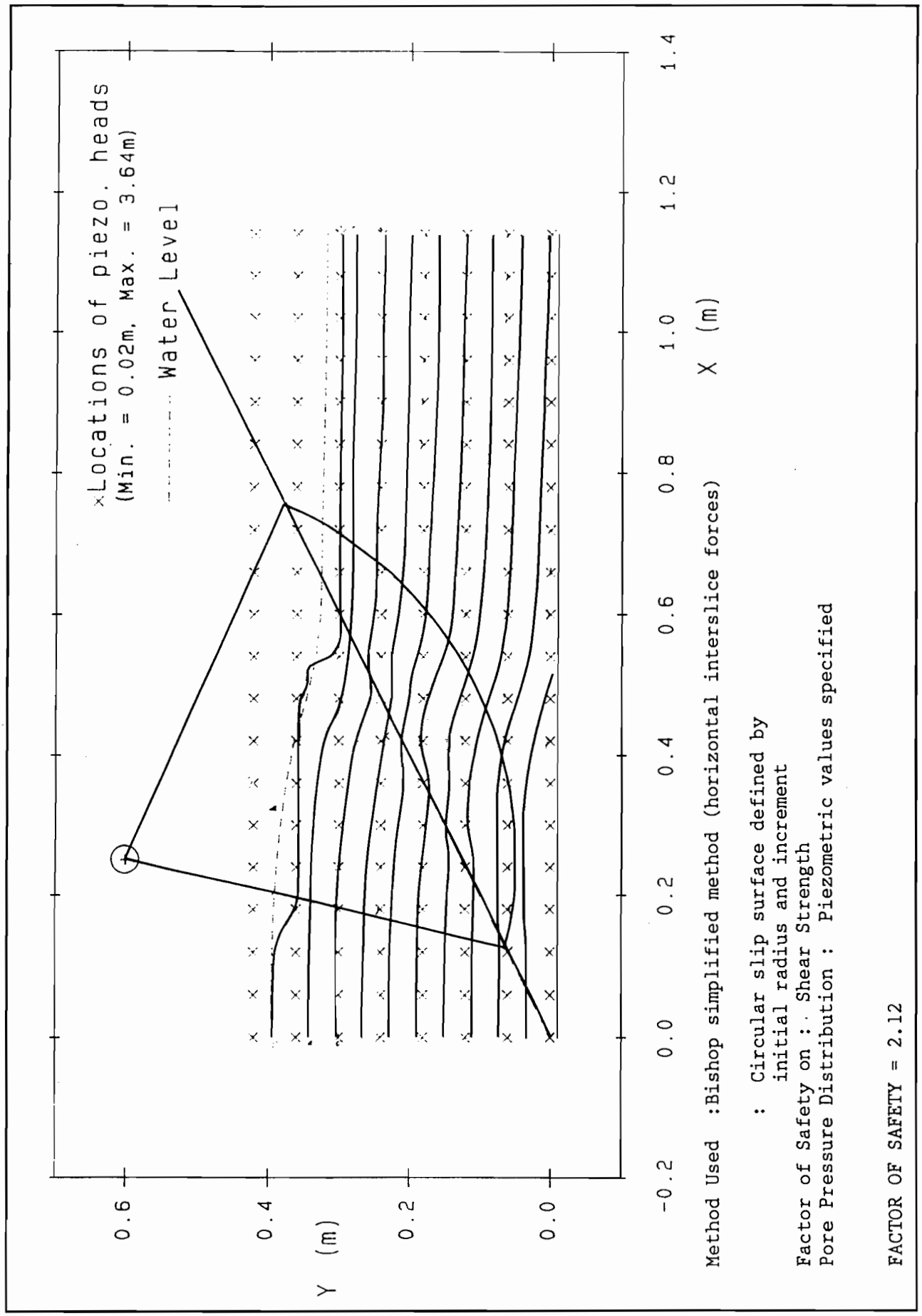

Fig 6.1 Example results of slope stability calculations.

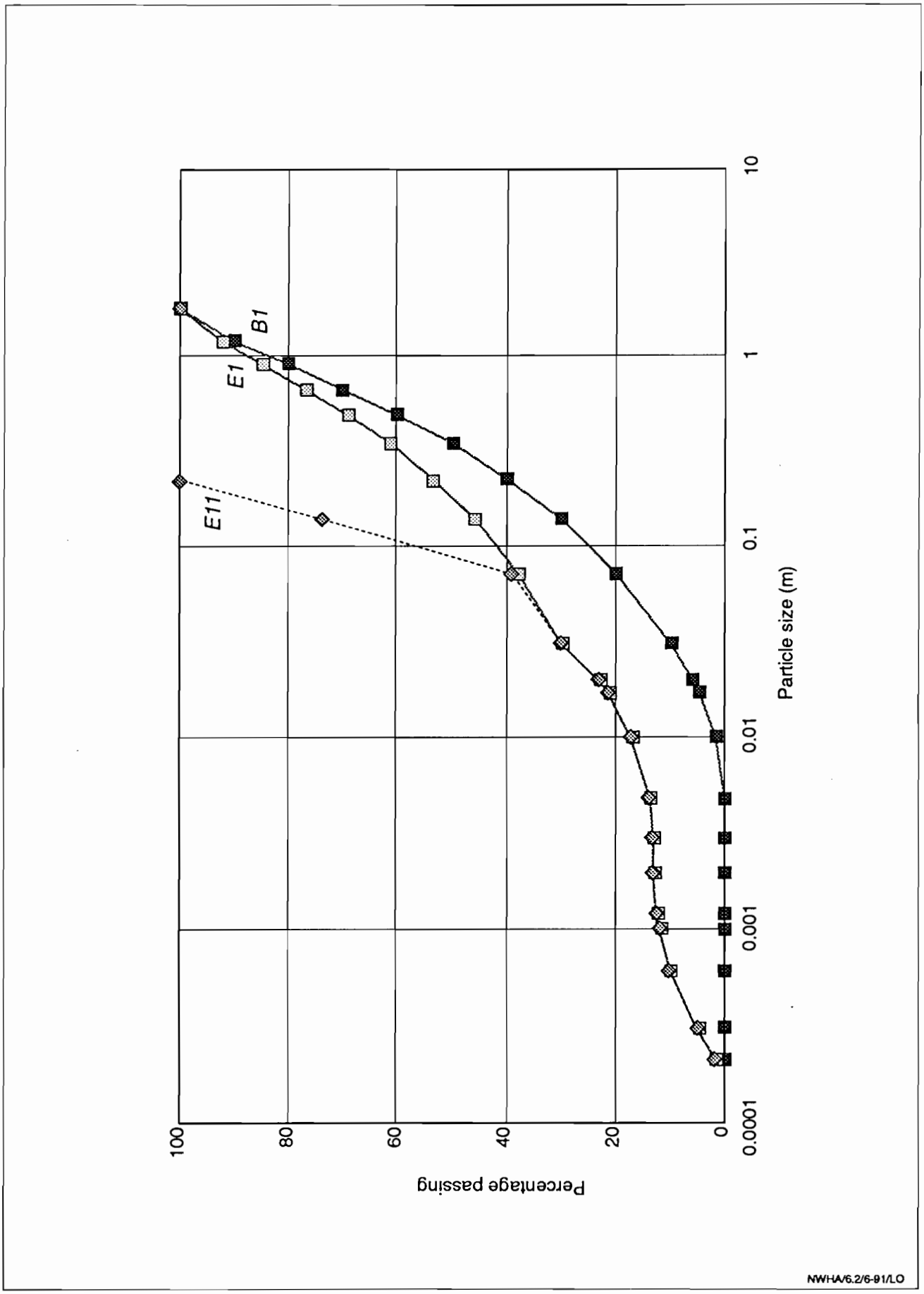

Fig 6.2 Size grading B1, E1 and E11

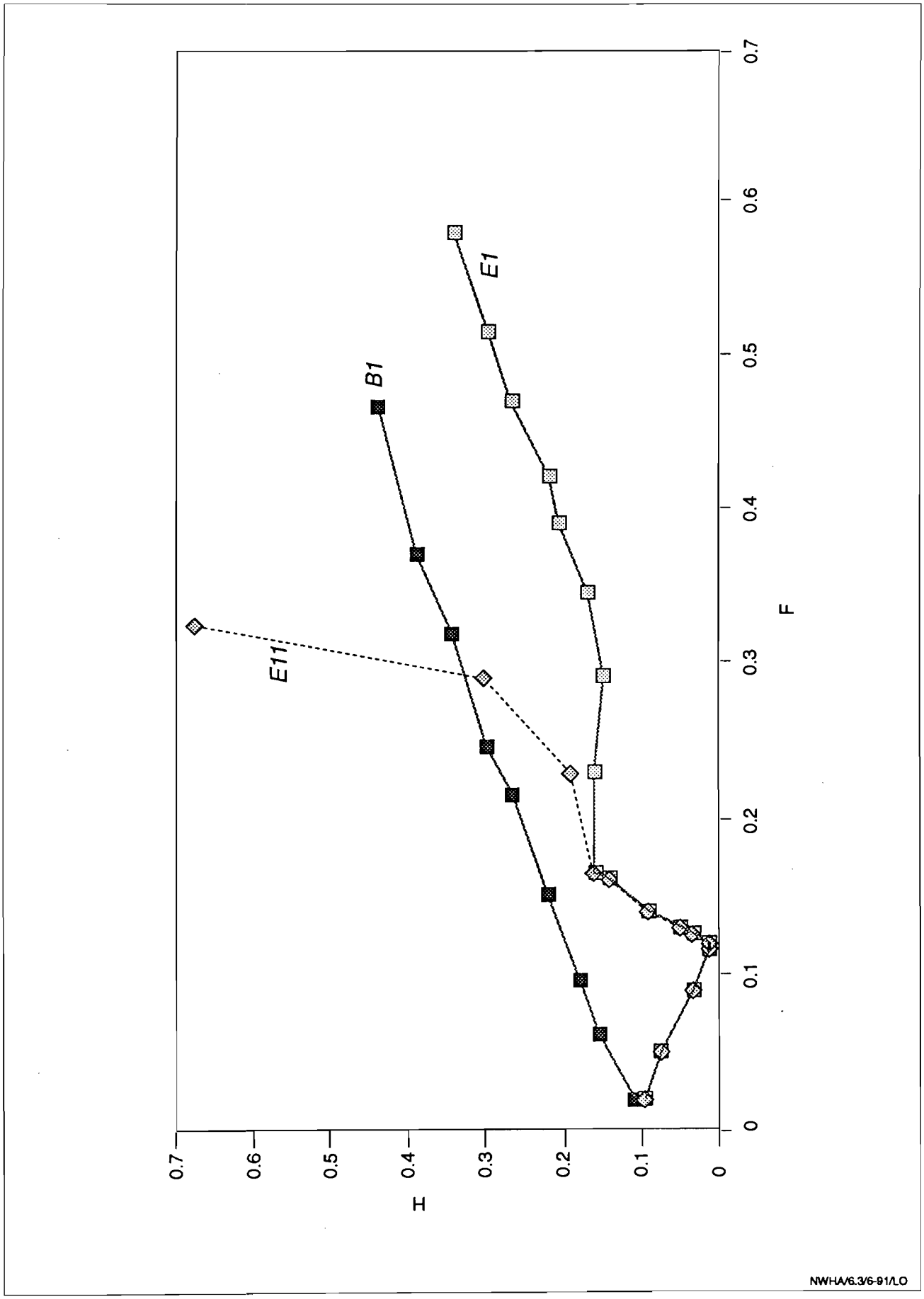

Fig 6.3 F-H diagram for stability of B1, E1 and E11

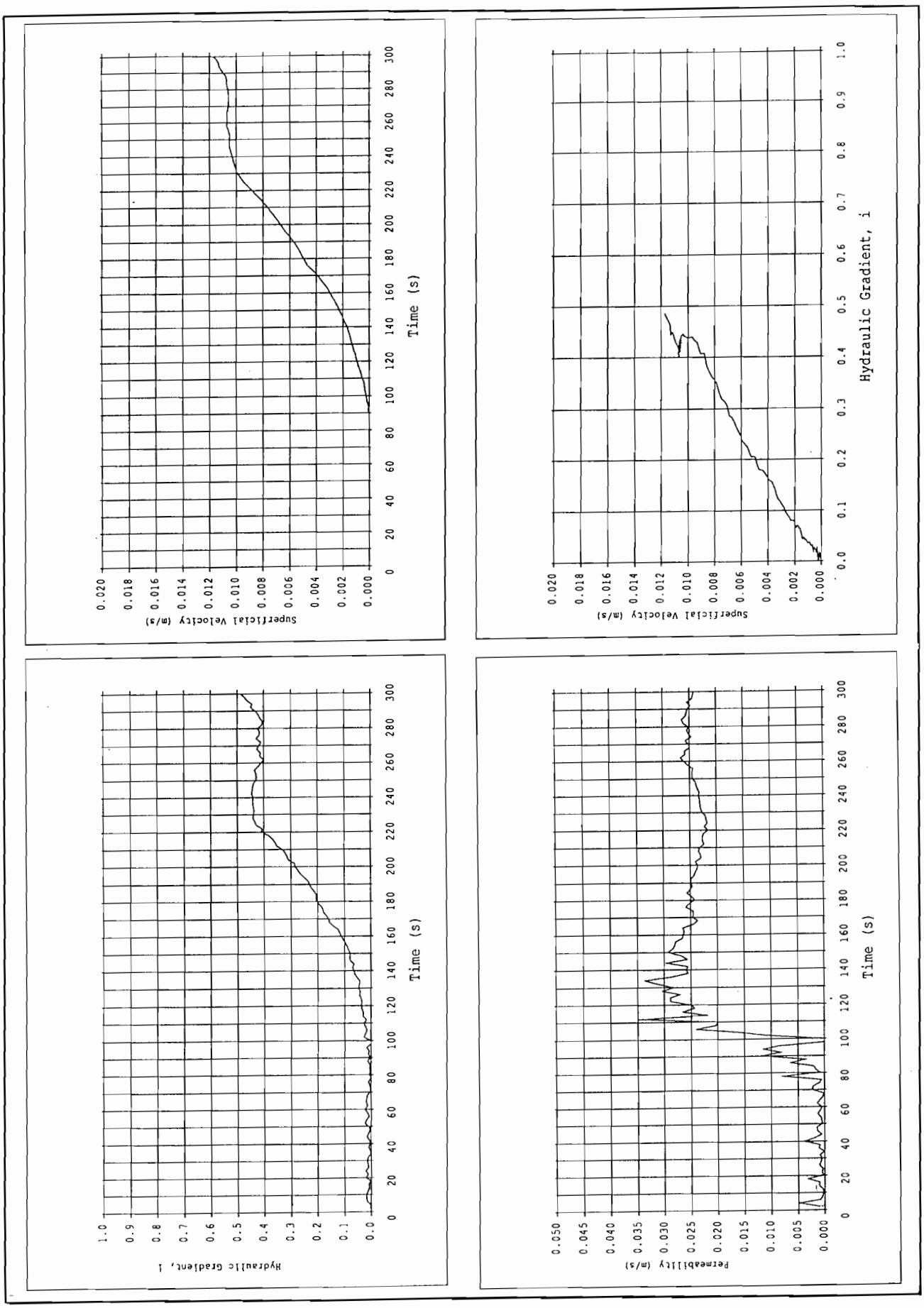

Fig 6.4 Steady state stability test (a), from Reference 6.7.

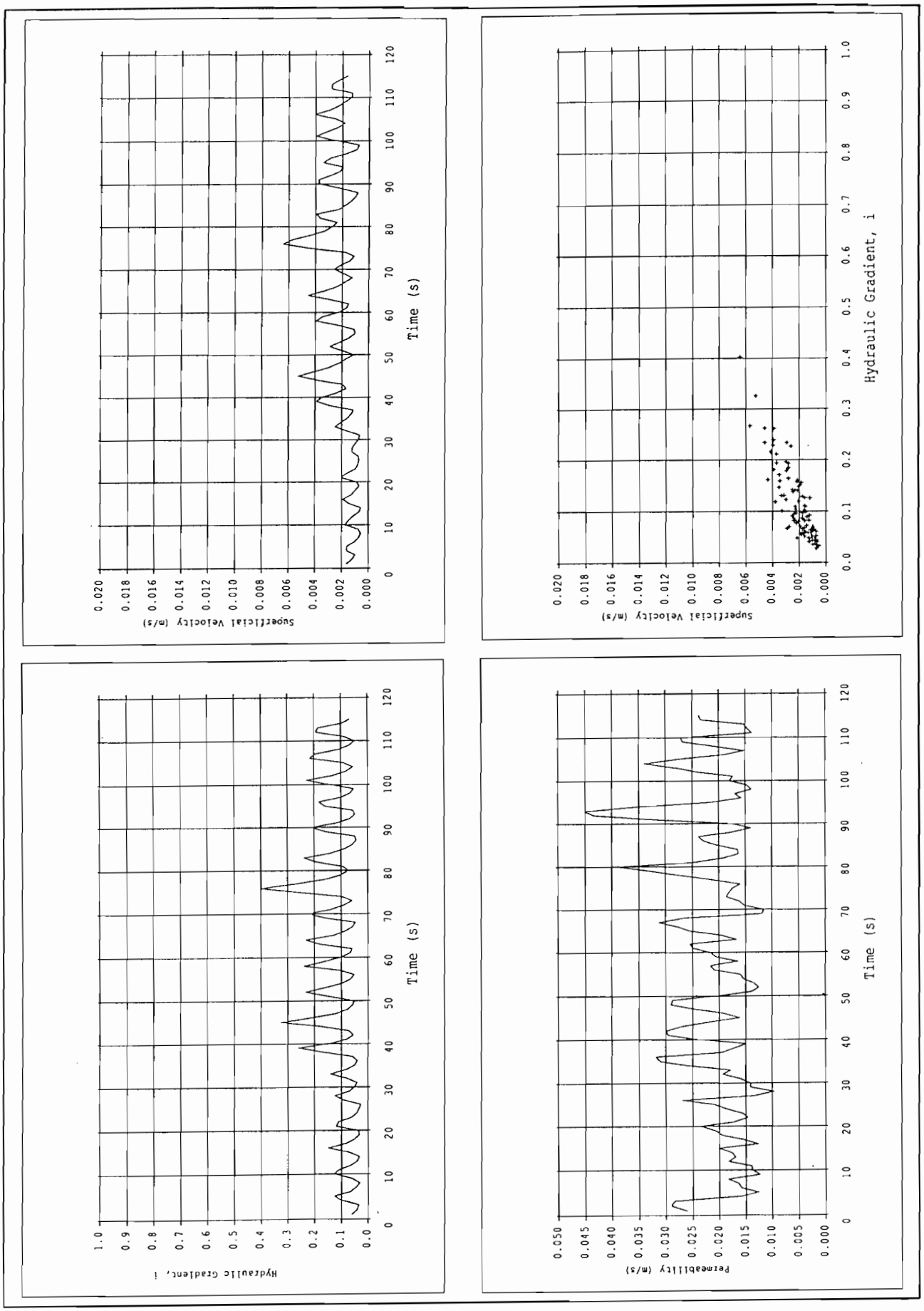

Fig 6.5 Unsteady stability test, from Reference 6.7.

Plates

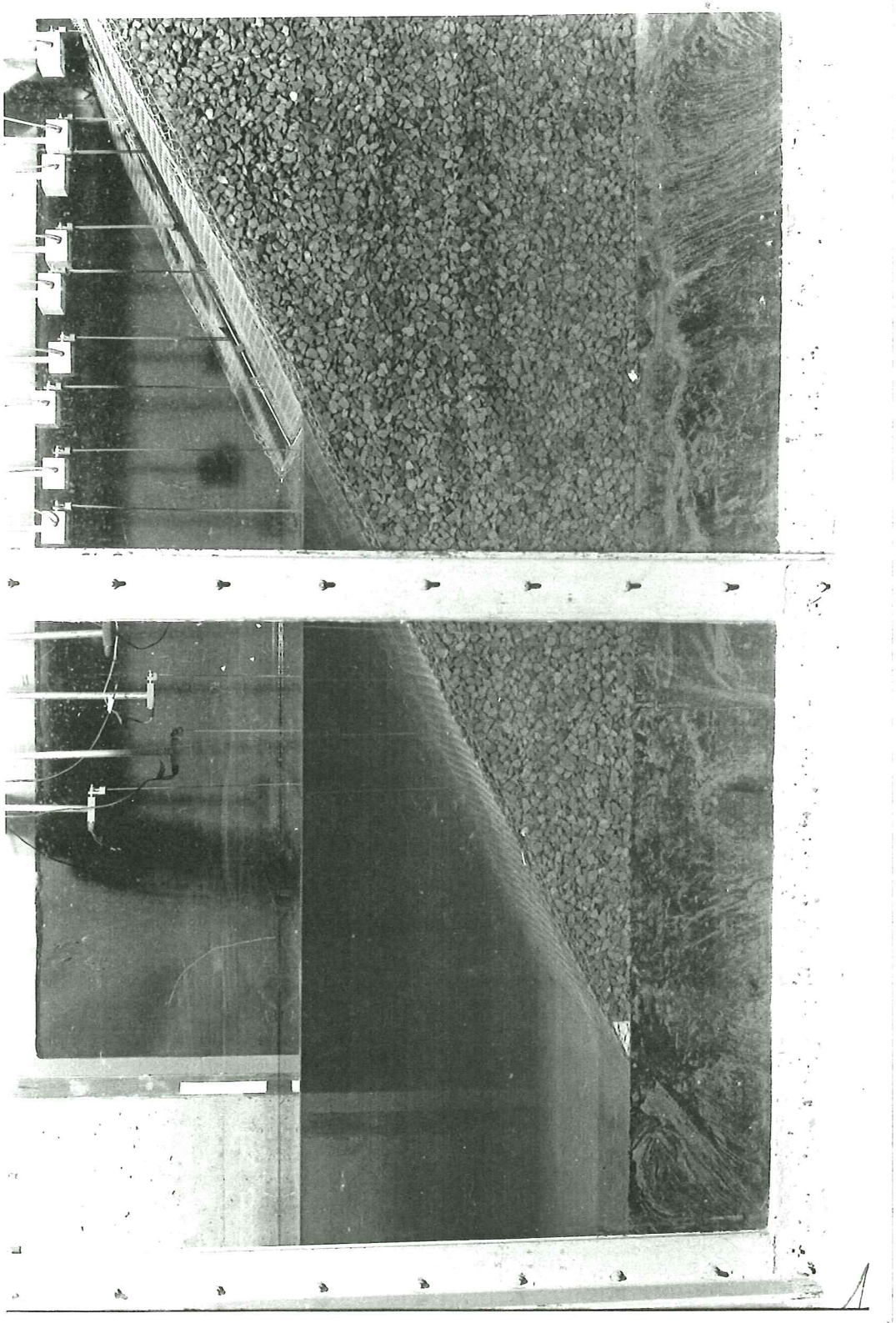

Plate 1 Initial wave flume tests.

Plate 2 Initial wave flume tests.

Plate 3 Initial wave flume tests.

Plate 4 Initial wave flume tests.

Plate 5 Initial wave flume tests.

Appendix

APPENDIX A

Workshop on wave impacts on coastal structures

1. INTRODUCTION

The quantitative description of wave impact loads has become more important in the design of breakwaters and sea walls, particularly where wave impact forces can lead to structural failure. Examples are given by the effect of repeated wave impacts on granular embankments, which can lead to cyclic increases in internal pore pressures, and hence geotechnical failure; and/or direct impact damage to slender-limbed concrete armour blocks.

The intensity and duration of wave impacts are strongly influenced by air entrained in the breaking wave. Air bubbles cannot however be reproduced to scale in model tests, reducing the accuracy of any predictions of impact pressure. Wave/structure impacts have been studied by coastal and offshore engineers, using mathematical and physical modelling, small and large scale experiments, and field data measurements. There is much experience on dealing with wave impacts, but this experience is often confined to relatively small teams.

This workshop was organised by Hydraulics Research at Wallingford on 1 November 1989, to share experience on measuring and/or modelling wave impact pressures or forces. The discussions fell under four headings:

Wave forces on coastal structures;
Numerical modelling of wave/structure interaction;
Laboratory experiments at large scale, and field data collection;
Laboratory and field measurement methods.

The programme of the workshop is given in Annex 1. The papers are given here under the headings above, rather than in the sessions timetabled.

Invitations to the seminar were sent to researchers involved in coastal and offshore engineering, and the design and use of measurement devices for the laboratory and/or field, as well as representatives of the Department of the Environment and the Department of Energy. Those attending are listed in Annex 2.

2. IMPACT FORCES/PRESSURES ON COASTAL STRUCTURES

2.1 The effects of wave impacts on coastal structures, NWH Allsop

Historically the forces acting on a breakwater or sea wall have only been estimated explicitly in those few instances where they contribute to the main failure mode(s). In many instances, particularly in the design of rock or concrete armour units for rubble structures and revetments, the design method determines the size of armour unit required to resist the given wave condition, using simple empirical relationships. The forces on individual armour units are not calculated.

New design methods being developed will give more information on the forces and/or pressures acting on such structures. Three particular areas are of interest under current projects at Hydraulics Research:

(a) Stability of close fitted concrete blockwork on embankment dams and revetments;
(b) Influence of wave impacts on pressures within the core of permeable structures;
(c) Direct impact loadings on slender limbs of concrete armour units.

Blockwork protection

In the UK, failures of blockwork protection appear to have been more common on embankment dams than on coastal structures. Generally individual blocks have been lifted by waves, allowing areas of underlayer to be washed out, and surrounding blockwork to be displaced. Damage has usually been confined to small areas, and has been repaired before damage has spread.

This failure mode may be treated as a quasi-static event. Each block has significant inertia, and impact pressures of very short duration will not cause movement. Failure is precipitated by the difference between the pressures acting into the slope from outside, and outwards from the underlayer. The maximum pressure difference occurs at the block situated just below still water level at maximum wave run-down. It is greatest for a relatively impermeable cover layer over a relatively permeable underlayer. The intensity and duration of wave impacts is not of great importance in the design of this type of protection. The design of the blockwork protection may therefore be addressed by empirical methods based on model test results, or field experience (Ref 4).

Hydro-geotechnical stability

There is evidence that repeated impact pressures on blockwork or asphalt protection may be transmitted to a sand core. This may cause cyclic increases in pore pressures, leading to geotechnical failure. Research in Germany and the Netherlands (Refs 5, 6) has shown that up to 50 km of Dutch sea dykes may be at risk from liquefaction of loosely compacted sand fill. This is most severe where the permeability of the underlayer/core material is low. The level and frequency of impact pressures will therefore constitute important design parameters.

The volume of rubble material in a breakwater depends critically on the side slopes and crest level. Conventional rock or concrete armouring must be large to resist wave forces at steep slopes. Some types of concrete armour appear to become more stable at steep slopes than at shallow angles. This is particularly true of hollow-cube armour as the COB or SHED. These units may offer the designer considerable savings in armour, and in rubble material. By their nature, however, high porosity armour units allow greater transmission of wave pressures, and hence pressure changes, to the mound material. A potential failure mode of some importance might be the gradual movement of material beneath the armour layer, particularly where the underlayer or core material is fine enough to pass through the voids in the armour. Again information is needed on the size and frequency of impact pressures.

Wave impacts on concrete armour units

Recent research in USA, the Netherlands, Denmark, and the UK, has addressed the relative fragility of concrete armour units with slender members. In many instances, the principal causes of armour unit failure has been the concentration of semi-static stresses within the armour layer, and/or strsses caused by inter-unit impacts. Hollow cube units are placed in very close proximity, with little opportunity for inter-unit collisions. Direct wave impacts on the limbs of such units might however cause structural failure. Studies to address this are described in Section 2.3 below.

2.2 Wave impacts on the Islay wave power device, TJT Whittaker and G Muller

A wave power device has been constructed in a rock gully on the island of Islay, Scotland. The device itself uses an oscillating water column driving air through a Wells turbine. The air chamber is contained within a concrete "hood" with a steeply sloping front

face, constructed into the rock gully. During the design of the wave power device, one of the areas of uncertainty was the size and frequency of wave impacts on the device. Little field data was available on wave impacts, and empirical design methods showed poor agreement. A research project was therefore set up to measure wave impact pressures on the device.

Two rows of 5 pressure transducers, mounted on steel beams, will be deployed on the concrete front face. Pressures will be sampled at up to 100 samples per second. The measurements will be processed on site by a Compaq PC. Further details of the arrangement are given in Annex 3.

2.3 Wave pressures on slender concrete armour units: model and fieldwork, DM Herbert

Under the direction of the Single Layer Armour research Club an attempt has been made to quantify the size and duration of wave impact pressures on slender limbed armour units such as the Cob and the Shed. The problem has been addressed using a combination of physical model tests and fieldwork deployment.

A physical model was constructed based on La Collette breakwater at St. Helier, Jersey. Pressures measurements were completed in the model using water filled hypodermic tubes to transmit pressures imposed on the surface of the Cob units to six pressure transducers buried deep in the mound. Wave impacting was found to be fairly sporadic. Typical impacts had rise times in the order of 10-20 milli-seconds, and were followed by a much longer quasi-hydrostatic pressure caused by wave run-up. Whereas the magnitude of the quasi-hydrostatic events was relatively similar, the impact spikes varied considerably in size.

The largest wave impacts were found to be equivalent to approximately 3.5 times the significant incident wave height, and occured on units sited close to still water level (SWL). There were marked reductions in impact size for units below SWL, where the unit is almost constantly submerged, and above SWL, where the vast majority of waves break prior to reaching the unit. Example results are shown in Annex 4.

The physical model enabled many different combinations of waves and water levels to be investigated but was prone to scale effects. The degree of aeration was likely to be underpredicted. This may have led to larger impacts of shorter duration than occur in prototype. It was therefore necessary to obtain some fieldwork data in order to attempt to quantify any scale effects.

Early in September 1989 four pressure transmitters were deployed on La Collette breakwater in similar positions to the transducers sited in the physical model. Output from the transmitters is recorded on an intelligent logger capable of storing up to 2.5 Gbytes of data per tape. The logger is triggered by an external signal from a tide gauge thus ensuring that data is only collected when significant wave impacting is likely.

It is hoped that data from these two pieces of work will be used together with a finite element model of a Cob unit developed by the University of Bristol. This model will allow potential stress concentrations to be identified, and determine if large wave impacts are responsible for the cracking of the relatively slender limbs.

2.4 Discussion

Three main areas were considered further. There was some discussion on reasons for the failure of large breakwaters, and particularly on the parameters required to assess potential failure of armour units. In the HR tests described by Herbert the force applied to the complete unit was measured in the flume experiments. Stresses induced in the unit depended also on the reaction conditions, presently unknown. In large scale tests at Hannover, tetrapod armour units had been instrumented for strain measurements, and tested in the Large Wave Flume (GWK).

Time intervals between samples, and the frequency responses of the measuring equipment, were also discussed. For the hollow cube units, the principal excitation frequencies had been derived from finite element analysis of the armour unit (Ref 9). From this work, Wastling suggested that the shortest event duration of interest for these units would be around 4 milli-seconds.

The possible errors in predicting wave impacts from scale models were highlighted. It was noted that tests by Furhboter had suggested that impacts from model waves of height above 0.5m would give reasonable agreement with full scale results.

3. NUMERICAL MODELLING OF WAVE IMPACTS

3.1 Numerical modelling and air/water interactions, DH Peregrine and MJ Cooker

A numerical model of 2-dimensional flow in breaking, and non- breaking waves, known as CHY, had been developed in the School of Mathematics at Bristol (Ref 10). The model used conformal mapping to increase the

speed and efficiency of calculation. It had been used to compute water surface profiles, and velocity distributions, for solitary waves impacting on a vertical wall. The calculations were taken very close to the point when the fluid starts to separate. The calculations suggest that velocities at the wall could be more than 3-4 times the maximum in the undisturbed breaker, and the force acting on the wall might exceed 32 times the hydrostatic load.

More detailed descriptions of the test results are given in Annex 5, and in References 11 and 12.

3.2 Use of a boundary element model to predict wave slam, RWK Shih

A two-dimensional boundary element model known as BEMTOOL had been developed initally at Imperial College (Ref 13), and subsequently improved at Hydraulics Research (Ref 14). The model's formulation was based on Cauchy's integral theorem, similar to the approach taken by Vinje & Brevig. The model was able to calculate water surface profiles, velocities and pressures up to the point of wave breaking. Input wave conditions included a piston wave-maker which could be set to give a wide range of wave types. The model operated in the physical plane, allowing the specification of sea bed and structure profiles of relatively complex form. The model could not however yet incorporate permeable boundaries. More details of the model are given in Reference 14.

3.3 Discussion

The capabilities of the two models were explored further. It was accepted that CHY was faster to run than BEMTOOL, although the models had not been compared directly. BEMTOOL however allowed a wider range of structure configurations and wave types to be studied.

4. WAVE IMPACTS AT LARGE SCALE

4.1 Wave impacts on vertical walls in the GWK, Hannover, H-W Partenscky

Many breakwaters and sea walls incorporate vertical faces. Wave impacts at such walls can be extremley severe. Methods to calculate impact forces / pressure were ill-supported by data. A programme of testing at large scale had been initiated at the Large Wave Flume (GWK) run by the Universities of Hannover and Braunschweig. The flume is 320m long, and can produce individual waves up to 2.5m in height. A vertical wall had been constructed in the flume, instrumented with 25 pressure transducers. Examples of test

results taken from References 2 and 3, included here as Annex 6, were shown.

Analysis of the impacts measured had lead to the development of a simple method for estimating the peak dynamic pressure, P_{dyn}:

$$P_{dyn} = K_L \rho g H_b$$

where H_b is the (maximum) breaking wave height at the structure, and K_L is an air content coefficient defined in terms of the percentage air content, P_A:

$$K_L = 5.4 [(100/P_A) -1]$$

Some of the pressures measured had rise times as short as 10 milli-seconds, but for comparisons with the theory pressures were averaged over the impact period, around 20-40 milli-seconds.

4.2 Wave impacts on a cylinder in the Delta Flume, Holland, J Chaplin

Tests had been conducted by a team of UK researchers led by City University in the Delta Flume of Delft Hydraulics to measure wave forces on cylinders. Wave pressures had been measured by 24 pressure cells around the cylinder.

A short film illustrated some aspects of the tests.

5. MEASUREMENT METHODS

5.1 Measurements in and of breaking waves, MW Griffiths

The measurement of velocities in breaking waves poses some particularly complex problems. Two techniques had been developed in the Physics Department at Edinburgh University to measure velocities at a point in space through a wave period, or conversely throughout an area at a moment in time. Laser doppler anemometry had been used to measure velocities and accelerations in the crests of breaking waves with sample periods as short as 0.5 milli-seconds. Particle image velocimetry with a high power (15 W) laser had been used to freeze particle motions over a sample area of 0.4m x 0.7m within a wave flume. More details are given in Annex 7.

Since the workshop, a new wave flume has been opened at Edinburgh. The scanning apparatus has been improved to allow a length of 1m to be covered.

Processing of the PIV photographs has now been automated, reducing processing to less than 30 minutes, rather than many hours.

5.2 Measurement of air in waves, P Hewson & J Griffiths

The importance of a knowledge of the air content of breaking waves had already been identified. There were however no devices able to quantify air concentrations, or bubble sizes, in unsteady flow. A research project had been started at Plymouth to develop devices that could measure air content, or similar, in the fresh water used in the hydraulic laboratory, and in salt water in the field. The measuring techniques required for these two situations were significantly different, and two separate devices would need to be developed.

A number of different techniques had already been explored, and were discussed in Annex 8.

5.3 Field measurement and analysis techniques, J Bishop

A major measurement exercise had been mounted on the Christchurch Bay Tower to validate wave theories used in the design of oil platforms etc in the North Sea. Water surface elevations, wave velocities, and forces on elements of the tower were recorded. Velocities were measured at a number of levels using perforated ball velocity meters. The results were compared with velocities predicted for waves of the measured heights.

5.4 Advances in instrumentation, R Cuffe

Field instruments tend to generate very large volumes of data. Pressure measurements often require very rapid response equipment. These requirements have required developments in recording, logging, and transducers, Annex 9.

It is usually most convenient to record at the measurement site direct onto magnetic tape. Historically, analogue signals were recorded as frequency modulated (FM) signals on ¼" or 1" tape. Specialist tape recorders were available, but were very expensive. Recent developments have allowed the use of commercial video recorders to carry digital signals. This increased the data volume held per tape, and reduced the cost of the recorder. Potential problems might arise with data quality if processing required many passes of the recorded tape. Future developments would probably include optical disks,

presently available in a Write Once Read Many times (WORM).

Computerised data logging is now generally driven by an "IBM compatible" PC, with data recorded to disk and/or tape. Very careful selection of the A/D converter, and the programming languages, are however essential to get the full benefit from the system. The major limitations of PC based systems appeared to be that they were difficult to multi-task, and to take samples at different rates.

Confusion often arose in setting the sampling rate required in relation to the signal bandwidth, instrument response, and signal rise time. In part this depends on the analysis to be carried out. A minimum sample rate should ensure that at least 3 samples are taken within the signal rise time. The sample rate, in samples per second, should be greater than 3 times the upper frequency band in Hz.

References

1. Allsop NWH "Hydro-geotechnical performance of rubble mound breakwaters" Report SR 183, Hydraulics Research, Wallingford, February 1991

2. Partenscky H-W "Dynamic forces due to waves breaking at vertical coastal structures" Proc 21st ICCE, Malaga, June 1988

3. Partenscky H-W & Tounsi K "Theoretical analysis of shock pressures caused by waves breaking at vertical structures" Proc 23rd IAHR congress, Ottawa, August 1989

4. Herbert DM & Allsop NWH "Wave protection in reservoirs: hydraulic model tests of blockwork stability" Report EX1725, Hydraulics Research, Wallingford, May 1988

5. Grune J "Anatomy of shock pressures (surface and sand core) induced by real sea state breaking waves" Proc conf Modelling soil-water-structure interactions, SOWAS 88, Delft, publ. Balkema, 1988

6. Ebbens EH, Molenkamp F & Ruygrok P "Effect of wave impact on asphalt revetments of Dutch sea dikes" Proc conf Modelling soil- water-structure interactions, SOWAS 88, Delft, publ. Balkema, 1988

7. Herbert DM & Hare GR "Physical model testing of a COB armoured structure" Report IT344, Hydraulics Research, Wallingford, January 1990, (Restricted)

8. Stephens RV "Preliminary field work and instrument trials" Report IT311, Hydraulics Research, Wallingford, July 1988, (Restricted)

9. Wastling MA "The effect of wave forces on individual limbs of single layer armour units" Report UBCE/C/90/8, University of Bristol, March 1990, (Restricted)

10. Tanaka M, Dold JW, Lewy M, & Peregrine DH "The instability and breaking of a solitary wave" J Fluid Mech, Volume 185, 1987

11. Cooker MJ & Peregrine DH "A model for breaking wave impact pressures" Proc 22nd ICCE, Delft, July 1990

12. Cooker MJ & Peregrine DH "Violent water motion at breaking wave impact" Proc 22nd ICCE, Delft, July 1990

13. Shih RWK "Wave induced uplift pressures acting on a horizontal platform" PhD thesis, Imperial College, University of London, 1989

14. Shih RWK "BEMTOOL: a two-dimensional numerical program based on boundary element model" Report IT 349, Hydraulics Research, Wallingford, November 1990

Annex 1

Programme for Workshop on Wave Impacts on Coastal Structures,
Hydraulics Research, Wallingford, November 1989

Annex 1

Programme for a workshop on wave impacts on coastal structures, Hydraulics Research, Wallingford

10.30-10.45		Welcome Objectives & Programme	S W Huntington J Chaplin (Chairman)
10.45-12.00		Session 1	
	1a	Wave forces on coastal structures	N W H Allsop
	1b	Wave impacts on the Islay wave power device	T J T Whittaker
	1c	Wave forces on slender Concrete units - model and field work	D M Herbert
		Discussion	
12.00-13.00		Session 2	
	2a	Numerical modelling and air/water interactions	D H Peregrine
	2b	Use of a boundary element model to predict wave slam	R W K Shih
		Discussion	
13.00-14.15		Lunch	
14.15-15.30		Session 3	
	3a	Wave impacts on vertical walls in the GWK, Hannover	H W Partenscky
	3b	Wave impacts on a cylinder in the Delta flume, Holland	J Chaplin
	3c	Measurements in, and of, breaking waves	M Griffiths
		Discussion	
15.30-16.45		Session 4	
	4a	Measurement of air in waves	P Hewson
	4b	Field measurement and analysis techniques	J Bishop
	4c	Advances in instrumentation	R Cuffe
		Discussion	
16.45-17.30		Closure discussion	A J Grass

Annex 2

List of participants, Workshop on Wave Impacts on Coastal Structures, Hydraulics Research, Wallingford, November 1989

Annex 2

List of participants, Workshop on wave impacts on coastal structures

Dr T J T Whittaker and Mr G Muller
Department of Civil Engineering
Queen's University
BELFAST BT7 1NN

Mr P Hewson, Mr P Bird and
Ms J Griffiths
Department of Civil Engineering
Polytechnic South West
Palace Court
PLYMOUTH PL1 2DE

Dr M Griffiths
Department of Physics
Edinburgh University
James Clerk Maxwell building
The King's Building
Mayfield Road
EDINBURGH EH9 3JZ

Mr J Bishop
6 The Hummicks
BEAULIEU
Hampshire SO4 27YU

Prof J Chaplin
City University
Northampton Square
LONDON EC1V 0HB

Dr A J Grass
Department of Civil Engineering
University College
Gower Street
LONDON
WC1 6BT

Dr M Whastling
University of Bristol
Department of Civil Engineering
Queen's Building
University Walk
BRISTOL BS8 1TR

Prof H W Partenscky
Franzius Institut
University of Hannover
Nienburger Strasse, 4
3000 HANNOVER 1
Federal Republic of Germany

Mr R Cuffe
Ship and Marine Data Systems Ltd
117 Fore Street
KINGSBRIDGE
Devon TQ7 1AL

Prof D H Peregrine, Mr M Cooker,
Dr D Diver
School of Mathematics
University of Bristol
University Walk
BRISTOL
BS8 1TW

Dr S W Huntington
Hydraulics Research
Wallingford

Mr C B Waters
Hydraulics Research
Wallingford

Mr N W H Allsop
Hydraulics Research
Wallingford

Dr D M Herbert
Hydraulics Research
Wallingford

Dr R W K Shih
Hydraulics Research
Wallingford